Determining the Mechanistic Plausibility for Acetyl-L-Carnitine as a Prognostic Biomarker in Sepsis

by

Marc McCann

A dissertation submitted in partial fulfillment
of the requirements for the degree of
Doctor of Philosophy
(Clinical Pharmacy Translational Science)
in the University of Michigan
2023

Doctoral Committee:

Professor Kathleen A. Stringer, Co-Chair
Associate Professor Haojie Zhu, Co-Chair
Professor Charles Burant
Clinical Associate Professor Jean Nemzek

Marc R. McCann

mrmccann@umich.edu

ORCID iD: 0000-0002-2132-6312

Dedication

The following is dedicated to my parents for their unconditional love and support throughout my life. Without them, I could not and would not have been able to follow my dreams of becoming a *scientist.*

Acknowledgements

It is both fortunate and unfortunate that the number of individuals who have helped mold me into the human I am today is truly innumerable; I simply cannot name everyone but *yinz* should know I love and cherish all the fundamental moments we have shared.

The first person I would like to thank is Dr. Kathleen Stringer, who has exemplified what it means to be a mentor and role model. Your tenacity and infectious excitement about research provided a constant source of motivation. It did not matter whether the experiment was a success or failure, I always left our meetings feeling better than before. The effort you made to be accessible regardless of your schedule is something I have greatly appreciated. You always treated me as a peer and valued my input, which was critical to my development as an aspiring scientist and leader. I will genuinely miss our weekly meetings even if they often ran over because we were derailed talking about football or one of our many shared interests. I would also like to thank you for welcoming me into your network of expert scientists that have aided my work, specifically, Dr. Michael Puskarich, Dr. Alan Jones, and Dr. Michael Maile who conducted the studies in patients with sepsis and septic shock then graciously afforded me the opportunity to use the data for my projects.

My work over the past few years simply would not have been possible without the aid and support from many individuals at the University of Michigan. I am particularly grateful for my committee members, Dr. Haojie Zhu, Dr. Charles Burant, and Dr. Jean Nemzek for their countless contributions throughout the arduous process of pursing graduate research. You all were a reliable source of information that was critical to the design, execution, and analysis of

my dissertation projects. To the members of the Stringer lab, Thomas Flott, Laura McLellan, and Cora McHugh, thank you for the immeasurable amount of help you gave through all the long and tedious experiments we ran together. I also want to give thanks to all the students and faculty in the Clinical Pharmacy department; specifically, Dr. Karen Farris, Dr. Dan Hertz, and Dr. Amit Pai. Through your sensible and charismatic leadership, you have created a program that truly values the students' opinions and actually implements our feedback. Additionally, I want to thank the members of my first lab at the University of Pittsburgh, Dr. Kerry Empey, Dr. Katie Eichinger, and Jess Kosanovich who provided the necessary foundational support and guidance that encouraged my interests in research.

I could not begin to describe the impact each member of my family has had on my development as a person. My two older brothers, Luke and Matt, have pushed me to strive for perfection in every aspect of my life through both conflict and love. They set the bar high for success from an early age and I was fortunate to learn from them. Of course, everything they taught me was learned from our incredible parents. My mum and dad fostered a family environment that facilitated tremendous personal growth from an early age. Our family dinner table conversations were likely more intense than any research debate I will ever encounter. My parents have taught me to be confident, pragmatic, reserved, and empathetic, but also how to find the right balance between them. As teachers, they knew the value of education and without their encouragement to challenge myself academically, I would not be in this position today. Being the youngest has many perks, but the greatest is having four remarkable role models to rely on and to them I am eternally grateful.

Next, I would like to thank my friends from West Manilla Ave, Dan Evans and Cody Alward, and the other golden eagles we went to school with, Jared Gulden, Pat Donovan,

Brandon Bates, Matt Hoey, and Michael Barrett who are always down to clown when I am in town. There are few things I enjoy more than hanging out with you all. I would also like to thank Dr. Jacob “Jake” Wissinger who I didn’t meet until pharmacy school at the University of Pittsburgh, but it feels like I have known you from the start. By the time I got to the University of Michigan, I had no expectations of making more life-long friends but thankfully I was wrong. From the first ice breaker event, Dr. Teddy Jennaro and I have been nearly inseparable, which was only exacerbated when Dr. Logan Smith joined the program. Thank you both for all the incredibly profound round table discussions at my apartment and the many fun times we have had. It has been a pleasure growing together as part-time pharmacists, aspiring scientists, and amateur golfers. I would also like to thank the many other friends from our Ann Abor crew who have made graduate school infinitely more enjoyable than it had any right to be.

Last but certainly not least, I want to express my sincerest gratitude to the sweetest and most remarkable woman I have ever met, Meghan McGowan. I still cannot believe you agreed to come to Michigan with me after so little time together but that just speaks to how special our relationship has been from the beginning and continues to grow with every passing day. The immense love and genuine compassion you give to the world is inspiring to myself and everyone around you. I know that wherever we end up next, it will be the most amazing adventure yet.

Preface

In the following work, each chapter contains an individual manuscript that is either currently published or in preparation. Chapter 1 contains an adapted version of the open access publication, *L-Carnitine and Acylcarnitines: Mitochondrial Biomarkers for Precision Medicine,* belonging to the MDPI Metabolites special issue Mitochondrial Metabolism and Bioenergetics. Chapter 2 represents the open access publication, *A Multivariate Metabolomics Method for Estimating Platelet Mitochondrial Oxygen Consumption Rates in Patients with Sepsis*, from the MDPI Metabolites journal section Endocrinology and Clinical Metabolic Research. Chapter 3 represents a manuscript draft that is under preparation with the title, *Metabolic Disruptions that Precede Organ Dysfunction in an Early Sepsis Mouse Model Persist in Patients with Sepsis and Septic Shock*.

Table of Contents

List of Tables

List of Figures

Abstract

Sepsis is a collection of clinical signs and symptoms that is described by life-threatening organ dysfunction inflicted by the body's own response to infection. The pathophysiological origins of organ dysfunction are not well understood, but mitochondrial metabolic dysfunction has been implicated as an influential factor. Serum lactate levels, a metabolite biomarker, are currently used to evaluate metabolism in patients with sepsis. Although lactate is clinically useful in many patients, overreliance on this single metabolite obfuscates the many disturbed metabolic pathways that likely influence the progression of sepsis-induced organ dysfunction. The carnitine pool represents a family of metabolites that are well-established markers of disturbed mitochondrial fatty acid oxidation. Recently, our group and others have identified elevations in acetyl-L-carnitine (C2) as the acylcarnitine with the most robust associations with sepsis-induced organ dysfunction, mortality, infection, and inflammation. The focus of the dissertation was to establish connections between C2 and various markers of mitochondrial dysfunction to mechanistically credential C2 as a candidate biomarker by expanding the metabolic interpretation of the signal in sepsis.

Developing multiple linear regression models with stepwise forward-backward variable selection, I identified metabolite signatures that were significantly associated with platelet derived mitochondrial oxygen consumption rates. One of the models included a negative association between whole blood C2 concentrations and baseline mitochondrial oxygen consumption rate, indicating that elevated C2 in the blood could represent lower mitochondrial function.

Leveraging serum baseline concentration data from patients with septic shock, I identified a relationship between mortality and measurements of C2 and individual intermediates of the tricarboxylic acid (TCA) cycle, a key step in energy production via oxidative phosphorylation. I used multiple linear regression models to determine that septic shock non-survivors at 28-days and 1-year had a stronger relationship between C2 and malate, when compared to survivors.

I also employed a mouse model of sepsis in conjunction with data from human sepsis and septic shock cohorts to characterize the tandem progression of sepsis-induced organ dysfunction and metabolic disturbances that present throughout sepsis. In the sepsis mouse model, I observed whole blood measurements of L-carnitine (LC) and the C2/LC ratio were decreased and increased, respectively, in the septic animals compared to the controls. This finding suggests that measuring carnitine metabolism has diagnostic value as an early predictor of sepsis. Analysis of the human cohorts revealed perturbations in the carnitine pool (LC, C2, C2/LC) were present and positively associated with various assessments of organ dysfunction. I also discovered perturbed metabolic pathways in the kidneys and livers of the septic animals that precede widespread, clinically detectable organ dysfunction and damage. Many of these organ metabolite signatures were correlated to changes in the whole blood C2/LC ratio, suggesting the whole blood C2/LC ratio reflects a broad range of metabolic abnormalities at the organ level. Additionally, several of the sepsis-induced organ metabolic disturbances in the animals were detected and associated with organ dysfunction in the human cohorts, including histidine, malate, alanine, glutamate, aspartate, lactate, and glutamine. These findings provide a mechanistic link between the metabolic response with the onset and progression of sepsis-induced organ dysfunction.

Overall, various markers of mitochondrial metabolic dysfunction were found to have profound connections to blood measurements of C2. This work provided evidence to support the use of C2 as a candidate biomarker for the comprehensive assessment of metabolism in patients with sepsis.

Chapter 1 Introduction

1.1 L-Carnitine and Acylcarnitines: Mitochondrial Biomarkers for Precision Medicine

1.1.1 Introduction

Mitochondria are widely investigated targets across different fields of biomarker discovery due to their expansive regulatory functions, which produce a vast range of molecules in response to disease and/or cellular dysfunction (1-6). Many metabolites are closely tied to components of mitochondrial function, but herein L-carnitine (LC) and the acylcarnitines (ACs) will be discussed for their untapped potential to serve as biomarkers for illness and drug response, including adverse drug reactions (ADRs).

The carnitine pool, comprised of LC and the acylated derivatives (ACs), is recognized for facilitating fatty acid β-oxidation (FAO) in mitochondria and peroxisomes (7, 8). The carnitine pool represents a group of mitochondrial derived metabolites, the blood concentrations of which generally reflect disorders of long-chain FAO, also known as the inborn errors of metabolism (9-11). The Health Resources & Services Administration of the U.S. Department of Health and Human Services recommends that neonatal screening includes tests for inborn errors of metabolism such as LC uptake or transport defects, medium-chain acyl-CoA dehydrogenase deficiency, long-chain L-3 hydroxyacyl-CoA dehydrogenase deficiency, very long-chain acyl-CoA deficiency, and trifunctional protein deficiency (12). LC and AC levels are not routinely measured outside of this neonatal screening. Consequently, the utility of LC and ACs as metabolic biomarkers has predominately centered around the implications of this screening and

the significant clinical impact of found defects, which have been extensively reviewed elsewhere (13, 14).

Recent advances in analytical methods coupled with the advancement of the science of metabolomics has brought LC and the acylated esters into the spotlight of biomarker discovery and research. Metabolomics is a systems biology science focusing on endogenous small molecules (<1500 Da) in a single biological sample, and pharmacometabolomics is the specific application regarding the metabolic response to drugs (15-17). Targeted measurements of free LC and the differing chain length ACs in the blood have revealed metabolic perturbations in patients across a variety of diseases and have been linked to drug toxicities. These findings bring new insights into the metabolic mechanisms that underlie certain diseases and ADRs. This knowledge may lead to the discovery of novel drug targets and influence therapeutic decision making.

1.1.2 Carnitine, Acylcarnitines, and Mitochondrial Bioenergetics

Primary Role: The Carnitine Shuttle

Mitochondria produce the majority of the primary energy currency, adenosine triphosphate (ATP), for the body through various oxidation pathways (18). Of note, glycolysis and FAO are complex processes that involve a series of enzymatic reactions and translocation of intermediate products. LC participates in a shuttle system to import long-chain fatty acids into the mitochondria for subsequent FAO, as shown in **Figure 1-1** (7, 9, 19).

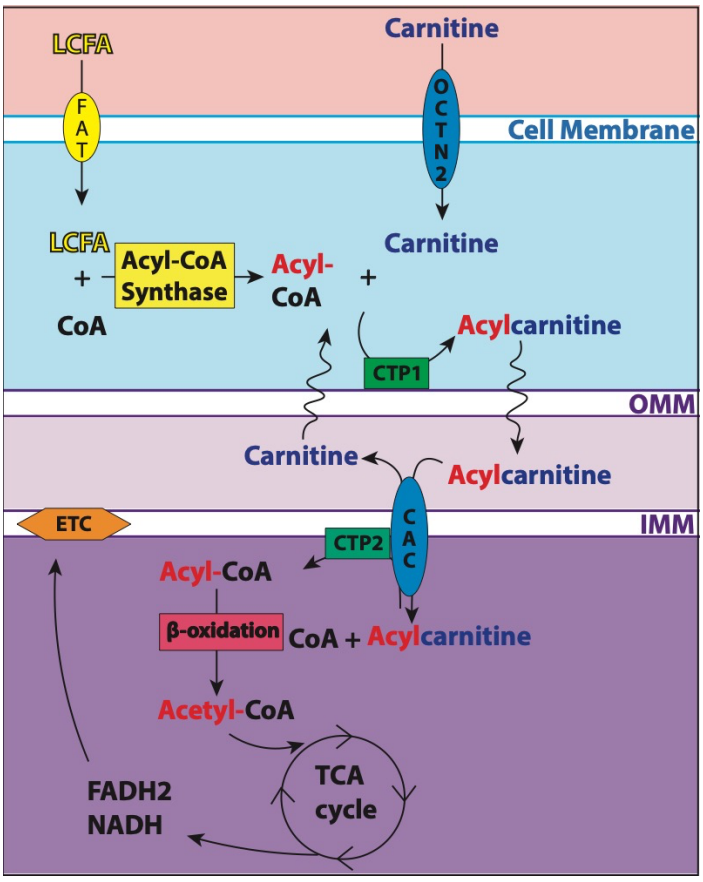

Figure 1-1 The Carnitine Shuttle.
The figure highlights the major components of the carnitine shuttle system that is required to import long-chain fatty acids (LCFA) into the mitochondria for oxidation. LCFA are converted to acyl-CoA via acyl-CoA synthase. Then the enzyme, carnitine palmitoyltransferase 1 (CPT1) produces acylcarnitines from acyl-CoA and free carnitine. Carnitine-acylcarnitine carrier (CAC; SLC25A20 gene) moves acylcarnitine across the inner mitochondrial membrane (IMM) as carnitine is exported out. CPT2 converts the acylcarnitine back into acyl-CoA and free carnitine. Acyl-CoA is then available for β-oxidation that produces 1 molecule of acetyl-CoA per cycle of oxidation, which enters the tricarboxylic acid (TCA) cycle. The cycle provides the necessary electron donors for the electron transport chain (ETC), thus powering oxidative phosphorylation

Endogenous Carnitine Homeostasis

LC is a small, polar molecule *de novo* synthesized from two amino acids, lysine and methionine, but, in humans, is largely acquired by dietary intake of animal products such as red meats, dairy, poultry, and fish (7, 8). The carnitine pool mostly resides in the skeletal muscle, but is also found in the blood, liver, kidney, brain, and heart (7). The plasma and tissues concentrations are heavily conserved, which allows for the detection of small perturbations. The normal plasma levels consists of 83% LC and 17% ACs, with acetylcarnitine (C2) representing

75% of the ACs (7). The compounds are highly regulated through reabsorption (98%) in the renal tubules and distribution in the tissues via the sodium dependent organic cation/carnitine transporter (OCTN) family (7, 8).

Historically, blood concentrations of LC and ACs are reported to distinguish groups within a study. For example, they are often compared between control and experimental arms, reported as changes from baseline, or as a ratio between the summed value of all measured ACs (or individual ACs) to free LC. Since LC is much higher in abundance relative to the ACs, an AC/LC ratio in the blood exceeding 0.4 is thought to represent disturbed mitochondrial metabolism (7). Additionally, ratios of ACs and other metabolites, such as free fatty acids, have also been used to assess different metabolic pathways (20-23).

Due to the tight regulation of the carnitine pool, perturbations in carnitine metabolism can also be identified through a quantitative, targeted analytical approach. Measurement of blood concentrations of specific ACs and LC may reveal the untapped potential of pinpointing disturbed metabolic pathways, which may help elucidate mechanisms that are affected by certain diseases and drugs.

Metabolic Pathways of Acylcarnitine Production

The total body carnitine pool is comprised of LC, short-chain (C2-C5), medium-chain (C6-C12), and long-chain (C14-C20) ACs (7, 24). The conventional abbreviation for ACs is shown as C followed by the chain length number, the number of saturated bonds after the colon, DC indicates a dicarboxylic acid, and an OH represents a hydroxyl group (e.g., C16:1-OH, 16 carbons with 1 double bond and a hydroxyl attached to the acyl group).

Notably, the short-chain ACs are derived from alternative energy sources, the branched chain amino acids (BCAAs; leucine, isoleucine, and valine) (25). During times of protein

catabolism, the BCAAs concentrations can increase, prompting utilization of LC. Specifically, propionylcarnitine (C3), C4-dicarboxylcarnitine (C4-DC), isovalerylcarnitine (C5) are produced during increased metabolism of leucine, isoleucine, and valine (25-27). Peroxisomes have also been implicated in the production of varying chain length ACs including C2, C3, C6, and C8 (10, 28-31). The peroxisomes oxidize very-long chain fatty acids (>C22) and branched chain fatty acids that are incompatible with mitochondrial enzymes (32). Peroxisomes utilize the carnitine shuttle to transport the end-products (acetyl-CoA, propionyl-CoA, and medium-chain acyl-CoA) into the mitochondria for complete oxidation via the TCA cycle (7, 33). Peroxisomal β-oxidation is mostly involved with fatty acid biosynthesis, whereas, mitochondrial β-oxidation is directed toward energy production (32). Due to this functional distinction, mitochondrial β-oxidation likely produces the majority of the medium- and long-chain ACs measured in the plasma (27, 32, 34, 35). Medium- and long-chain ACs are produced when fatty acid supply exceeds demand and/or the capacity of mitochondrial β-oxidation and the TCA cycle enzymes (23).

Ultimately, the mitochondria remain the primary machinery that regulate the oxidation pathways of fatty acids, glucose, and BCAAs. Incomplete fatty acid oxidation, and disruptions to glycolysis and BCAA metabolism can be assessed by measuring blood concentrations of LC and various ACs. Targeted measurements of the carnitine pool may unveil mechanistic insights that open new avenues of translational research, allowing clinicians to connect disturbances in mitochondrial metabolism to clinical phenotypes and outcomes.

1.1.3 Disease-induced Alterations to Carnitine Metabolism

Disruption in mitochondrial metabolic function is attributable to a number of diseases. This has raised interest in the measurement of blood levels of LC and ACs to further understand how changes in mitochondrial macronutrient metabolism inform disease manifestation,

progression, and severity. Herein we address recent findings that demonstrate how disrupted carnitine metabolism informs the phenotypes of several major diseases, potentially elucidating mechanistic pathways that could provide pharmacodynamic targets.

Diabetes Mellitus

Patients with diabetes have underlying disruptions in carbohydrate and lipid metabolism that present as elevated blood glucose levels due to impaired insulin sensitivity or production (35). The metabolic interplay between insulin-dependent glucose metabolism and FAO are major areas of interest in diabetes research. The pathogenesis of insulin resistance and diabetes have been linked to intramitochondrial disturbances, specifically involving incomplete or reduced FAO and lipotoxicity (27, 36). Prevailing theories suggest incomplete FAO causes lipids (long-chain ACs, acyl-CoA, ceramide, diacylglycerol) to accumulate in the cytosol leading to disruption and inhibition of insulin signaling (27, 35, 37). It remains unclear whether the short-chain ACs reflect or inflict insulin resistance in diabetic patients (27). However, it is clear that C2 is involved with the regulation of metabolic flexibility, since LC utilization and C2 production are important for maintaining glucose homeostasis (23). Unchecked lipid oxidation can stifle the response to insulin and hinder the switch from lipid to glucose metabolism following a carbohydrate meal, which is likely amplified in patients with impaired insulin sensitivity. The associated increase in C2 production helps regulate this transition by reducing acetyl-CoA concentrations, thus allowing glucose oxidation to progress. Then, increases in malonyl-CoA concentrations ultimately suppress FAO through CPT1 inhibition, completing the switch from fat to glucose oxidation.

Numerous studies have reported disruptions in the carnitine pool with differential impact on levels of long- and short-chain ACs (27, 36). Type II diabetes (T2D) patients with

complications (e.g., retinopathy, hyperlipidemia, neuropathy) had 25% lower serum LC levels than diabetic patients without complications (38). Impaired insulin-dependent uptake of LC is a possible explanation, however, increased production of other ACs may also reduce the levels of LC in diabetic patients (27). The results of this study also highlight how measurement and interpretation of specific ACs profiles can inform of specific disruptions in metabolism. For example, positive correlations between hemoglobin A1c (HbA1c), a clinical parameter of glucose control, with plasma C2 and various short- and medium-chain ACs have been reported in T2D (22, 39). A positive relationship between C2 and HbA1c suggests that patients with worse glucose control (higher HbA1) are unable to maintain glucose homeostasis despite implementation of the C2 salvage pathway. The relationship between HbA1c with the short- and medium- chain ACs indicates a global metabolic dysfunction disrupting glucose, BCAA, and fatty acid metabolism. Plasma LC, BCAA-derived short-chain (C3, C4, C4-DC, C5), and medium-chain (C6, C8, C10:1), and long-chain (C14:1, C16, C18, C18:1) ACs were all significantly increased in T2D patients compared to lean, non-diabetic individuals after an overnight fast (22). The widespread disruption to the whole carnitine pool after an overnight fast emphasizes the inability of T2D patients to switch between fuel sources compared to healthy individuals. Another study that compared insulin resistant obese subjects and healthy lean subjects showed significantly increased concentrations of C3, C5, C6, and C8:1 in the insulin resistant group (40). The disruption in short-chain ACs suggests diabetes and insulin resistance also impacts metabolism of BCAAs, which is a growing area of study in diabetes research (41).

Patients with insulin resistance and diabetes often present with perturbed long-chain ACs. The most plausible mechanism that contributes to this is intracellular inhibition/disruption of long-chain fatty acids on insulin signaling (27, 35). A prospective study published by the

American Diabetes Association found that plasma levels of long-chain ACs were the most predictive of the ACs for the development of T2D (36). Patients with gestational diabetes and newly diagnosed T2D had increased levels of serum medium-chain ACs with fewer differences in long-chain ACs levels (42). The authors speculated that this finding indicates mitochondrial dysfunction is minimal in the early stages of T2D. Moreover, patients in the early stages of diabetes development are able to complete more cycles of FAO leading to medium-chain AC production, compared to long-term diabetic patients who succumb to FAO dysfunction (fewer cycles), and as a result produce more long-chain ACs.

These examples illustrate that measurements of LC and its derivatives can inform about the different components of mitochondrial metabolic function in diabetic patients. Associations between HbA1c and increased C2 or other ACs are indicative of global metabolic dysfunction that extends beyond hyperglycemia. Long-chain ACs seem to be the most predictive of the development of T2D, however, the medium-chain esters may also be helpful in identifying early or transient diabetes in patients. Different scenarios of LC and AC concentrations likely reflect distinct metabolic dysfunction in this population, which opens the door for new targeted therapeutic interventions or prognostic tests. Interestingly, there are a growing number of studies that show supplementation with LC improves glucose homeostasis through stimulation of the C2 salvage pathway that invokes metabolic flexibility (23, 43, 44). Albeit larger studies are necessary to validate and strengthen the biomarker potential and the therapeutic benefits of targeting these pathways before translation into clinical practice is attainable.

Cancer

Reprogrammed metabolism, a hallmark characteristic of cancer, provides the necessary conditions for growth in substrate dependent environments (45). The Warburg effect, which

favors glycolysis, leads to an upregulation in the compensatory pathways to fuel the TCA cycle, specifically, increased oxidation of BCAAs and fatty acids (46). Considering these adaptations, the carnitine pool is uniquely positioned to reflect the changes that occur during cancer development and progression. Targeted measurement of LC and ACs may afford new opportunities in cancer diagnosis, prognosis, and even new pharmacological targets. Herein we discuss the forms of cancer for which there is evidence of disrupted carnitine metabolism.

Hepatocellular carcinoma (HCC) is primarily caused by chronic inflammation and liver damage stemming from various insults such as hepatitis B, hepatitis C, and nonalcoholic fatty liver disease (NAFLD) (47). The liver is a major regulator of energy metabolism and the primary location of LC biosynthesis (47, 48). In cases of severe liver damage, such as HCC, there are reports of impaired FAO leading to elevated ACs in the blood (47, 49). Several studies have reported similar findings about the ability of serum concentrations of LC, short-chain, medium-chain, and long-chain ACs to differentiate patients with HCC from those with liver disease or healthy controls. The authors observed increased LC, decreased short- and medium-chain ACs, and increased long-chain ACs (49-52). Differences in the AC response to disease can inform the metabolic landscape without the need for an invasive measurement such as a liver biopsy. The distinct pattern of decreased short- and medium-chain esters with increased long-chain ACs indicates the disruption is likely early in FAO. The increase in LC could represent a number of metabolic impairments such as a reduced uptake of LC or cell death leading to an intracellular LC contribution to the blood level. Based on the available studies, measured carnitines may offer a diagnostic tool to distinguish HCC patients from healthy subjects or those with other liver diseases.

Irregularities in AC concentrations have been identified in other cancers as well. A metabolomics analysis conducted using the plasma of breast cancer patients with matched controls found an association between C2 and the risk of breast cancer (53). It logically follows that cancer presenting in different tissues would have differing effects on carnitine metabolism. The signal in breast cancer patients pointing to C2 as the lone AC suggests the malignant tissue invokes the metabolic flexibility pathway as it switches between glucose and fat utilization. Another metabolomics study aimed to discriminate colorectal adenoma, colorectal cancer, and healthy subjects (54). The authors found that serum ACs spanning the whole spectrum from short-chain to long-chain as consistently differentiated between the patient groups. The findings suggest that ACs may have value as early detection biomarkers of colorectal adenoma and colorectal cancer. Yet another metabolomics analysis in serum concluded differences in carnitine metabolism between papillary thyroid cancer and benign nodules (55). Yao et al observed increased serum concentrations of medium- and long-chain ACs in the cancer cohort compared to the benign group. In line with previous conclusions, the increase in medium- and long-chain ACs suggests that patients are in an early to mid-stage of cancer development. This type of inferencing, if further studied and properly validated, could add new criteria to the staging of cancers, which could significantly influence therapeutic decision making.

The prolific metabolic switching observed in various cancers emphasizes the crucial role metabolic flexibility plays in this disease, which is reflected in the blood LC and AC profile (56). The diversity of cancer is vast, manifesting in different tissues through various mechanisms, yet current evidence suggests that differential concentrations of ACs may have diagnostic value for certain forms. By measuring the carnitine pool, clinicians and researchers can identify pathways that are exploited by cancer cells, which could lead to new biomarkers or druggable targets.

Heart Failure

Due to the advancements in cardiovascular treatments and increased life span of the aging population, a paradoxical increase in patients with heart failure is occurring (57, 58). In these patients, dysfunctional myocardial tissue has known energy disruptions and shortcomings that include decreased ATP and phosphocreatine, as well as, abnormalities in FAO (57). Considering this disruption, the carnitine profile represents measurable metabolites in the blood that directly reflect the metabolic derangement present in the failing heart (59). Additionally, the healthy heart primarily uses FAO for energy, but showcases metabolic flexibility by utilizing glucose, lactate, ketone bodies, and amino acids, further supporting the utility of the carnitine pool in understanding the metabolic consequences of heart failure.

A recently published study reported that plasma long-chain ACs were significantly elevated in patients with heart failure compared to controls (60). Furthermore, the elevated AC signal (C16, C18:2, C18:1, C16:1-OH/C14:1-DC, C20:4) increased linearly with decreasing left ventricular ejection fraction, which is a defining clinical characteristic of heart failure. The signal enabled the authors to distinguish between the two heart failure phenotypes since the long-chain ACs were higher in those with reduced ejection fraction (HFrEF) compared to the subjects with preserved ejection fractions (HFpEF). The phenotypic distinction suggests the ACs have potential utility in supporting the current heart failure classification as an objective measure of heart failure staging but would need further replication and validation. A more clinically guided study by Ahmed et al identified several groups of plasma ACs that were associated with defined clinical outcomes (61). Groups of mostly medium- and long-chain ACs were found to be associated with all-cause mortality or all-cause hospitalization, when adjusted for known predictors of each outcome. However, only the long-chain AC group (C16, C18:2, C18:1, C18,

C20:4) was associated with lower peak VO_2 (a negative clinical characteristic of heart failure), cardiovascular death/hospitalization, and heart failure exacerbation. Furthermore, the individual levels of C16, C18:1, and C18:2 were significantly higher in patients with end-stage heart failure prior to left ventricular assist device implantation and decreased with improved circulatory support. The findings of this study suggest long-chain ACs have clinical utility in assessing disease severity in the heart failure population. After validation in larger cohorts, clinicians could eventually personalize therapy based on a given patient's AC profile. A metabolomic analysis conducted by Ruiz et al found that plasma LC and numerous ACs differentiated between a healthy control group and patients with heart failure (62). The heart failure patients had higher levels of LC and various chain-length ACs (C2, C4, C6, C8, C10, C12, C14, C16, C18, C18:1, C18:2) than in the control group, when adjusted for sex, age, renal function, and insulin resistance. Additionally, C2 and the medium-chain ACs were positively associated with NT-ProBNP, a clinical marker of disease severity, suggesting that the increase in metabolite concentrations were indicative of worsening disease. Interestingly, the researchers stratified the heart failure group by diabetes status and found C2 to be increased in the diabetic subgroup. The full range of ACs reflect the widespread disruption to FAO, as well as BCAA and glucose oxidation that occurs in heart failure. However, the C2 distinction by diabetes status likely reflects that patients with heart failure have more disruptions in FAO than glucose metabolism. This is further supported by other studies predominantly showing the long-chain ACs as the differentiating ACs in heart failure.

Of all the ACs, the long-chain ACs seem to be the most associated with heart failure clinical outcomes. They also may play a physiological role in exacerbating the disease progression. The known biological effects of long-chain ACs suggest a possible mechanism of

inflicting cellular damage through promoting skeletal muscle inflammation, reactive oxygen species (ROS) production, cellular stress, and insulin resistance (60). More research in this area is warranted to strengthen the prognostic usefulness of long-chain ACs and to further elucidate the perturbed mitochondrial pathways as potential therapeutic targets.

Sepsis and Septic Shock

Despite the United States spending over an estimated $41 billion on sepsis care, it continues to be a leading cause of mortality with rates rising above 40% in those identified with septic shock (63, 64). In 2016, characterization of the syndrome was reevaluated to develop a consensus definition that more accurately reflected the advancements in our pathobiological understanding (64). Broadly, sepsis is "a life-threatening organ dysfunction caused by a dysregulated host response to an infection" (64). Septic shock is the more severe form that includes persistent hypotension and elevated lactate concentrations (64). Sepsis is acknowledged to be a syndrome rather than a specific illness due to the limited comprehension of the pathobiology, interpatient heterogeneity, and lack of a gold standard diagnostic test (64). The last 30 decades of research have uncovered more biological pathways (cardiovascular, hormonal, neuronal, metabolic, bioenergetic) are perturbed by sepsis than simply the immune response, as previously thought (64). The metabolic component is increasingly recognized as one of the potential causes of sepsis-induced organ dysfunction, a driving factor of mortality rates in this population (15, 65-67). Maintaining normal carnitine homeostasis is vital for mounting an immune response, especially in the case of a severe infection such as sepsis (68). The connection between the carnitine pool and sepsis via the immune system and metabolism makes targeted analysis of these compounds a valuable pursuit.

Several studies have observed a range of sepsis-induced disruptions in carnitine metabolism between survivors and non-survivors of sepsis and septic shock (69-73). A comprehensive study by Langley et al found the short- and medium-chain AC plasma profiles to be the most pronounced between sepsis survivors and non-survivors at 28 days (69). The ACs (C2, C5, C6, C8, C10) were significantly increased in the non-survivors even after adjusting for renal function. Absence of the long-chain ACs from these findings point to a similar conclusion found in some of the diabetes studies. Increased short- and medium-chain esters may reflect newly developed FAO dysfunction, meaning that β-oxidation cycles successfully shortened the long-chain fatty acids before eventual disruption. These findings were further corroborated by another study that reported disruptions in the short- and medium-chain plasma AC profiles of sepsis patients (70). The authors noted increased levels of various short- and medium-chain ACs were associated with markers of hepatic and renal function and infection/inflammation. However, only C2 was associated with all of these indices and 28-day mortality. The distinction separating C2 from the other ACs in this study poses an interesting hypothesis. The higher plasma C2 levels in the non-survivors compared to the survivors might be due to the unsuccessful switch between nutrient sources leading to the overproduction of C2 in an attempt to achieve metabolic flexibility. The ability or inability to switch between fuel sources during the high metabolic demands of sepsis could influence the immune response to the infection, organ dysfunction, and ultimately, survival. Puskarich et al. found distinct LC and AC serum profiles in septic shock patients between 28-day survivors and non-survivors at baseline and following supplementation with intravenous LC (71). This finding suggests that increased concentrations of LC, C2, C3, and C8 at baseline are predictive for sepsis mortality. This conclusion also corroborates the findings of the previously mentioned sepsis studies that showed sepsis-induced

perturbations in the short- and medium-chain ACs. Interestingly, the researchers also hypothesized that the use of LC supplementation provoked a latent phenotype in the metabolome, including the carnitine pool, that informed the response to the therapeutic intervention (17). Furthermore, a pharmacometabolomics analysis of a clinical trial using intravenous LC in patients with septic shock reports that baseline C2 concentrations are predictive of a mortality benefit from the treatment (74).

Indeed, the carnitine pool profile is informative of the metabolic derangement that presents during sepsis. The short- and medium- chain ACs appear to be the more prominently disturbed esters in this disease state. The presence of the short-chain ACs could indicate greater oxidation of the BCAA, whereas the medium-chain compounds may reflect disturbed peroxisomal FAO or partially impaired mitochondrial FAO. Regardless, targeted measurements of the carnitine pool offer insights into the metabolic derangement of sepsis that provide opportunities to develop new pharmacologic interventions and prognostic biomarkers.

1.2 Sepsis is a Metabolic Syndrome

1.2.1 Metabolic Derangement

The development of sepsis presents with a global metabolic derangement that encompasses a wide range of metabolic pathways. Metabolomics approaches can be used to identify specific targeted sets of metabolites like the carnitine pool or using an untargeted platform capturing a broad range of compounds (15). Researchers can use either approach to discern metabolic signatures that can yield patient phenotypes that may be useful for prognosis and diagnosis. Numerous studies on patients with sepsis have found metabolite signals in various biospecimens that are differentiating between survivors and non-survivors, sepsis and healthy controls, and early vs late onset sepsis in neonates (17, 69-72, 75). After the differentiating

metabolites are identified, the directionality of the concentrations and the metabolic pathways involved aid in the interpretation of the results. Metabolic pathways such as amino acid metabolism, mitochondrial FAO, TCA cycle, and the pentose phosphate pathway have all been shown to be perturbed in patients with sepsis (15). Associations between sepsis-induced organ dysfunction and various metabolite groups, such as the carnitine pool and amino acid metabolites, have been reported (70, 76). Establishing connections between the disturbed metabolic pathways and clinically relevant outcomes is critical to facilitate the translation of metabolites to validated biomarkers. Viewing sepsis from a metabolic perspective affords the opportunity for early identification of prognostic phenotypes and sheds light on metabolic mechanisms that could serve as potential drug targets for new therapies.

1.2.2 Metabolic Pathobiology of Sepsis-induced Organ Dysfunction

The full extent of the mechanisms leading to sepsis-induced organ dysfunction are incompletely understood. However, the past few decades of research have shed light on the complex interplay between the initial infectious insult and the metabolic consequences that follow. Broadly, the early pro-inflammatory response coincides with a hierarchical reallocation of energy consumption through a preferential use of glycolysis over oxidative phosphorylation and the downregulation of non-essential cellular pathways (77-79). This metabolic restructuring is thought to be an adaptive response to limit or prevent apoptotic tissue damage from occurring due to an uncontrolled energy imbalance (79). As a result, the downregulation of oxidative phosphorylation and high energy non-essential pathways is at least partially responsible for the early reduced organ function observed in sepsis (77). The inability to switch from the initial pro-inflammatory/glycolytic response to the anti-inflammatory/oxidative phosphorylation phase has been associated with chronic inflammation and perturbed organ recovery (80). In fact, the failure

to restore homeostatic metabolic processes has been linked to the development of persistent inflammation, immunosuppression, and catabolism syndrome (81).

The mitochondria facilitate many of the metabolic processes that are disturbed during sepsis progression (66). An estimated 98% of the total body oxygen consumption occurs within the mitochondria which is consumed during the production of ATP via oxidative phosphorylation (66). Apart from their role as the powerhouse of the cell, they are also involved in the production of reactive oxygen species, intracellular calcium regulation, thermoregulation, apoptosis, and hormone production (66). Due to the diversity of biological roles, mitochondrial function is a broadly used term that can be assessed by measuring different metrics such as oxygen consumption rate, mitochondrial membrane potential, and mitochondria-linked metabolite concentrations (15, 82, 83). The presence of mitochondrial dysfunction in sepsis has been widely characterized in clinical and preclinical studies(15, 64-66, 84). The organelles and their DNA are also recognized as Damage-Associated Molecular Patterns that further instigate the inflammatory response (78). Overall, mitochondrial dysfunction has been implicated as one of the potential causes of sepsis-induced organ dysfunction (66, 67).

Due to the critical role of oxygen in the production of ATP, inadequate oxygenation of tissues was believed to be the main connection between mitochondrial dysfunction and sepsis-induced organ dysfunction or failure (67). The hypothesis is derived from the known impact of systemic inflammation on the cardiovascular system (66). The reported cardiovascular dysfunction is heavily influenced by mitochondrial pathways such as oxidative stress, abnormal calcium handling, and down regulation of mitochondrial genes (78). Other irregularities like coronary microvascular changes, increased vascular permeability, nitrosative stress, and disrupted tissue microcirculatory also contribute to organ hypoperfusion and tissue hypoxia (78).

This framework has since been undermined by the reports of minimal cell death in the organs from sepsis patients, coupled with the observations of increased oxygen tensions in both human sepsis and animal models of sepsis (66, 85, 86). Tissue hypoxia may occur in some areas, but it is not the sole driver of sepsis-induced organ dysfunction due to the paradoxical lack of cell death observed in affected organs.

1.2.3 Acetyl-L-carnitine as a Sepsis Biomarker

Lactate is currently the gold standard metabolite biomarker that guides treatment regimens and presides in the Sepsis-3 definition of septic shock (64). While it is well supported as a prognostic biomarker for mortality and organ failure, the mechanistic understanding is misattributed to anaerobic glycolysis due to tissue hypoxia (78, 86). Lactate production does occur during anaerobic metabolism; however, it can also be generated from liver dysfunction, drug inhibited metabolism, and adrenergic stimulated aerobic glycolysis (78, 87). Lactate serves as an important metabolic intermediate that is used to generate glucose through gluconeogenesis and contribute to oxidative phosphorylation through a conversion to pyruvate (86). The role as a fuel source is particularly important during a high energy demand condition like sepsis. Organ specific lactate studies are sparce but there is evidence to suggest that the splanchnic bed consumes lactate when the muscles are hypoxic, the brain and heart consume lactate under duress, the kidneys convert it to glucose, and both the lungs and skeletal muscle generate lactate (86, 88). Garcia-Alvarez et al suggest that elevated lactate levels in sepsis are not a reliable marker of tissue hypoxia and more likely evident of a stress induced metabolic adaptation that uses accelerated glycolysis to increase lactate stores as an alternative fuel source (86). From a clinical perspective, lactate has limited use as a biomarker beyond the first 8 hours of treatment and in cases of septic shock (89). Additionally, researchers found that 47% of subjects enrolled

in a multinational study of patients with sepsis had normal serum lactate levels (<2 mmol/L) during their first day in the ICU, yet mortality rates in this group remained high at 17% (87). Overall, lactate levels are a useful biomarker in sepsis, but far from perfect, leaving room for new biomarkers to help fill the gaps.

Adopting the aerobic glycolytic interpretation, increased lactate levels in sepsis may only serve to capture a small piece of the full metabolic derangement of sepsis. As previously mentioned, carnitine and the acylcarnitines are known markers of mitochondrial dysfunction that are primarily produced via mitochondrial FAO (7). Numerous reports have shown impaired carnitine metabolism in patients with sepsis and septic shock, with C2 as the most consistently associated with mortality, organ failure, and inflammation (69-73). Measurements of the carnitine pool may offer a more direct insight into sepsis-associated mitochondrial dysfunction than lactate. Since the carnitine pool indicates impaired mitochondrial FAO, it helps represent the metabolic blind spot that is not reflected in the glycolytic lactate signal.

However, the sepsis-induced metabolic mechanisms leading to the production of C2 are not specifically characterized. The production of C2 can occur at the end of mitochondrial FAO but has the unique capability to act as an acetyl- group sink through conversion of acetyl-CoA via carnitine acetyltransferase (CAT) when acetyl-CoA accumulates beyond the ability of the TCA cycle to utilize it (90). The main role of carnitine-acylcarnitine carrier (CAC; SLC25A20 gene) is to transport acylcarnitine molecules into the mitochondrial matrix (see **Figure 1-1**) but it can also move ACs in the opposite direction. Since CAC can transport ACs out of the mitochondria, blood concentrations of C2 reflect intracellular levels as well as the regulation of acetyl-CoA and free CoA (7, 10, 27). Increased production of C2 represents a critical mechanism for buffering the metabolic status between fed (glucose oxidation) and fasted (fat oxidation)

states, referred to as metabolic flexibility (23, 91). Acetyl-CoA is a known inhibitor of pyruvate dehydrogenase (PDH), a critical enzyme involved in cellular respiration of glucose (7, 90, 92). Conversely, LC has been shown to stimulate PDH in human muscle *in vivo* and *in vitro*, possibly through the reduction of acetyl-CoA (an inhibitor) by converting it to C2, thus supporting metabolic flexibility (93, 94). Acetyl-CoA, through conversion to malonyl-CoA, also has the capacity to block CPT1 from transporting long chain acylcarnitines for mitochondrial FAO (91). In the context of sepsis research, the group identified with negative clinical outcomes typically present with elevated levels of C2 and other acylcarnitines. Increased blood concentrations of C2 suggests that acetyl-CoA accumulation likely occurs, indicating that fat and glucose oxidation pathways may also become inhibited in these patients that are desperate to maintain bioenergetic homeostasis. Furthermore, if the blood concentrations of C2 are indicative of acetyl-CoA accumulation then it suggests that the metabolic pathways generating acetyl-CoA are not the main concern but more so the downstream mitochondrial machinery that are failing to utilize this critical molecule. Therefore, it is imperative to further interrogate the metabolic implications of an elevated C2 by studying the relationship between blood concentrations of C2 with other mitochondrial function measurements including mitochondrial oxygen consumption rate (mOCR), TCA cycle metabolites, and acetyl-CoA.

1.3 Innovation

Herein, the proposed research to further connect the rise in C2 concentrations to downstream mitochondrial pathways will include investigating associations with mOCR, TCA cycle metabolites, and acetyl-CoA. The following list highlights the innovative approach.

Novel mitochondrial function measurement: The gold standard for measuring mitochondrial function *in vivo* requires tissue biopsies (95). I will use platelets from humans with sepsis as a

"circulating organ" surrogate to assess mitochondrial function, which precludes the need for tissue biopsies. This method has been optimized and applied to the sepsis population with success (96, 97).

Mechanistic discovery approach: To my knowledge, the metabolic, organ perturbations that precede the rise in serum C2 levels are unknown. This knowledge gap would be financially and pragmatically difficult to investigate in a human or large animal model of sepsis. With the proposed cecal ligation and puncture (CLP) mouse model of sepsis, I can elucidate sepsis-induced metabolic disruptions in organs over time. I expect these findings to inform the changes in metabolic signals that occur during the development of sepsis-induced multiorgan dysfunction/failure.

Combined measurement of metabolomics and mitochondrial metabolic function: To address the broad scope of mitochondrial function, I will combine two approaches to better inform mitochondrial energy status in sepsis. There is preliminary evidence to support that elevated serum C2 informs sepsis outcomes, but the mechanistic plausibility remains understudied. A multifaceted approach investigating likely causes of elevated C2 in sepsis will provide a more comprehensive understanding of the candidate biomarker.

1.4 Long-term goal, Objective, and Central Hypothesis

The long-term goal is to advance understanding of the metabolic mechanisms that underlie sepsis pathogenesis in order to discover biomarker candidates and drug target opportunities. The overall objective of this proposal is to advance knowledge of the mechanistic relationships between C2 and various mitochondrial function assessments in different models of sepsis. The central hypothesis is that blood C2 concentration is associated with organ acetyl-CoA levels and mitochondrial function measurements. The rationale for the proposed work is that a

metabolic link between organ acetyl-CoA levels, mitochondrial function, and blood C2 concentrations in sepsis could further the utility of C2 as a biomarker of sepsis mortality and identify targets for therapeutics.

1.5 Specific Aims and Rationales

1.5.1 Aim 1

Elucidate the extent of the association between platelet mitochondrial respiration and C2

I hypothesized that whole blood C2 levels from sepsis patients can inform mitochondrial respiration measurements as assessed by linear regression models. Assessing mitochondrial function is vital to understanding metabolic status in sepsis patients as it has been linked to multiorgan failure, a defining characteristic of sepsis severity (66). Measuring mitochondrial oxygen consumption, or respiration, provides a direct approach to quantifying oxidative phosphorylation, a major component of metabolism. This measurement is typically performed on mitochondria from a muscle biopsy, but these samples are not easily obtained, especially from critically ill patients such as those with sepsis. Platelets are uniquely positioned to inform sepsis metabolism because they contain mitochondria as well as influence coagulation, innate immunity, and may play a role in multiorgan dysfunction (98). Accordingly, recent studies have found associations between increased platelet mitochondrial respiration with sepsis mortality and organ failure (96, 97). Increased serum C2 has been associated with the same sepsis clinical parameters (70, 71). To my knowledge, there have not been any studies connecting mitochondrial respiration to C2 levels in the blood collected from sepsis patients. Measured C2 in the blood has the potential to act as an early distress signal of mitochondrial dysfunction in sepsis. The rationale for this aim was that platelets are readily available and can serve as

"surrogate organs" for the assessment of mitochondrial function that may be reflected in the C2 levels from the blood.

1.5.2 Aim 2

Identify the differential associations between C2 and TCA cycle metabolite concentrations in sepsis survivors and non-survivors.

I hypothesized that there will be stronger associations between C2 and individual TCA cycle metabolites in sepsis non-survivors (28-day) compared with sepsis survivors. Characterizing the relationship between C2 and individual TCA cycle metabolites between sepsis survivors and non-survivors will aid in understanding the contribution of a disrupted TCA cycle makes to sepsis-induced elevations in C2 that are linked to mortality. In health (normal physiology), concentrations of TCA cycle metabolites are relatively low and held constant (99). However, under high metabolic stress like in sepsis, TCA cycle metabolite concentrations may increase due to higher energy demand characterized by increased metabolism of carbon sources like lipids, glucose, and amino acids that replenish the cycle intermediates via anaplerotic reactions (99, 100). This is illustrated in a paper by Langley et al, that found increased levels of C2 and various TCA cycle metabolites (oxaloacetate, α-ketoglutarate) in the blood of sepsis non-survivors (69). Based on these findings, we expected that the metabolic perturbations brought on by sepsis will include a disruption of the TCA cycle.

1.5.3 Aim 3

Investigate the temporal relationship between plasma C2 and organ acetyl-CoA concentrations using a mouse model of sepsis.

I used an established CLP mouse model to acquire longitudinal measurements of organ acetyl-CoA and plasma C2. My working hypothesis was that sepsis-induced changes in plasma C2 will reflect organ acetyl-CoA over time. Patients are admitted to the hospital at different time points along the sepsis disease timeline, which increases the variability of an already highly heterogeneous population. Due to this timing, clinicians and researchers likely miss the initial start of sepsis, which could contain crucial metabolic information as patients transition from health to disease as sepsis progresses. Altered metabolic parameters, such as changes in tissue mitochondrial metabolic function and blood levels of C2, have been associated with organ function and mortality in sepsis (66, 70). However, certain questions remain unanswered regarding the origin and timing of C2 production during sepsis. The objective of this aim was to characterize the relationship between concentrations of C2 in the plasma and acetyl-CoA in the major organs over the course of sepsis. Serial tissue biopsies are controversial and impractical to acquire in critically ill patients so I employed a CLP mouse model of sepsis to attain this objective. This model allowed for assessment of whole organ acetyl-CoA with simultaneous measures of plasma C2. Use of our recently developed swine model of sepsis would not be cost effective to achieve this objective because serial sacrificing of animals for whole organ acetyl-CoA measurements is required.

1.6 References

1. Grazioli S, Pugin J. Mitochondrial Damage-Associated Molecular Patterns: From Inflammatory Signaling to Human Diseases. Front Immunol. 2018;9:832.
2. Boyapati RK, Dorward DA, Tamborska A, Kalla R, Ventham NT, Doherty MK, et al. Mitochondrial DNA Is a Pro-Inflammatory Damage-Associated Molecular Pattern Released During Active IBD. Inflamm Bowel Dis. 2018;24(10):2113-22.

3. Wilkins HM, Weidling IW, Ji Y, Swerdlow RH. Mitochondria-Derived Damage-Associated Molecular Patterns in Neurodegeneration. Front Immunol. 2017;8:508.
4. Kraft BD, Chen L, Suliman HB, Piantadosi CA, Welty-Wolf KE. Peripheral Blood Mononuclear Cells Demonstrate Mitochondrial Damage Clearance During Sepsis. Crit Care Med. 2019;47(5):651-8.
5. Khatami F, Payab M, Sarvari M, Gilany K, Larijani B, Arjmand B, et al. Oncometabolites as biomarkers in thyroid cancer: a systematic review. Cancer Manag Res. 2019;11:1829-41.
6. Picca A, Guerra F, Calvani R, Bucci C, Lo Monaco MR, Bentivoglio AR, et al. Mitochondrial Dysfunction and Aging: Insights from the Analysis of Extracellular Vesicles. Int J Mol Sci. 2019;20(4).
7. Reuter SE, Evans AM. Carnitine and acylcarnitines: pharmacokinetic, pharmacological and clinical aspects. Clin Pharmacokinet. 2012;51(9):553-72.
8. Evans AM, Fornasini G. Pharmacokinetics of L-carnitine. Clinical pharmacokinetics. 2003;42(11):941-67.
9. Knottnerus SJG, Bleeker JC, Wüst RCI, Ferdinandusse S, L IJ, Wijburg FA, et al. Disorders of mitochondrial long-chain fatty acid oxidation and the carnitine shuttle. Rev Endocr Metab Disord. 2018;19(1):93-106.
10. Wanders RJA, Ruiter JPN, L IJ, Waterham HR, Houten SM. The enzymology of mitochondrial fatty acid beta-oxidation and its application to follow-up analysis of positive neonatal screening results. J Inherit Metab Dis. 2010;33(5):479-94.
11. Merritt JL, Norris M, Kanungo S. Fatty acid oxidation disorders. Ann Transl Med. 2018;6(24).
12. American College of Medical Genetics. Newborn Screening: Towards a Uniform Screening Panel and System. Genetic Med. 2006;8(5).
13. Almannai M, Alfadhel M, El-Hattab AW. Carnitine Inborn Errors of Metabolism. Molecules. 2019;24(18).
14. Nasser M, Javaheri H, Fedorowicz Z, Noorani Z. Carnitine supplementation for inborn errors of metabolism. Cochrane Database Syst Rev. 2012;2012(2):Cd006659.

15. Eckerle M, Ambroggio L, Puskarich MA, Winston B, Jones AE, Standiford TJ, et al. Metabolomics as a Driver in Advancing Precision Medicine in Sepsis. Pharmacotherapy. 2017;37(9):1023-32.
16. Kaddurah-Daouk R, Weinshilboum RM. Pharmacometabolomics: implications for clinical pharmacology and systems pharmacology. Clin Pharmacol Ther. 2014;95(2):154-67.
17. Puskarich MA, Finkel MA, Karnovsky A, Jones AE, Trexel J, Harris BN, et al. Pharmacometabolomics of l-carnitine treatment response phenotypes in patients with septic shock. Ann Am Thorac Soc. 2015;12(1):46-56.
18. Kohoutova M, Dejmek J, Tuma Z, Kuncova J. Variability of mitochondrial respiration in relation to sepsis-induced multiple organ dysfunction. Physiol Res. 2018;67(Supplementum 4):S577-s92.
19. El-Gharbawy A, Vockley J. Defects of Fatty Acid Oxidation and the Carnitine Shuttle System. Pediatr Clin North Am. 2018;65(2):317-35.
20. Saiki S, Hatano T, Fujimaki M, Ishikawa KI, Mori A, Oji Y, et al. Decreased long-chain acylcarnitines from insufficient beta-oxidation as potential early diagnostic markers for Parkinson's disease. Sci Rep. 2017;7(1):7328.
21. Bogusiewicz A, Horvath TD, Stratton SL, Mock DM, Boysen G. Measurement of acylcarnitine substrate to product ratios specific to biotin-dependent carboxylases offers a combination of indicators of biotin status in humans. J Nutr. 2012;142(9):1621-5.
22. Mihalik SJ, Goodpaster BH, Kelley DE, Chace DH, Vockley J, Toledo FG, et al. Increased levels of plasma acylcarnitines in obesity and type 2 diabetes and identification of a marker of glucolipotoxicity. Obesity (Silver Spring). 2010;18(9):1695-700.
23. Bruls YM, de Ligt M, Lindeboom L, Phielix E, Havekes B, Schaart G, et al. Carnitine supplementation improves metabolic flexibility and skeletal muscle acetylcarnitine formation in volunteers with impaired glucose tolerance: A randomised controlled trial. EBioMedicine. 2019;49:318-30.
24. Dambrova M, Makrecka-Kuka M, Kuka J, Vilskersts R, Nordberg D, Attwood MM, et al. Acylcarnitines: Nomenclature, Biomarkers, Therapeutic Potential, Drug Targets, and Clinical Trials. Pharmacol Rev. 2022;74(3):506-51.
25. Zhang S, Zeng X, Ren M, Mao X, Qiao S. Novel metabolic and physiological functions of branched chain amino acids: a review. J Anim Sci Biotechnol. 2017;8:10.

26. Lake AD, Novak P, Shipkova P, Aranibar N, Robertson DG, Reily MD, et al. Branched chain amino acid metabolism profiles in progressive human nonalcoholic fatty liver disease. Amino Acids. 2015;47(3):603-15.
27. Schooneman MG, Vaz FM, Houten SM, Soeters MR. Acylcarnitines: Reflecting or Inflicting Insulin Resistance? Diabetes. 2013;62(1):1-8.
28. Ramsay RR. The role of the carnitine system in peroxisomal fatty acid oxidation. Am J Med Sci. 1999;318(1):28-35.
29. Jakobs BS, Wanders RJ. Fatty acid beta-oxidation in peroxisomes and mitochondria: the first, unequivocal evidence for the involvement of carnitine in shuttling propionyl-CoA from peroxisomes to mitochondria. Biochem Biophys Res Commun. 1995;213(3):1035-41.
30. Osmundsen H, Bremer J, Pedersen JI. Metabolic aspects of peroxisomal beta-oxidation. Biochim Biophys Acta. 1991;1085(2):141-58.
31. Wanders RJ, Tager JM. Lipid metabolism in peroxisomes in relation to human disease. Mol Aspects Med. 1998;19(2):69-154.
32. Demarquoy J, Le Borgne F. Crosstalk between mitochondria and peroxisomes. World J Biol Chem. 2015;6(4):301-9.
33. Wanders RJ, Waterham HR, Ferdinandusse S. Metabolic Interplay between Peroxisomes and Other Subcellular Organelles Including Mitochondria and the Endoplasmic Reticulum. Front Cell Dev Biol. 2015;3:83.
34. National Center for Biotechnology Information. PubChem Database. Palmitoylcarnitine, CID=461, https://pubchem.ncbi.nlm.nih.gov/compound/Palmitoylcarnitine (accessed on Feb. 19, 2020) [
35. Bene J, Hadzsiev K, Melegh B. Role of carnitine and its derivatives in the development and management of type 2 diabetes. Nutr Diabetes. 2018;8.
36. Sun L, Liang L, Gao X, Zhang H, Yao P, Hu Y, et al. Early Prediction of Developing Type 2 Diabetes by Plasma Acylcarnitines: A Population-Based Study. Diabetes Care. 2016;39(9):1563-70.
37. McCoin CS, Knotts TA, Adams SH. Acylcarnitines—old actors auditioning for new roles in metabolic physiology. Nat Rev Endocrinol. 2015;11(10):617-25.

38. Poorabbas A, Fallah F, Bagdadchi J, Mahdavi R, Aliasgarzadeh A, Asadi Y, et al. Determination of free L-carnitine levels in type II diabetic women with and without complications. Eur J Clin Nutr. 2007;61(7):892-5.
39. Adams SH, Hoppel CL, Lok KH, Zhao L, Wong SW, Minkler PE, et al. Plasma Acylcarnitine Profiles Suggest Incomplete Long-Chain Fatty Acid β-Oxidation and Altered Tricarboxylic Acid Cycle Activity in Type 2 Diabetic African-American Women1–3. J Nutr. 2009;139(6):1073-81.
40. Newgard CB, An J, Bain JR, Muehlbauer MJ, Stevens RD, Lien LF, et al. A Branched-Chain Amino Acid-Related Metabolic Signature that Differentiates Obese and Lean Humans and Contributes to Insulin Resistance. Cell Metab. 2009;9(4):311-26.
41. Bloomgarden Z. Diabetes and branched-chain amino acids: What is the link? J Diabetes. 2018;10(5):350-2.
42. Batchuluun B, Al Rijjal D, Prentice KJ, Eversley JA, Burdett E, Mohan H, et al. Elevated Medium-Chain Acylcarnitines Are Associated With Gestational Diabetes Mellitus and Early Progression to Type 2 Diabetes and Induce Pancreatic beta-Cell Dysfunction. Diabetes. 2018;67(5):885-97.
43. Noland RC, Koves TR, Seiler SE, Lum H, Lust RM, Ilkayeva O, et al. Carnitine insufficiency caused by aging and overnutrition compromises mitochondrial performance and metabolic control. The Journal of biological chemistry. 2009;284(34):22840-52.
44. Muoio DM, Noland RC, Kovalik J-P, Seiler SE, Davies MN, DeBalsi KL, et al. Muscle-specific deletion of carnitine acetyltransferase compromises glucose tolerance and metabolic flexibility. Cell metabolism. 2012;15(5):764-77.
45. DeBerardinis RJ, Chandel NS. Fundamentals of cancer metabolism. Sci Adv. 22016.
46. Vyas S, Zaganjor E, Haigis MC. Mitochondria and Cancer. Cell. 2016;166(3):555-66.
47. Li S, Gao D, Jiang Y. Function, Detection and Alteration of Acylcarnitine Metabolism in Hepatocellular Carcinoma. Metabolites. 2019;9(2).
48. Rui L. Energy metabolism in the liver. Compr Physiol. 2014;4(1):177-97.
49. Enooku K, Nakagawa H, Fujiwara N, Kondo M, Minami T, Hoshida Y, et al. Altered serum acylcarnitine profile is associated with the status of nonalcoholic fatty liver disease (NAFLD) and NAFLD-related hepatocellular carcinoma. Sci Rep. 2019;9(1):10663.

50. Zhou L, Wang Q, Yin P, Xing W, Wu Z, Chen S, et al. Serum metabolomics reveals the deregulation of fatty acids metabolism in hepatocellular carcinoma and chronic liver diseases. Anal Bioanal Chem. 2012;403(1):203-13.
51. Chen S, Kong H, Lu X, Li Y, Yin P, Zeng Z, et al. Pseudotargeted metabolomics method and its application in serum biomarker discovery for hepatocellular carcinoma based on ultra high-performance liquid chromatography/triple quadrupole mass spectrometry. Analytical chemistry. 2013;85(17):8326-33.
52. Zhou L, Ding L, Yin P, Lu X, Wang X, Niu J, et al. Serum metabolic profiling study of hepatocellular carcinoma infected with hepatitis B or hepatitis C virus by using liquid chromatography-mass spectrometry. J Proteome Res. 2012;11(11):5433-42.
53. His M, Viallon V, Dossus L, Gicquiau A, Achaintre D, Scalbert A, et al. Prospective analysis of circulating metabolites and breast cancer in EPIC. BMC Med. 2019;17(1):178.
54. Farshidfar F, Kopciuk KA, Hilsden R, McGregor SE, Mazurak VC, Buie WD, et al. A quantitative multimodal metabolomic assay for colorectal cancer. BMC Cancer. 2018;18(1):26.
55. Yao Z, Yin P, Su D, Peng Z, Zhou L, Ma L, et al. Serum metabolic profiling and features of papillary thyroid carcinoma and nodular goiter. Mol Biosyst. 2011;7(9):2608-14.
56. Smith RL, Soeters MR, Wüst RCI, Houtkooper RH. Metabolic Flexibility as an Adaptation to Energy Resources and Requirements in Health and Disease. Endocrine reviews. 2018;39(4):489-517.
57. Turer AT. Using metabolomics to assess myocardial metabolism and energetics in heart failure. J Mol Cell Cardiol. 2013;55:12-8.
58. Albert CL, Tang WW. Metabolic Biomarkers in Heart Failure. Heart Fail Clin. 2018;14(1):109-18.
59. Murashige DA-O, Jang CA-O, Neinast MA-O, Edwards JA-O, Cowan AA-O, Hyman MA-O, et al. Comprehensive quantification of fuel use by the failing and nonfailing human heart. Science. 2020;370(1095-9203 (Electronic)):364-8.
60. Hunter WG, Kelly JP, McGarrah RW, 3rd, Khouri MG, Craig D, Haynes C, et al. Metabolomic Profiling Identifies Novel Circulating Biomarkers of Mitochondrial Dysfunction Differentially Elevated in Heart Failure With Preserved Versus Reduced Ejection Fraction: Evidence for Shared Metabolic Impairments in Clinical Heart Failure. J Am Heart Assoc. 2016;5(8).

61. Ahmad T, Kelly JP, McGarrah RW, Hellkamp AS, Fiuzat M, Testani JM, et al. Long-Chain Acylcarnitine Metabolites are Associated with Adverse Outcomes and Reversible with Mechanical Circulatory Support in Systolic Heart Failure. J Am Coll Cardiol. 2016;67(3):291-9.
62. Ruiz M, Labarthe F, Fortier A, Bouchard B, Thompson Legault J, Bolduc V, et al. Circulating acylcarnitine profile in human heart failure: a surrogate of fatty acid metabolic dysregulation in mitochondria and beyond. Am J Physiol Heart Circ Physiol. 2017;313(4):H768-h81.
63. Buchman TG, Simpson SQ, Sciarretta KL, Finne KP, Sowers N, Collier M, et al. Sepsis Among Medicare Beneficiaries: 1. The Burdens of Sepsis, 2012-2018. Crit Care Med. 2020;48(3):276-88.
64. Singer M, Deutschman CS, Seymour CW, Shankar-Hari M, Annane D, Bauer M, et al. The Third International Consensus Definitions for Sepsis and Septic Shock (Sepsis-3). JAMA. 2016;315(8):801-10.
65. Carre JE, Singer M. Cellular energetic metabolism in sepsis: the need for a systems approach. Biochim Biophys Acta. 2008;1777(7-8):763-71.
66. Singer M. The role of mitochondrial dysfunction in sepsis-induced multi-organ failure. Virulence. 2014;5(1):66-72.
67. Brealey D, Singer M. Mitochondrial Dysfunction in Sepsis. Curr Infect Dis Rep. 2003;5(5):365-71.
68. Famularo G, De Simone C, Trinchieri V, Mosca L. Carnitines and its congeners: a metabolic pathway to the regulation of immune response and inflammation. Ann N Y Acad Sci. 2004;1033:132-8.
69. Langley RJ, Tsalik EL, van Velkinburgh JC, Glickman SW, Rice BJ, Wang C, et al. An integrated clinico-metabolomic model improves prediction of death in sepsis. Sci Transl Med. 2013;5(195):195ra95.
70. Chung KP, Chen GY, Chuang TY, Huang YT, Chang HT, Chen YF, et al. Increased Plasma Acetylcarnitine in Sepsis Is Associated With Multiple Organ Dysfunction and Mortality: A Multicenter Cohort Study. Crit Care Med. 2019;47(2):210-8.
71. Puskarich MA, Evans CR, Karnovsky A, Das AK, Jones AE, Stringer KA. Septic Shock Nonsurvivors Have Persistently Elevated Acylcarnitines Following Carnitine Supplementation. Shock. 2018;49(4):412-9.

72. Ferrario M, Cambiaghi A, Brunelli L, Giordano S, Caironi P, Guatteri L, et al. Mortality prediction in patients with severe septic shock: a pilot study using a target metabolomics approach. Sci Rep. 2016;6:20391.
73. Rogers AJ, McGeachie M, Baron RM, Gazourian L, Haspel JA, Nakahira K, et al. Metabolomic derangements are associated with mortality in critically ill adult patients. PLoS One. 2014;9(1):e87538.
74. Puskarich MA, Jennaro TS, Gillies CE, Evans CR, Karnovsky A, McHugh CE, et al. Pharmacometabolomics identifies candidate predictor metabolites of an L-carnitine treatment mortality benefit in septic shock. Clin Transl Sci. 2021;14(6):2288-99.
75. Fanos V, Caboni P, Corsello G, Stronati M, Gazzolo D, Noto A, et al. Urinary (1)H-NMR and GC-MS metabolomics predicts early and late onset neonatal sepsis. Early human development. 2014;90 Suppl 1:S78-83.
76. Puskarich MA, McHugh C, Flott TL, Karnovsky A, Jones AE, Stringer KA. Serum Levels of Branched Chain Amino Acids Predict Duration of Cardiovascular Organ Failure in Septic Shock. Shock. 2021;56(1):65-72.
77. Pool R, Gomez H, Kellum JA. Mechanisms of Organ Dysfunction in Sepsis. Crit Care Clin. 2018;34(1):63-80.
78. Arina P, Singer M. Pathophysiology of sepsis. Curr Opin Anaesthesiol. 2021;34(2):77-84.
79. Gómez H, Kellum JA, Ronco C. Metabolic reprogramming and tolerance during sepsis-induced AKI. Nat Rev Nephrol. 2017;13(3):143-51.
80. Han SH, Malaga-Dieguez L, Chinga F, Kang HM, Tao J, Reidy K, et al. Deletion of Lkb1 in Renal Tubular Epithelial Cells Leads to CKD by Altering Metabolism. J Am Soc Nephrol. 2016;27(2):439-53.
81. Singer M. Critical illness and flat batteries. Crit Care. 2017;21(Suppl 3):309.
82. Chacko B, Kramer P, Ravi S, Benavides G, Mitchell T, Dranka B, et al. The Bioenergetic Health Index: a new concept in mitochondrial translational research. Clin Sci (Lond). 2014;127(Pt 6):367-73.
83. Zorova LD, Popkov VA, Plotnikov EY, Silachev DN, Pevzner IB, Jankauskas SS, et al. Mitochondrial membrane potential. Anal Biochem. 2018;552:50-9.

84. Ohtoshi M, Jikko A, Asano M, Uchida K, Ozawa K, Tobe T. Ketogenesis during sepsis in relation to hepatic energy metabolism. Res Exp Med (Berl). 1984;184(4):209-19.
85. Brealey D, Karyampudi S, Jacques TS, Novelli M, Stidwill R, Taylor V, et al. Mitochondrial dysfunction in a long-term rodent model of sepsis and organ failure. Am J Physiol Regul Integr Comp Physiol. 2004;286(3):R491-7.
86. Garcia-Alvarez M, Marik P, Bellomo R. Sepsis-associated hyperlactatemia. Crit Care. 2014;18(5):503.
87. Sauer CM, Gómez J, Botella MR, Ziehr DR, Oldham WM, Gavidia G, et al. Understanding critically ill sepsis patients with normal serum lactate levels: results from U.S. and European ICU cohorts. Sci Rep. 2021;11(1):20076.
88. Levy B. Lactate and shock state: the metabolic view. Curr Opin Crit Care. 2006;12(4):315-21.
89. Bakker J, Postelnicu R, Mukherjee V. Lactate: Where Are We Now? Crit Care Clin. 2020;36(1):115-24.
90. Schroeder MA, Atherton HJ, Dodd MS, Lee P, Cochlin LE, Radda GK, et al. The cycling of acetyl-coenzyme A through acetylcarnitine buffers cardiac substrate supply: a hyperpolarized 13C magnetic resonance study. Circ Cardiovasc Imaging. 2012;5(2):201-9.
91. Muoio DM. Metabolic inflexibility: when mitochondrial indecision leads to metabolic gridlock. Cell. 2014;159(6):1253-62.
92. Hansford RG, Cohen L. Relative importance of pyruvate dehydrogenase interconversion and feed-back inhibition in the effect of fatty acids on pyruvate oxidation by rat heart mitochondria. Arch Biochem Biophys. 1978;191(1):65-81.
93. Arenas J, Huertas R, Campos Y, Diaz AE, Villalon JM, Vilas E. Effects of L-carnitine on the pyruvate dehydrogenase complex and carnitine palmitoyl transferase activities in muscle of endurance athletes. FEBS Lett. 1994;341(1):91-3.
94. McAllister A, Allison SP, Randle PJ. Effects of dichloroacetate on the metabolism of glucose, pyruvate, acetate, 3-hydroxybutyrate and palmitate in rat diaphragm and heart muscle in vitro and on extraction of glucose, lactate, pyruvate and free fatty acids by dog heart in vivo. Biochem J. 1973;134(4):1067-81.
95. Brand M, Nicholls D. Assessing mitochondrial dysfunction in cells. Biochem J. 2011;435(Pt 2):297-312.

96. Puskarich MA, Kline JA, Watts JA, Shirey K, Hosler J, Jones AE. Early alterations in platelet mitochondrial function are associated with survival and organ failure in patients with septic shock. J Crit Care. 2016;31(1):63-7.
97. Sjovall F, Morota S, Hansson MJ, Friberg H, Gnaiger E, Elmer E. Temporal increase of platelet mitochondrial respiration is negatively associated with clinical outcome in patients with sepsis. Crit Care. 2010;14(6):R214.
98. Dewitte A, Lepreux S, Villeneuve J, Rigothier C, Combe C, Ouattara A, et al. Blood platelets and sepsis pathophysiology: A new therapeutic prospect in critically ill patients? Ann Intensive Care. 2017;7.
99. Bar-Or D, Carrick M, Tanner A, 2nd, Lieser MJ, Rael LT, Brody E. Overcoming the Warburg Effect: Is it the key to survival in sepsis? J Crit Care. 2018;43:197-201.
100. Englert JA, Rogers AJ. Metabolism, metabolomics, and nutritional support of patients with sepsis. Clin Chest Med. 2016;37(2):321-31.

Chapter 2 A Multivariate Metabolomics Method for Estimating Platelet Mitochondrial Oxygen Consumption Rates in Patients with Sepsis

2.1 Abstract

Background: Sepsis-induced alterations in mitochondrial function contribute to organ dysfunction and mortality. Measuring mitochondrial function in vital organs is neither feasible nor practical, highlighting the need for non-invasive approaches. Mitochondrial function may be reflected in the concentrations of metabolites found in platelets and whole blood (WB) samples. We proposed to use these as alternates to indirectly estimate platelet mitochondrial oxygen consumption rate (mOCR) in sepsis patients.

Methods: We determined the relationships between platelet mOCR and metabolites in both platelets and WB as measured by quantitative 1H-NMR metabolomics. The associations were identified by building multiple linear regression models with stepwise forward-backward variable selection. We considered the models to be significant with an ANOVA test (p-value $\leq$ 0.05) and a positive predicted-R2.

Results: The differences in adjusted-R2 and ANOVA p-values (platelet adj-R2: 0.836 (0.0003), 0.711 (0.0004) vs WB adj-R2: 0.428 (0.0079)) from the significant models indicate the platelet models were more associated with platelet mOCR.

Conclusions: Our data suggest there are groups of metabolites in WB (leucine, acetylcarnitine) and platelets (creatine, ADP, glucose, taurine) that are associated with platelet mOCR. Thus, WB and platelet metabolites could be used to estimate platelet mOCR.

2.2 Introduction

Sepsis mortality rates range from 25-30%, and the incidence of sepsis is increasing in the aging population. It is of paramount importance to advance clinical approaches for the diagnosis and treatment of the disease (1, 2). The global effects of sepsis impact numerous bodily systems including the cardiovascular, endocrine, and immune, but recently, there has been growing attention paid to the effects of sepsis on metabolism (3, 4). By definition, sepsis is a dysregulated host response to a pathogen that leads to life-threatening organ dysfunction (1). The causative mechanism underlying organ dysfunction is likely multifaceted, but recent reports suggest mitochondrial dysfunction plays a major role (5). Understanding mitochondrial function in sepsis represents an opportunity to develop novel and targeted therapeutics, but the assessment of mitochondrial function in humans is challenging and not always attainable in critically ill patients. As such, new diagnostic approaches to the assessment of mitochondrial dysfunction are needed.

Mitochondrial function is a term that broadly encompasses different aspects such as respiration rates, metabolite synthesis, calcium regulation, and membrane potential (6). Some of these can be measured using isolated platelets, which offers a potential solution to the problem of evaluating mitochondrial function using tissue biopsies in the sepsis population. Altered platelet mitochondrial function has been observed in numerous human disease states including type II diabetes (7), aging (8), asthma (9), and sepsis (10-16). The results of the sepsis studies generally show an increase in mitochondrial activity. Although, this is not a consistent finding, which warrants further study on this topic. Critically, platelet mitochondrial respiration, or mitochondrial oxygen consumption rates (mOCR), has been found to be associated with sepsis clinical parameters such as severity of illness, organ failure, and mortality (11, 12).

Metabolomics, the measurement of small molecules (<1500 Daltons), or metabolites, in a single biological sample, is another effective approach to study the impact of sepsis on mitochondrial function (17). Recently, Chacko et al., showed that the platelet metabolome in healthy subjects is functionally integrated with platelet mOCR (18). These advancements suggest the assessment of metabolites may provide a reliable surrogate measurement of platelet mitochondrial function in a manner more suitable to human clinical trials, thus bridging the translational research gap.

To our knowledge, the evaluation of the relationship between whole blood (WB) metabolomics, platelet metabolomics, and platelet mitochondria bioenergetics has not been previously reported. This work is needed to determine the extent of the association between platelet mOCR and metabolites identified and quantified in isolated platelets and WB. The primary aim of the study was to test the hypothesis that variations in platelet mitochondrial function as measured by mOCR are associated with WB and isolated platelet metabolites in sepsis patients. As a secondary aim, we sought to detect distinct metabolite signatures between whole blood and isolated platelets using quantitative ^{1}H-nuclear magnetic resonance (NMR) metabolomics and correlation analysis. Using multiple linear regression (MLR) models, we identified groups of metabolites in WB (leucine, acetylcarnitine) and platelets (creatine, ADP, glucose, taurine) that are associated with platelet mOCR.

2.3 Materials and Methods

2.3.1 Setting

This was a prospective observational study of patients that were treated with an institutional quantitative resuscitation protocol for sepsis in the emergency department of the University of Mississippi Medical Center; a separate cohort of subjects were enrolled for the purpose of acquiring WB and platelet samples to serve as negative, non-sepsis controls. The

protocol was IRB-approved (IRB#2016-0076) at the University of Mississippi Medical Center. All patients or their legally authorized representative (sepsis patients) provided written informed consent. All methods described apart from the NMR analysis were conducted by the researchers at the University of Mississippi Medical Center.

2.3.2 Participants

The enrollment period took place from 09/2016-9/2018. Enrollment criteria were the following: 1) Suspected or confirmed infection; 2) Any two of four criteria of systemic inflammatory response in ED (19); 3) Age ≥ 18; 4) Lactate ≥ 2.0 mmol/L; 5) Enrollment within 2 hours of initiation of quantitative resuscitation protocol (20). Exclusion criteria were: 1) any primary diagnosis other than sepsis; 2) established Do Not Resuscitate status; 3) transferred from another hospital with sepsis therapy already initiated; 4) cardiopulmonary resuscitation (chest compression or defibrillation) prior to enrollment; 5) patient or legal representative unable to understand and sign informed consent.

Controls patients were eligible if they were admitted to the emergency department and had no medical conditions that required chronic administration of medication expected to affect platelet function (aspirin, PGY12 inhibitors, etc). Unlike the sepsis cohort, these patients were not admitted to the intensive care unit. Controls were attempted to be matched to sepsis patients in a 1:1 fashion by sex, race, and age +/- 10 years. Not all patients enrolled had an eligible control match enrolled. This control group was chosen to represent an acutely ill cohort of the same race, sex, and age as the sepsis cohort so that differences in the group were more likely to be attributed to sepsis rather than general acute illness or differences in baseline demographics known to impact mitochondrial function (21).

2.3.3 Collection of Blood Samples

After discarding a waste of 3-5 mL, three WB samples (12 mL each) were collected by direct venipuncture or from an indwelling line into K2 EDTA-containing Vacutainer tubes (BD 367863; Becton-Dickinson, Franklin Lakes, NJ USA); each tube was inverted 6 to 8 times to ensure distribution of the anti-coagulant. Samples were immediately placed on ice and promptly transported to the laboratory. The blood sample for WB metabolomics was aliquoted into screw-top cryotubes (1mL), flash-frozen in liquid nitrogen and immediately stored (-80°C). An aliquot of WB from each subject was shipped frozen on dry ice to the University of Michigan's NMR Metabolomics Laboratory.

2.3.4 Platelet Isolation for Assessment of Mitochondrial Respiration

Platelet isolation for measurement of mOCR was performed as previously described with minor modifications (12). Briefly, blood (12 mL) was centrifuged (200 x g for 6 min at room temperature). The platelet-rich plasma layer was transferred to another tube and centrifuged (4500 x g for 5 min at 4°C) to pellet the platelets. The nearly cell-free plasma layer was transferred to a new tube, leaving approximately 0.25 mL of plasma in the original tube. This remaining plasma was used to resuspend the platelet pellet to produce ultra-rich plasma. Platelets in the ultra-rich plasma were counted with an automated cell counter (Cellometer AutoM10; Nexcelom Bioscience, Lawrence, MA) and diluted with additional plasma as needed to achieve a concentration of ~200 x 10^6 cells/mL. This cell concentration has previously been shown to be optimal for mitochondrial respiration assessment (11). Measurements were performed in the patient's own plasma instead of buffer media consistent with prior work by our group (12), as mOCR appear to be influenced by factors in the plasma (22).

2.3.5 Sample Extraction for Metabolomics

Platelets were isolated and counted as described above. In preparation for metabolomics assay, resuspended platelets were centrifuged (4500 x g, 5 mins, at 4°C), decanted, and then resuspended in 1 mL of methanol (20°C). Cell lysis was achieved by flash freezing samples in liquid nitrogen for 30s and allowing them to thaw to room temperature before storage at -80°C. Frozen samples were shipped on dry ice to the University of Michigan's NMR Metabolomics Laboratory for analysis, where they were stored at -80°C. Immediately before assay, samples underwent a second freeze-thaw cycle by flash freezing in liquid nitrogen and thawing to room temperature (23). The researchers at the NMR Metabolomics Laboratory were blinded to the experimental arms.

Platelet pellets were on ice for the duration of the extraction. Samples were transferred to 5-mL centrifuge tubes and chloroform was added to each resuspended pellet to create a 1:1 methanol:chloroform solution. An additional 250uL of 1:1 methanol:chloroform was added, then 1mL DI water, followed by a final 500uL addition of DI water. After each solvent addition, samples were vortexed (30s). After the final addition of water, samples were vortexed until they were white and opaque. Samples were chilled in ice-water bath (15 min), then centrifuged (1000 x g, 15 min, at 4°C). After centrifugation, a thin pellet of cellular debris and precipitated protein separated the upper aqueous layer of the extracted sample from the lower chloroform layer. The aqueous supernatant was removed, lyophilized and resuspended in 50mM phosphate buffer in deuterium oxide in preparation for NMR. WB samples were prepared for NMR by methanol:chloroform precipitation as previously described (24).

2.3.6 Platelet Mitochondrial Respiration Measurements

Mitochondrial oxygen consumption was measured using a high-resolution respirometer (Oxygraph O2k; Oroboros Instruments, Innsbruck, Austria) by a technician that was aware of the

experimental groups. The device was calibrated, and the data were acquired in accordance with the manufacturer's instructions as previously reported (12). The platelet concentrations in the chamber were entered into the manufacturer provided software (DatLab 5.2; Oroboros Instruments, Innsbruck, Austria), which allowed for normalization of the results to cell count at the end of the experiment.

As previously described, each mOCR was measured in the following order; Basal, State 4o, maximum (Max) respiration (12). Briefly, unstimulated platelets provided the resting Basal respiration rate of oxidative phosphorylation. Following the baseline measurement, oligomycin (3 µL; 4 µg/ mL from 95% HPLC pure oligomycin A) was added to prevent ATP production by inhibiting ATP synthase (complex V), representing the oxygen consumed by proton leakage across the inner mitochondrial membrane (State 4o). Then, sequential additions (2µL, then 1µL) of carbon cyanide 4-(trifluoromethoxy) phenylhydrazone (FCCP; 20 mM – yellow) were added to measure Max respiration (25). Our Max rate represents the maximum respiration when using an intact cell model such as this, however, it does not represent the same maximum rate as determined when using isolated mitochondria in the presence of excess substrates (6). It is important to note that these measurements included oxygen consumption of the plasma, along with other extra-mitochondrial activity. In order to account for these contributions, rotenone (3 µL) and antimycin A (3 µL) were added at the end of the assay to final concentrations of 0.6 µmol/L and 1.8 mmol/L, respectively, to measure the residual OCR that is independent of mitochondrial oxygen consumption; this value was subtracted from each mOCR measurement. The selected respiration rates have been published in previous studies of platelet mitochondrial function in sepsis patients (11, 12). These mOCR are measured in intact platelets rather than permeabilized cells or isolated mitochondria. This minimizes the cellular disruptions inflicted by

the isolation or permeabilization process, a critical step when using reactive clinical samples such as platelets from sepsis patients. We suspended the platelets in each patient's own plasma to further replicate the in vivo environment. All chemicals for the platelet mitochondrial experiments were purchased from Sigma-Aldrich (St. Louis, MO).

2.3.7 Quantitative 1-D-^{1}H-NMR Metabolomics

At the time of assay, samples were thawed on ice and prepared for NMR analysis as previously described (24). Details of NMR acquisition can be found in the Supplementary Materials (S4.7.1). NMR spectra were acquired at the University of Michigan BioNMR Core Laboratory on a Bruker 18.8 Tesla (800 MHz) NMR spectrometer ascend magnet equipped with a 5mm Triple resonance inverse detection TCI cryoprobe and Bruker NEO console, operated by TopSpin 4.0.7 software. Details of NMR spectra acquisition, the pulse sequence and spectral analysis can be found in the Supplementary Materials (S4.7.1). Resulting metabolomics data were scaled to correct for differences in initial sample volume (for WB samples) or cell count (isolated platelets) before statistical analysis.

2.3.8 Data Analysis

Missing values were imputed using half of the minimum value of each respective metabolite concentration. The data were then normalized by natural-log transformation. Descriptive statistics were used to summarize patient demographic data. All statistical analyses were performed, and all correlation matrices were constructed in RStudio (RStudio Team 2015. RStudio: Integrated Development for R. RStudio, Inc., Boston, MA). The primary associations were done using each mOCR as the dependent (response, y) variable and the natural-log transformed metabolite concentrations as the independent (predictors, x) variables for a MLR

model. Each MLR model was built using the stepwise forward-backward variable selection method when given the respective metabolites. The metabolites were entered or removed from the model based on the default p-values, 0.1 and 0.3, respectively. Adjusted-R^2 shows the goodness-of-fit of the model to the data and predicted-R^2 protects against overfitting the model. The R code for the MLR models is provided in the Supplementary Materials (S4.8.1).

To test significance of the models, ANOVA was used to compare each final model to the full model which included all possible metabolites as predictors. Resulting p-values of ≤ 0.05 were considered significant. MetaboAnalyst 4.0 (https://www.metaboanalyst.ca/) was used to conduct a pathway analysis of the metabolites from the final MLR models (26). Pearson's correlation was utilized to test the associations between the platelet and WB metabolites.

2.4 Results

2.4.1 Patient Demographics

Thirty-one patients with sepsis and 14 control subjects were enrolled. Of the 31 sepsis subjects, 17 had mOCR matched to WB NMR metabolomics, while 14 had completed mOCR matched to platelet NMR metabolomics. Viable metabolomics data were obtained from 9 of the control subjects due to technical errors with the cell counter that precluded adjustment of metabolite concentrations to platelet count. The patient demographics and clinical parameters of the sepsis patients and control subjects are presented in **Table 2-1,** separated by regression analysis group. The sepsis cohort, when grouped by inclusion in WB or platelet regression analyses, were moderately ill sepsis patients with median sequential organ failure assessment (SOFA) scores of 5 (IQR 3, 9), and 4.5 (IQR 3, 8.5), with 28-day mortality rates of 12% and 7%, respectively.

Variable	Sepsis patients		Controls (n=9)
	Whole blood (n=17)	Platelet (n=14)	
Age (IQR)*	59 (52-67)	57 (50-67)	53 (32-56)
Race (%)			
White	8 (47)	8 (57)	2 (22)
African-American	9 (53)	6 (43)	7 (78)
Ethnicity (%)			
Non-Hispanic	17 (100)	14 (100)	9 (100)
Hispanic	0 (0)	0 (0)	0 (0)
Sex (%)			
Male	10 (59)	8 (57)	4 (44)
Female	7 (41)	6 (43)	5 (56)
28-day mortality (%)	2 (12)	1 (7)	0 (0)
BMI kg/m^2 (IQR)*	25.6 (23-34)	26.6 (23-33)	31.5 (24-46)
Preexisting conditions (%)			
Coronary artery disease	2 (12)	2 (14)	0 (0)
End-stage renal disease	2 (12)	2 (14)	0 (0)
Chronic obstructive pulmonary disease	5 (29)	5 (36)	1 (11)
Chronic heart failure	0 (0)	0 (0)	1 (11)
Cirrhosis	1 (6)	0 (0)	0 (0)
Peripheral vascular disease	1 (6)	1 (7)	0 (0)
Cerebrovascular accident	1 (6)	2 (14)	0 (0)
Malignancy	4 (24)	1 (7)	0 (0)
Vital signs (IQR)*			
Heart rate (beats/min)	102 (86-106)	102 (87-107)	85 (77-88)
Systolic blood pressure (mmHg)	110 (104-119)	110 (98-116)	145 (128-149)
Diastolic blood pressure (mmHg)	65 (59-72)	64 (59-68)	84 (81-98)
Baseline laboratory (SD)			
Creatinine (mg/dL)	1.8 (1.3)	1.6 (1.2)	n/a
Platelet count (x1000 cells/mm^3)	205 (148)	182 (100)	n/a
White blood count (x1000 cells/mm^3)	15 (7.8)	15.75 (8.2)	n/a
Disease severity (IQR)*			
SOFA (enrollment)	5 (3-9)	4.5 (3-8.5)	n/a

Lactate mM (enrollment)	1.8 (1.2-2.1)	2 (1.2-2.1)	n/a

Table 2-1 Patient demographics and clinical parameters
* Median (interquartile range); n/a = not applicable

2.4.2 Multiple Linear Regression Models Analysis

The descriptive statistics for Basal, State 4o, and Max respiration rates of the sepsis patients are presented in **Table 2-2**. We identified 31 WB and 19 platelet metabolites in at least 70% of samples (the list and concentrations of detected WB and platelet metabolites used for the analysis can be found in the excel file of the Supplementary Materials (*S2.2.1*); the entire data set can be found at the NIH Metabolomics Workbench: https://www.metabolomicsworkbench.org/ doi: 10.21228/M8FX1M). Additionally, missing values for 12 WB and 13 platelet metabolites were imputed with half of the lowest measured concentration value of each respective metabolite. A representative NMR spectrum of WB and platelet samples can be found in the Supplementary Materials (***Figure S1***).

Statistic	Basal	**State 4o**	**Max**
Median	0.0861	0.0191	0.1141
IQR	0.0626 - 0.1117	0.0060 - 0.0267	0.1010 - 0.1364

Table 2-2 Mitochondrial Oxygen Consumption Descriptive Statistics
IQR= interquartile range; all units are pmol/(sec*106 platelets)

The results of the MLR models relating metabolite concentrations (independent variable) to each mOCR (dependent variable) are presented in **Table 2-3**. Models using platelet metabolites were more highly associated with the platelet mOCR than those from the WB metabolites, as shown by the differences in adjusted-R^2 and the ANOVA results. Predicted-R^2 values followed the same hierarchy between platelet and WB models, but also revealed that the model with State 4o and WB metabolites was overfit, as evidenced by the substantial difference between the adjusted-R^2 and the negative predicted-R^2 (-0.111). Models meeting our criteria of significant ANOVA result and a positive predicted-R^2 are shown as the top 3 models in **Table 2-**

3. The stepwise models demonstrated the best relationship between State 4o and metabolites, a weaker relationship between Basal mOCR and metabolites, and no statistically significant relationships involving Max respiration.

Response (y)	Covariates (x)	β Coefficient (p-value)	Adj.-R^2	Pred.- R^2	ANOVA (p-value)
State 4o	PLT.Creatine	-0.009 (0.081)	0.836	0.629	(0.0003)*
	PLT.ADP	0.066 (0.000)*			
	PLT.Choline	-0.047 (0.000)*			
	PLT.Glucose	0.015 (0.026)*			
Basal	PLT.ADP	0.141 (0.000)*	0.711	0.608	(0.0004)*
	PLT.Taurine	-0.107 (0.000)*			
Basal	WB.Leucine	0.084 (0.002)*	0.428	0.308	(0.0079)*
	WB.Acetylcarnitine	-0.049 (0.066)			
State 4o	WB.Alanine	0.042 (0.060)	0.281	-0.111	(0.039)*
	WB.2.Hydroxybutyrate	0.026 (0.099)			
Max	WB.3.Hydroxybutyrate	0.017 (0.049)*	0.236	-0.033	(0.0595)
	WB.AMP	0.032 (0.088)			
Max	PLT.Creatine	0.022 (0.080)	0.170	-0.147	(0.0801)

Table 2-3 Multiple Linear Regression results
PLT.metabolite = platelet metabolite, WB.metabolite= whole blood metabolite; * indicates p-value ≤ 0.05

Significant metabolites selected for inclusion in the final model were entered into MetaboAnalyst for a pathway analysis. However, due to the small number of significant compounds, results were not interpretable. Rather, we reviewed the literature surrounding the biological relevance of the metabolites in the context of sepsis. A literature review by Eckerle et al., reported statistically significant metabolites that were found to be related to 3 pathways, namely, energy metabolism, mitochondrial dysfunction, and platelet activation and/or aggregation (**Table 2-4**) (17).

Sepsis Pathway	**Metabolites**	
	Whole blood	*Platelet*
Energy metabolism	Leucine	Creatine, ADP*, Choline*, Glucose*
Mitochondrial dysfunction	Acetylcarnitine	n/a

Platelet activation/aggregation	Taurine	ADP*, Choline*, Glucose*

Table 2-4 Selected Metabolites Biological Relevance to Sepsis
* Metabolites that are related to several sepsis pathways; n/a = not applicable; (17)

2.4.3 Evaluation of Platelet Isolation and Metabolite Detection Methods

To evaluate the relationship between platelet and WB metabolites in states of both sepsis and non-sepsis critical illness, we created two correlation matrices of platelet metabolites and WB metabolites in the sepsis and control subjects, respectively, which are reported in **Figure 2-1**. There were several significant correlations present in the sepsis group that were not observed in the controls, further emphasizing the metabolic perturbations provoked by the disease.

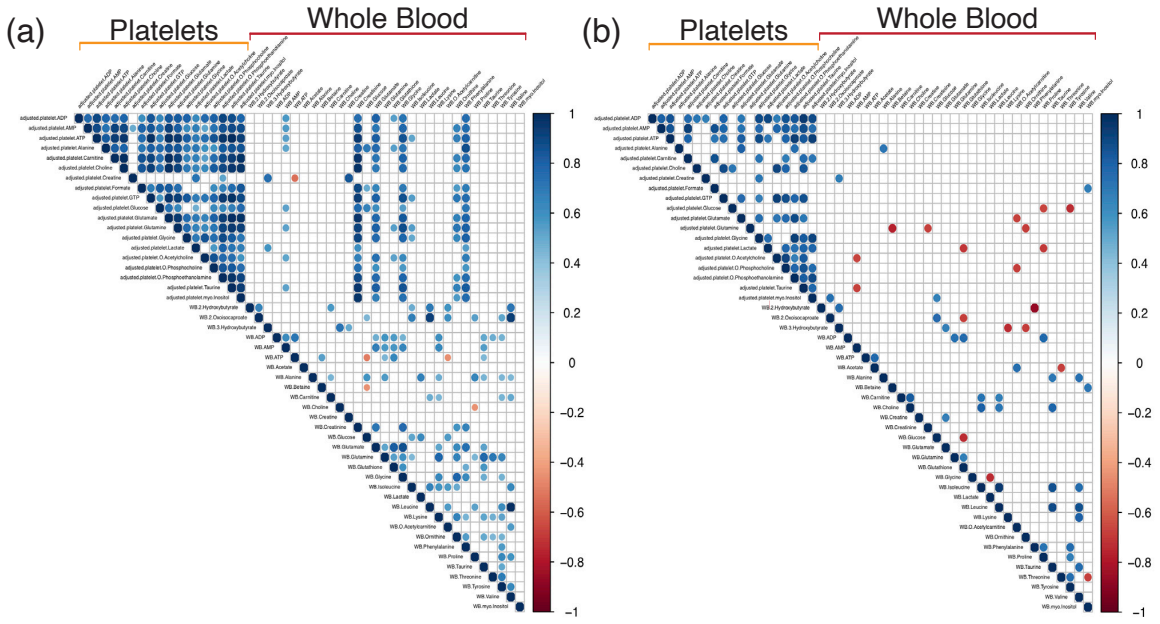

Figure 2-1 Comparing Correlations between Whole Blood and Platelet Metabolites in Septic and Healthy Subjects
Significant associations were found between whole blood and platelet metabolites. In sepsis patients, (a) several whole blood metabolites (creatinine, glutamate, glycine, ornithine, phenylalanine) were significantly and positively correlated with at least 12/19 (63%) of the detected platelet metabolites; these are contained within the red box. These significant correlations were not present in the (b) control subjects. P-values of < 0.05 were considered significant. Matrices were generated in RStudio using Pearson's correlation coefficient (r) with a scale of -1 to 1.

2.5 Discussion

This study provides evidence supporting the use of either platelet or WB metabolites to indirectly estimate platelet mOCR in patients with sepsis. As anticipated, platelet metabolites more accurately reflect platelet mOCR than WB metabolites, and the metabolite associations between the biofluids are more pronounced in sepsis-patients than in controls. Our data illustrate that certain WB (leucine, acetylcarnitine) and platelet metabolites (creatine, ADP, glucose, taurine) are significantly associated with platelet mOCR as measured by high-resolution respirometry. This demonstrates that an informative, non-invasive approach to the assessment of mitochondrial function could be employed when it is not feasible to acquire tissue or platelet mitochondria for mOCR measurements in real-time, such as in the context of human clinical investigations.

Groups of WB metabolites showed a significant relationship to the Basal (unstimulated) mitochondrial respiration measurement when using a stepwise forward-backward variable selection MLR model building method. Stronger statistical models were achieved with platelet metabolites as potential predictors (adj-R^2: 0.836, 0.711 vs adj-R^2: 0.428) with the same model building method. This is logical because platelet mitochondria likely contribute substantially to the components of the platelet metabolome. Moreover, the difference in model strength might be explained by the relatively lower biomass of platelets compared to other tissues. Of note, the associations between metabolites with Basal and State 4o respiration differ. This is expected, as Basal respiration represents the passive energy production state, while State 4o is a non-physiologic state, which indirectly measures the leakage of protons across the inner mitochondrial membrane. Increased levels of State 4o may represent ROS-associated damage to the inner mitochondrial membrane, and increased uncoupling protein leading to reduced energy output (25, 27, 28). This suggests it may be possible to use different metabolites (or metabolite panels) to probe various mitochondrial processes.

Three models met the criteria of significant ANOVA results and positive predicted-R^2 values. The metabolites identified via these models appear to have biological significance with sepsis and the prespecified goal of the project, namely, development of non-invasive reflections of altered mitochondrial function, adding to the clinical relevance of these findings (**Table 2-4**).

In regard to specific metabolites and pathways, it is worth noting that both of the platelet models included ADP, which highlights the importance of this molecule in sepsis. ADP and creatine are both substrates of ATP synthesis, but ADP is also maintained in high concentrations within the dense granules of platelets as they utilize the compound to activate aggregation (29-31). Platelet aggregation is also strongly influenced by choline, which is a precursor to platelet

activating factor (32). Sepsis is characterized as a hypercoagulable state, so it is logical that ADP and choline are highlighted in this biological and clinical model of sepsis.

Other metabolic signals were also evident. Glucose metabolism in sepsis has been extensively studied. In the context of activated platelets, there is evidence to support increases in glucose uptake, glycolysis, lactate, and glycogenolysis (33). Notably, the role of taurine in sepsis is unclear; but it is highly concentrated in platelets and reportedly reduces coagulation and increases during animal hibernation (34, 35). We find the latter observation interesting, because it may play a role in the sepsis hibernation hypothesis, which theorizes downregulated mitochondrial respiration acts as defensive strategy to prevent sepsis-induced cell death (36).

Lastly, acetylcarnitine and leucine have ties to sepsis through mitochondrial dysfunction and energy metabolism, respectively. Leucine is a branched chain amino acid, which are used as a source of energy during sepsis (37). Recently, Puskarich et al., and Chung et al., both found acetylcarnitine to be associated with mortality and organ failure in sepsis (38, 39). These findings, in conjunction with ours, further support the previously observed relationship between acetylcarnitine, platelet mitochondrial respiration, mortality and organ failure (12). Additional studies are needed to identify the mechanisms that underpin the associations, but these biological relationships support the utility of a metabolomics approach to estimate platelet mitochondrial function.

Despite the well-characterized metabolic derangement of sepsis, there is a major inability to accurately and longitudinally assess mitochondrial function in these patients due to the ethical and practical concerns of obtaining muscle/tissue biopsies. As such, there remains a clinical and critical need to non-invasively evaluate sepsis-induced changes in mitochondrial function for several reasons. First, mitochondrial function has been identified as increasingly important in

contributing to multiorgan dysfunction (5, 40). Second, a reliable and practical method could be more easily translated into clinical use to identify metabolically impaired phenotypes. There is a growing body of literature to support the use of measuring mitochondrial function in peripheral blood cells from patients with sepsis (10-16). The clinical significance of platelet mitochondrial function is evident in recent reports that show associations between increased respiration with mortality and organ failure (11, 12). To our knowledge, this is the first study to relate metabolomics data from two distinct biofluids with platelet mitochondrial bioenergetics. These results are consistent with other studies using intact platelets isolated from human blood samples. The high resolution respirometry used in these studies is generally considered the gold standard for measuring mitochondrial oxygen consumption. However, this experimental technique has several pitfalls that may prevent its translation into the clinical toolbox. The time sensitive method requires skilled technicians to collect fresh blood samples, isolate platelets and execute the respirometer protocol without the ability to freeze for later use or reruns. As such, this is not a high throughout procedure. Therefore, the purpose of this study was to discover and evaluate sets of metabolites that reflect platelet mOCR, potentially bypassing the need for high-resolution respirometry in clinical settings. We recognize our hypothesis-generating results only lay the groundwork that must be refined and validated in larger cohorts and more generalizable populations, but the future directions seem promising.

The stronger association between the platelet mOCR and platelet metabolome supports the secondary goal of evaluating our platelet isolation methods using quantitative ^{1}H-NMR spectroscopy. The apparent differences in detected metabolites and significant correlations between the platelet and WB metabolomes supports the successful optimization of our platelet metabolomics approach. Indeed, the appearance of associations between the WB and platelet

metabolomes in the subjects with sepsis emphasizes the prolific metabolic response that sepsis provokes. Platelets release metabolites into the blood upon activation, which offers a potential mechanistic explanation for this observation (29-31). Albeit, there were fewer control subjects than in the sepsis group so this may affect the lack of associations between the platelet and WB metabolites in this group.

We recognize there are several limitations of our study. First and foremost, this is a small, single center sample, and the specific metabolites and panels should be viewed skeptically and reproduced prior to broader application. Just as important, the associations pursued were matched to platelets, which represent a small biomass that may or may not reflect vital organ mitochondrial function. Future studies should attempt to make this pathophysiologic link. It is worth noting that the maximum respiration models were consistently weaker than those of the other two mOCR. The lack of significant relationships with Max respiration and measured metabolites is reasonable, as this represents an artificial experimental state of maximum respiratory capacity that is not reflected in the body and would not necessarily be expected to be related to measured peripheral metabolites. In regards to patient outcomes, we did not reproduce the previously reported association between maximum respiratory rate and SOFA score (12), although this may reflect our small sample size and relatively low and homogeneous severity of illness compared to prior reports. Again, due to a relatively lower severity of illness, we did not observe significant differences in respiratory rates and mortality as previously reported (11, 12). When building an MLR model with such interrelated variables like metabolites, we considered the possibility of collinearity between them. However, this is not of concern as the intention of our model was to use metabolite sets to estimate platelet mOCR and not individual metabolites. We refrained from interpreting the β Coefficients from the MLR models to avoid over

speculation about the relationships between individual metabolites and mitochondrial respiration. The ANOVA tested the difference between the selected models and the saturated models that includes every measured metabolite for that biofluid. The full model has more predictors than the sample size, which puts the test at risk of overfitting. However, the resulting p-values were not excessively small, so we do not believe the ANOVA test was overfit. Although, due to the small sample size, the test result could have been idiosyncratic to our population, leading to the need for external validation. Ideally, we would have compared the models from sepsis patients and non-sepsis controls, however, the mOCR data from the controls was considered unusable due to technician errors that occurred during experimentation. Albeit, this limitation did not prevent us from achieving the goal of the study, which was to determine if metabolomics data are reflective of platelet mitochondrial respiration. A follow-up study is necessary to identify potential differences and clinical significance between the metabolic associations in sepsis and non-sepsis subjects. The cross-sectional design of the study was also a limitation that precluded us from evaluating metabolic changes over time.

2.6 Conclusions

In conclusion, WB (leucine, acetylcarnitine) and platelet (creatine, ADP, glucose, taurine) metabolites have potential use as surrogates for estimating platelet mitochondrial function. This strategy, which circumvents the need for tissue sampling and the use of high-resolution respirometry, could be a viable approach to assess mitochondrial function in patients with sepsis. Further studies are warranted to corroborate these findings in a larger, more generalizable cohort.

2.7 Supplementary Materials

The following are available online at https://www.mdpi.com/2218-1989/10/4/139/s1; S2.2.1 WB and platelet metabolites with mOCR data; **Figure S1**: Representative NMR spectra from whole blood and platelet extracts; S4.7.1 Acquisition of Quantitative 1-D-1H-NMR Metabolomics Data; S4.8.1 Stepwise forward-backward variable selection model building R code.

2.8 Author Contributions

Conceptualization, M.R.M. and M.A.P.; methodology, M.R.M., C.E.M., M.K., and T.S.J.; formal analysis, M.R.M., M.A.P., and T.S.J.; investigation, M.A.P., C.E.M., and M.K.; resources, C.E.M., M.K., K.A.S., and M.A.P.; data curation, C.E.M., M.A.P., and M.R.M.; writing—Original draft preparation, M.R.M., and C.E.M.; writing—Review and editing, M.R.M., C.E.M., K.A.S., M.A.P., and A.E.J.; visualization, M.R.M..; supervision, M.A.P., K.A.S., and A.E.J.; project administration, M.A.P., K.A.S., M.K. and C.E.M.; funding acquisition, M.A.P., and K.A.S. All authors have read and agreed to the published version of the manuscript.

2.9 Funding

This work was supported by funding from the National Institute for General Medical Sciences (NIGMS), K23GM113041 (MAP) and R01GM111400 (KAS). The content is solely the responsibility of the authors and does not necessarily represent the official views of NIGMS or the NIH.

2.10 Acknowledgments

We would like to acknowledge Casey Schooff and Andrew Benjamin who assisted with sample processing and Larisa Yeomans who helped with the acquisition of NMR spectra. We would also like to acknowledge the enrolled patients that graciously provided their samples to support ongoing efforts in research.

2.11 Conflicts of Interest

The authors declare no conflict of interest. The funders had no role in the design of the study; in the collection, analyses, or interpretation of data; in the writing of the manuscript, or in the decision to publish the results.

2.12 References

1. Singer M, Deutschman CS, Seymour CW, Shankar-Hari M, Annane D, Bauer M, et al. The Third International Consensus Definitions for Sepsis and Septic Shock (Sepsis-3). JAMA. 2016;315(8):801-10.
2. Fleischmann C, Scherag A, Adhikari NK, Hartog CS, Tsaganos T, Schlattmann P, et al. Assessment of Global Incidence and Mortality of Hospital-treated Sepsis. Current Estimates and Limitations. Am J Respir Crit Care Med. 2016;193(3):259-72.
3. Simmons J, Pittet JF. The Coagulopathy of Acute Sepsis. Curr Opin Anaesthesiol. 2015;28(2):227-36.
4. Greco E, Lupia E, Bosco O, Vizio B, Montrucchio G. Platelets and Multi-Organ Failure in Sepsis. Int J Mol Sci. 2017;18(10).
5. Singer M. The role of mitochondrial dysfunction in sepsis-induced multi-organ failure. Virulence. 2014;5(1):66-72.
6. Brand M, Nicholls D. Assessing mitochondrial dysfunction in cells. Biochem J. 2011;435(Pt 2):297-312.

7. Avila C, Huang RJ, Stevens MV, Aponte AM, Tripodi D, Kim KY, et al. Platelet mitochondrial dysfunction is evident in type 2 diabetes in association with modifications of mitochondrial anti-oxidant stress proteins. Exp Clin Endocrinol Diabetes. 2012;120(4):248-51.
8. Merlo Pich M, Bovina C, Formiggini G, Cometti GG, Ghelli A, Parenti Castelli G, et al. Inhibitor sensitivity of respiratory complex I in human platelets: a possible biomarker of ageing. FEBS Lett. 1996;380(1-2):176-8.
9. Xu W, Cardenes N, Corey C, Erzurum SC, Shiva S. Platelets from Asthmatic Individuals Show Less Reliance on Glycolysis. PLoS One. 2015;10(7):e0132007.
10. Sjovall F, Morota S, Frostner EA, Hansson MJ, Elmer E. Cytokine and nitric oxide levels in patients with sepsis--temporal evolvement and relation to platelet mitochondrial respiratory function. PLoS One. 2014;9(7):e103756.
11. Sjovall F, Morota S, Hansson MJ, Friberg H, Gnaiger E, Elmer E. Temporal increase of platelet mitochondrial respiration is negatively associated with clinical outcome in patients with sepsis. Crit Care. 2010;14(6):R214.
12. Puskarich MA, Kline JA, Watts JA, Shirey K, Hosler J, Jones AE. Early alterations in platelet mitochondrial function are associated with survival and organ failure in patients with septic shock. J Crit Care. 2016;31(1):63-7.
13. Lorente L, Martin MM, Lopez-Gallardo E, Blanquer J, Sole-Violan J, Labarta L, et al. Decrease of oxidative phosphorylation system function in severe septic patients. J Crit Care. 2015;30(5):935-9.
14. Lorente L, Martin MM, Lopez-Gallardo E, Iceta R, Blanquer J, Sole-Violan J, et al. Higher platelet cytochrome oxidase specific activity in surviving than in non-surviving septic patients. Crit Care. 2014;18(3):R136.
15. Protti A, Fortunato F, Caspani ML, Pluderi M, Lucchini V, Grimoldi N, et al. Mitochondrial changes in platelets are not related to those in skeletal muscle during human septic shock. PLoS One. 2014;9(5):e96205.
16. Protti A, Fortunato F, Artoni A, Lecchi A, Motta G, Mistraletti G, et al. Platelet mitochondrial dysfunction in critically ill patients: comparison between sepsis and cardiogenic shock. Crit Care. 2015;19:39.

17. Eckerle M, Ambroggio L, Puskarich MA, Winston B, Jones AE, Standiford TJ, et al. Metabolomics as a Driver in Advancing Precision Medicine in Sepsis. Pharmacotherapy. 2017;37(9):1023-32.
18. Chacko BK, Smith MR, Johnson MS, Benavides G, Culp ML, Pilli J, et al. Mitochondria in precision medicine; linking bioenergetics and metabolomics in platelets. Redox Biol. 2019;22:101165.
19. Bone RC, Balk RA, Cerra FB, Dellinger RP, Fein AM, Knaus WA, et al. Definitions for sepsis and organ failure and guidelines for the use of innovative therapies in sepsis. The ACCP/SCCM Consensus Conference Committee. American College of Chest Physicians/Society of Critical Care Medicine. Chest. 1992;101(6):1644-55.
20. Jones AE, Brown MD, Trzeciak S, Shapiro NI, Garrett JS, Heffner AC, et al. The effect of a quantitative resuscitation strategy on mortality in patients with sepsis: a meta-analysis. Crit Care Med. 2008;36(10):2734-9.
21. Sjovall F, Ehinger JK, Marelsson SE, Morota S, Frostner EA, Uchino H, et al. Mitochondrial respiration in human viable platelets--methodology and influence of gender, age and storage. Mitochondrion. 2013;13(1):7-14.
22. Belikova I, Lukaszewicz AC, Faivre V, Damoisel C, Singer M, Payen D. Oxygen consumption of human peripheral blood mononuclear cells in severe human sepsis. Crit Care Med. 2007;35(12):2702-8.
23. Paglia G, Magnúsdóttir M, Thorlacius S, Sigurjónsson ÓE, Guðmundsson S, Palsson BØ, et al. Intracellular metabolite profiling of platelets: Evaluation of extraction processes and chromatographic strategies. Journal of Chromatography B. 2012;898:111-20.
24. McHugh CE, Flott TL, Schooff CR, Smiley Z, Puskarich MA, Myers DD, et al. Rapid, Reproducible, Quantifiable NMR Metabolomics: Methanol and Methanol: Chloroform Precipitation for Removal of Macromolecules in Serum and Whole Blood. Metabolites. 2018;8(4).
25. Chacko B, Kramer P, Ravi S, Benavides G, Mitchell T, Dranka B, et al. The Bioenergetic Health Index: a new concept in mitochondrial translational research. Clin Sci (Lond). 2014;127(Pt 6):367-73.
26. Chong J, Wishart DS, Xia J. Using MetaboAnalyst 4.0 for Comprehensive and Integrative Metabolomics Data Analysis. Current Protocols in Bioinformatics. 2019;68(1):e86.

27. Divakaruni AS, Brand MD. The regulation and physiology of mitochondrial proton leak. Physiology (Bethesda). 2011;26(3):192-205.
28. Cheng J, Nanayakkara G, Shao Y, Cueto R, Wang L, Yang WY, et al. Mitochondrial Proton Leak Plays a Critical Role in Pathogenesis of Cardiovascular Diseases. Adv Exp Med Biol. 2017;982:359-70.
29. de Stoppelaar SF, van 't Veer C, van der Poll T. The role of platelets in sepsis. Thromb Haemost. 2014;112(4):666-77.
30. Puri RN, Colman RW. ADP-induced platelet activation. Crit Rev Biochem Mol Biol. 1997;32(6):437-502.
31. Horjus DL, Nieuwland R, Boateng KB, Schaap MCL, van Montfrans GA, Clark JF, et al. Creatine kinase inhibits ADP-induced platelet aggregation. Sci Rep. 2014;4.
32. Michel V, Yuan Z, Ramsubir S, Bakovic M. Choline transport for phospholipid synthesis. Exp Biol Med (Maywood). 2006;231(5):490-504.
33. Fidler TP, Middleton EA, Rowley JW, Boudreau LH, Campbell RA, Souvenir R, et al. Glucose Transporter 3 Potentiates Degranulation and Is Required for Platelet Activation. Arterioscler Thromb Vasc Biol. 2017;37(9):1628-39.
34. Miglis M, Wilder D, Reid T, Bakaltcheva I. Effect of taurine on platelets and the plasma coagulation system. Platelets. 2002;13(1):5-10.
35. Hayes KC, Pronczuk A, Addesa AE, Stephan ZF. Taurine modulates platelet aggregation in cats and humans. Am J Clin Nutr. 1989;49(6):1211-6.
36. Kohoutova M, Dejmek J, Tuma Z, Kuncova J. Variability of mitochondrial respiration in relation to sepsis-induced multiple organ dysfunction. Physiol Res. 2018;67(Supplementum 4):S577-s92.
37. Van Wyngene L, Vandewalle J, Libert C. Reprogramming of basic metabolic pathways in microbial sepsis: therapeutic targets at last? EMBO Mol Med. 2018;10(8).
38. Puskarich MA, Evans CR, Karnovsky A, Das AK, Jones AE, Stringer KA. Septic Shock Nonsurvivors Have Persistently Elevated Acylcarnitines Following Carnitine Supplementation. Shock (Augusta, Ga). 2018;49(4):412-9.
39. Chung KP, Chen GY, Chuang TY, Huang YT, Chang HT, Chen YF, et al. Increased Plasma Acetylcarnitine in Sepsis Is Associated With Multiple Organ Dysfunction and Mortality: A Multicenter Cohort Study. Crit Care Med. 2019;47(2):210-8.

40. Crouser ED. Mitochondrial dysfunction in septic shock and multiple organ dysfunction syndrome. Mitochondrion. 2004;4(5-6):729-41.

Chapter 3 Investigating the Metabolic Underpinnings of Sepsis-induced Organ Dysfunction Using a Mouse Model of Sepsis, and Human Sepsis and Septic Shock Data

3.1 Stronger Associations between C2 and Individual TCA Cycle Metabolites in Sepsis Non-Survivors compared with Sepsis Survivors

Under a stressful and high energy demanding condition like sepsis, patients may present with abnormal TCA cycle metabolite concentrations due to the increased metabolism of carbon sources such as lipids, glucose, and amino acids or from modulation of the TCA cycle enzymes and anaplerotic pathways (1-4). The acylcarnitines are known to reflect disruptions in β-oxidation of fatty acids, which is intended to supply acetyl-CoA to the TCA cycle. Due to the proximity of acylcarnitine generation to the TCA cycle, I hypothesized that the production of C2 could reflect an expanded view of mitochondrial dysfunction including both disruptions in FAO and the TCA cycle. To add clinical context to this hypothesis, multiple linear regression analysis was applied to determine if the metabolic relationships between C2 and the intermediates of the TCA cycle were stronger in the septic shock non-survivors compared to the survivors. Positive findings from this analysis provided evidence expanding the mechanistic, metabolic interpretation of altered C2 levels while demonstrating a distinct signal between non-survivors and survivors.

The data used for the primary analysis was generated from the phase 1 clinical trial studying the therapeutic benefit of supplemental intravenous L-carnitine in patients with septic shock (RACE) (5). To avoid the potential effects of the therapy on mortality, I used the baseline metabolite concentrations from the placebo group (n=61). The patients included in the analysis

had serum metabolites quantified using the acylcarnitine and the Glycolysis/TCA/Nucleotide targeted platforms conducted by the Michigan Regional Comprehensive Metabolomics Resource Core. The TCA platform quantified citrate/isocitrate, succinate, fumarate, and malate vie ion-pair chromatography mass spectrometry. The targeted acylcarnitine platform quantified 8 acylcarnitine derivatives (LC, C2, C3, C4, C5, C8, C14, C16) and reported 14 others. The multiple linear regression models were structured with C2 concentration as the dependent variable with independent variables for the TCA cycle intermediate concentrations, binary mortality (28-day; 1-year), and an interaction term between the two covariates (**Equation 3-1**). Each of the detected TCA cycle intermediates and mortality terms were substituted into the models. The goal was to identify a significant interaction term (p-value ≤ 0.05), which would indicate a difference in the metabolic relationship between the non-survivors and survivors.

$$C2 = \beta o + \beta 1(TCA) + \beta 2(mortality) + \beta 3(TCA * mortality)$$

Equation 3-1. Multiple Linear Regression Model Format
The metabolite concentrations were natural log transformed and scaled. The mortality variables were dichotomized with 0=survivor and 1=non-survivor. TCA= tricarboxylic acid cycle intermediate

The models using malate at 28-days (β3= -0.51; p=0.055), malate at 1-year (β3= -0.54; p=0.036), and succinate at 1-year (β3= -0.68; p=0.038) were found to have significant interaction terms (**Figure 3-1**). We added clinical parameters to the significant models to adjust for age, sex, BMI, and SOFA, but inclusion of the variables did not impact the interaction terms, so they were removed. The slope term, β1, denoting the relationship between malate and C2 was greater in magnitude in the non-survivors compared to the survivors at 28-days (-0.528 vs -0.0184), and 1-year (-0.421 vs 0.118). Therefore, in support of the hypothesis, the relationship between malate and C2 was stronger in the septic shock non-survivors compared with the survivors. However, β1 indicating the association between succinate and C2 were similar in magnitude between the

non-survivors and survivors at 1-year (-0.295 vs 0.379). The significant interaction slope of the succinate at 1-year model illustrated a different metabolic relationship based on mortality but did not support the hypothesis that the non-survivors' metabolic relationship is stronger. Interestingly, when substituted for C2 as the dependent variable, lactate did not have any relationships with the TCA cycle metabolites between the survivors and non-survivors. Overall, the findings demonstrate that the relationship between C2 and different TCA cycle intermediates are differentiating between mortality groups, suggesting that changes in these key mitochondrial metabolites are closely linked to mortality. Thus, the C2 signal in septic shock reflects an expanded interpretation of mitochondrial dysfunction including a perturbed TCA cycle. The next steps were to validate the results in a less sick sepsis cohort to interrogate the extent to which illness severity influences the metabolic relationships.

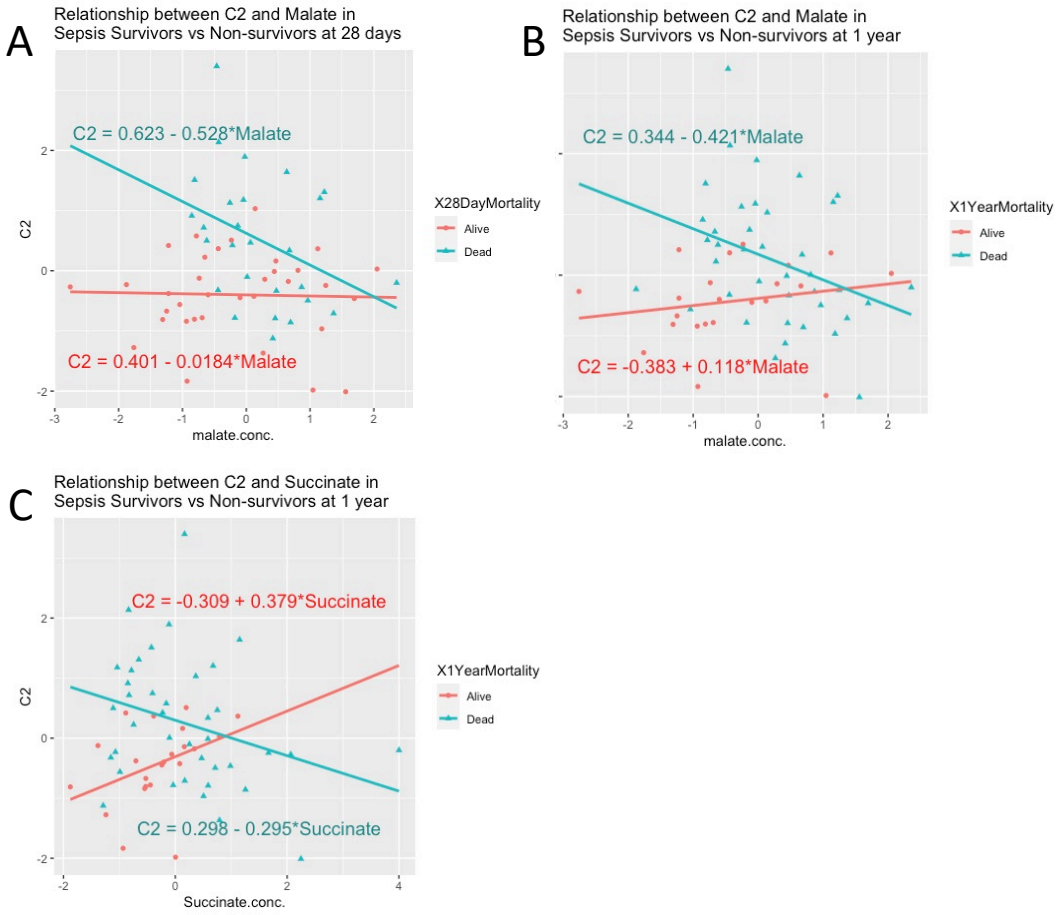

Figure 3-1. Multiple Linear Regression Model Results
The models with significant interaction slopes included (A) malate at 28-days, (B) malate at 1-year, and (C) succinate at 1-year. The regression lines for each mortality group are distinguished by color; red= survivors, blue=non-survivors.

The central biorepository (CBR) at the University of Michigan provided plasma samples from ICU patients identified with sepsis (n=134) that did not meet the Sepsis-3 definition for septic shock due to a lactate level ≤ 2 mmol/L (6). **Table 3-1** compares the median SOFA scores, 28-day mortality, and 1-year mortality between the CBR and RACE cohorts.

	CBR n=134	RACE n=61
Median SOFA	6	12
28-day mortality	28%	44%
1-year mortality	44%	64%

Table 3-1. Comparing SOFA, 28-day, and 1-year mortality between groups
CBR represents the less sick sepsis cohort, whereas the RACE data are from septic shock patients.

The plasma samples were analyzed using the same targeted approaches as the RACE patient samples (acylcarnitines and Glycolysis/TCA/Nucleotide platforms). Using multiple linear regression interaction models, we assessed the relationships among C2 and the TCA cycle intermediates between sepsis non-survivors and survivors. However, we were unable to validate the same metabolic relationships between C2 and malate or succinate. We also did not find any new significant interaction models that were not present in the primary analysis results. These findings suggest that sepsis and septic shock represent different stages of metabolic disruption. Further exploration is necessary to identify the extent of the metabolic differences between the early stages of sepsis through septic shock. Such findings would uncover metabolic mechanisms that influence the progression of sepsis-induced organ dysfunction, which may reveal new therapeutic targets.

Nevertheless, an important connection was identified among the sepsis and septic shock cohorts. C2 was positively correlated to organ dysfunction as measured through the SOFA score (CBR $r=0.42$, $p<0.00$; RACE $r=0.44$, $p<0.00$). Consequently, our secondary analysis sought to characterize the metabolite signals at the different stages of sepsis, determine how they relate to changes in organ dysfunction, and explore the mechanistic origins of the C2 signal we observe in patients with sepsis.

3.2 Metabolic Disruptions that Precede Organ Dysfunction in an Early Sepsis Mouse Model Persist in Patients with Sepsis and Septic Shock.

3.2.1 Introduction

The Sepsis-3 guidelines include a consensus statement that an unregulated infection leads to a cascade of disruptions in bodily systems that result in prolific organ damage, dysfunction, and/or failure that ultimately drives the mortality and morbidity in patients (6). Specifically, the cardiovascular, neuronal, endothelial, immune, bioenergetic, and metabolic systems are all affected during the progression of sepsis-induced organ dysfunction, but the underlying mechanisms remain poorly understood (6-8). This poses as a major barrier to identifying and developing targeted therapeutics for patients with sepsis (6, 7).

Despite this lack of knowledge, there have been advancements in the understanding of sepsis pathobiology, and metabolism has emerged as a critical component (2, 7, 9, 10). For example, lactate, a metabolic product of glycolysis, is codified in the Sepsis-3 guidelines definition which has led to its use as a biomarker in treatment algorithms (6, 11). More recently, using metabolomics, we and others have identified mitochondrial metabolic signals (e.g., acylcarnitines) in the blood that are associated with sepsis severity, organ dysfunction, mortality, and persistent critical illness (10, 12-16). These findings have raised our curiosity about the

origins and timing of these signals, and the extent to which changes in blood metabolite levels reflect organ specific perturbations in metabolism and function. This information is needed for moving the sepsis definition to one that is grounded in mechanism.

Metabolomics is a versatile systems biology approach that measures endogenous metabolites in a single biological sample (9, 17). To date, most sepsis metabolomics studies have been cross-sectional. However, longitudinal organ-focused studies are needed to characterize the chronological progression of sepsis-induced changes in organ metabolism and function. Importantly, since metabolic pathways are highly conserved across mammalian species (18), metabolism can serve as a "translational bridge" between experimental and clinical sepsis, enabling mechanistic studies. Herein, we present two human sepsis cohorts and an experimental murine model of sepsis that show mitochondrial metabolic signals in the blood reflect disruptions in organ-level metabolism that is a harbinger of organ injury and dysfunction.

3.2.2 Methods

Human sepsis and septic shock cohorts

After obtaining consent, plasma samples from patients in the intensive care unit with sepsis were collected through the University of Michigan Central Biorepository (CBR) as a secondary research method. Patients were selected based on the criteria that their most recent serum lactate measured prior to research sample collection was ≤ 2 mmol/L to exclude patients with septic shock. The samples were then sent to the Michigan Regional Comprehensive Metabolomics Research Core (MRC2) to be assayed via liquid chromatography mass spectrometry (LC-MS) on their targeted platforms, Acylcarnitines and Glycolysis/TCA/Nucleotides. The Acylcarnitine platform quantified 8 compounds using internal standards (L-carnitine, C2, C3, C4, C5, C8, C14, C16) and provided peak areas for 21 other

acylcarnitines. The Glycolysis/TCA/Nucleotides platform quantified 6 compounds using internal standards (glucose, lactate, succinate, malate, citrate/isocitrate, adenosine triphosphate) and provided peak areas for 50 other compounds.

The data from patients with septic shock were part of a secondary analysis from a phase 2 placebo controlled clinical trial (RACE) studying the therapeutic effects of intravenous L-carnitine (5). Patients were consented and enrolled within 24 hours of septic shock recognition. For this analysis, we used the baseline serum samples from patients in the placebo arm that were previously assayed by the MRC2 using the same targeted platforms (19). There were minor differences in the Glycolysis/TCA/Nucleotides assay due to changes made by the MRC2. Specifically, the RACE samples were assayed using ion-pair chromatography mass spectrometry and the quantified compounds were citrate/isocitrate, succinate, fumarate, and malate with 29 other metabolite peak areas provided. Also for the RACE dataset, the Acylcarnitine platform provided peak areas for 16 other acylcarnitines, as opposed to the 21 detected in the CBR cohort. Due to this difference, we only considered the common metabolites detected (56 total) in both data sets for the analyses (**Table 3-2**). We compared the demographics between the two cohorts in **Table 3-3**.

LC.conc	C2.conc	C2.LC	C3.conc	C4.conc	C5.conc	C6	C8:1
C8.conc	C10:1	C10	C12:1	C12	C14:1	C14.conc	C16:1
C20:4	C18:2	C20:3	C16.conc	C18:1	C20:2	C18	C20:1
C20:0	Citrate/ Isocitrate.conc	Lactate.conc	Malate.conc	Succinate.conc	Taurine	Creatinine	Glutamine
Proline	Asparagine	Citrulline	Deoxyuridine	Valine	Hypoxanthine	Leucine/ Isoleucine	Tyrosine
Glutamate	Aspartate	Phenylalanine	Gluconate	Tryptophan	Pyruvate	Pantothenic acid	alpha-ketoglutarate
Threonine	Alanine	Histidine	Creatine	Methionine	Xanthine	Hexose 6-phosphate	Fumarate

Table 3-2 Common metabolites between the sepsis (CBR) and septic shock (RACE) cohorts detected via the Acylcarnitines and the Glycolysis/TCA/Nucleotides platforms.
-.conc indicates an internal standard quantified compound, all others are peak areas.

Variable	Sepsis cohort CBR (n = 134)	Septic Shock cohort RACE (n = 61)	p-value
Demographics			
Age, years (IQR)	59 (49, 69)	61 (48, 71)	0.8
Male, n (%)	83 (62%)	33 (54%)	0.3
Female, n (%)	51 (38%)	28 (46%)	
Physiologic variables			
Body mass index (IQR)	29 (24, 35)	27 (22, 35) ‡	0.1
Laboratory values			
Clinical lactate, mmol/L (IQR)	1.3 (0.9, 1.6)	3.8 (2.7, 6.7) ‡	<0.0001*
Carnitine values			
L-carnitine (LC), µM	56.1 (42.6, 94.6)	38.4 (25.6, 59)	<0.0001*
Acetylcarnitine (C2), µM	13.3 (8.2, 22.6)	17.3 (11.5, 29.8)	0.006*
C2/LC ratio	0.22 (0.16, 0.36)	0.51 (0.35, 0.74)	<0.0001*
Severity of Illness			
Total SOFA score (IQR)	4 (3, 7)	9 (7, 11)	<0.0001*
$SOFA_{renal}$ (IQR)	1 (0, 4)	1 (1, 2) ‡	0.9
$SOFA_{liver}$ (IQR)	0 (0, 1)	1 (0, 2)	0.009*
Mortality			
28-day, n (%)	37 (28%)	27 (44%)	0.03*
1-year, n (%)	60 (45%)	39 (64%)	0.01*

Table 3-3. Demographics between sepsis (CBR) and septic shock (RACE) patients.
‡ sample size differs due to missing data; RACE BMI n=60, RACE lactate n=50, RACE SOFArenal n=59;
* Denotes the Mann-Whitney test p-value <0.05

Cecal Ligation and Puncture Mouse Model of Sepsis

This study followed the guidelines of the Institutional Animal Care and Use Committee (IACUC) of the University of Michigan, which approved the animal procedures and animal care methods used for this study. Male and female (12-13 weeks) C57BL/6J mice (The Jackson Laboratory, Bar Harbor, Maine) included in the study received routine housing as previously described for at least 5 days prior to surgery for acclimatization (20). Under isoflurane anesthesia (VetOne, Boise, Idaho), the cecal ligation and puncture (CLP) surgery was performed using a 50% ligation of the cecum with two punctures using a 26-gauge needle as previously described to obtain a 50-70% mortality rate (20). At induction, the mice received 1.5 mL of warmed saline

containing 0.05 mg/kg buprenorphine subcutaneously with 4 additional doses in 100 µL of warmed saline every 12 hours up to 48 hours, depending on the termination time point. Cages were randomly assigned to receive the CLP or sham laparotomy in which we did not ligate or puncture the cecum. The 6- and 24-hour termination time point groups had 10 CLP and 10 sham animals. Due to the anticipated mortality at these time points, we included 2 and 6 extra animals in the 30- and 48-hour CLP groups, respectively, to ensure we had a minimum of 10 animals per group. The final counts for each time point are shown in **Table 3-4**.

group	T0 hours	T6 hours	T24 hours	T30 hours	T48 hours
CLP		10 (5 male; 5 female)	10 (5 male; 5 female)	11 (5 male; 6 female)	14 (7 male; 7 female)
sham		10 (5 male; 5 female)	10 (5 male; 5 female)	10 (5 male; 5 female)	10 (5 male; 5 female)
healthy	10 (5 male; 5 female)				

Table 3-4. Demographic table containing the number of animals per group, time point, and sex distribution.
N=95 total animals

Tissue Collection and Processing

At termination, the mice underwent isoflurane anesthesia for tissue collection via the freeze clamp procedure intended to quench the *in vivo* metabolism, as previously described (21). Briefly, laparotomy was performed, and the left renal blood vessels were clamped then the kidney was excised and cut longitudinally before being submerged in 10% neutral buffered formalin (24895887, Sigma-Aldrich) for 18 hours followed by 70% ethanol until histological analysis was performed. The right medial liver lobe received the same collection for histological analysis. The right kidney blood vessels were clamped, and the excised tissue was washed in a glucose (10 mM) and pyruvate (0.5 mM) solution then simultaneously frozen and flattened using liquid nitrogen cooled paddle forceps and stored in cryotubes containing argon. The left liver lobe, heart, and lungs were also excised, and freeze clamped. Plasma (1:1 v/v, 100 µL whole blood into 100 µL of 3.4 mM EDTA PBS (1X)) samples were collected via the tail snip method

at termination to be assayed via the VETSCAN VS2 comprehensive diagnostic profile for the clinical biomarkers; creatinine (CRE), total bilirubin (TBIL), amylase (AMY), albumin (ALB), total protein (TP), blood urea nitrogen (BUN), and alanine transaminase (ALT). Whole blood (30 µL) was also collected at termination for internal standard quantified measurements of L-carnitine and acetylcarnitine via LC-MS at the University of Michigan Pharmacokinetic and Mass Spectrometry Core.

Freeze clamped kidney and liver samples were homogenized and extracted using a methanol/chloroform/water extraction solution, as previously described (22). Briefly, methanol/chloroform (1:2 v/v, 1mL -20 ºC) was added to homogenization tubes containing steel beads with 50-100 mg of the kidney or left liver lobe. Dry ice was added to cool the bead homogenizer (Beadbug 6, Benchmark Scientific). The tissues were bead homogenized for 3 cycles of 20s with 30s rest intervals at 4350 rpm, then cooled at -20 ºC for 2 minutes between each run (3 runs total). The tubes containing matched halves of the organs were combined in 5 mL tubes, placed on ice, and pulse sonicated for 20s (Sonic Dismembrator model 100, Fisher Scientific). Samples were added to 15 mL conical tubes containing cold chloroform/HPLC grade water (1:1 v/v, 1.6 mL 4 ºC) to the samples, vortexed for 10s, and let rest on ice for 15 minutes before centrifugation (13,400 x g, 30 min at 4 ºC). The resulting aqueous fraction was filtered (0.2 µm) then lyophilized.

^{1}H-Nuclear Magnetic Resonance (NMR) Spectroscopy

Post-lyophilization, samples were resuspended in a 50 mM phosphate buffer in D2O. After being resuspended, samples were vortexed to fully resuspend all solids, and then measured and transferred to labeled cryotubes using a 1 mL glass serological pipet. If the sample volume was less than 500 µL, D2O was added to the sample to bring its volume up to 500 µL. 50 µL of

DSS-d6 of known concentration was then added to all samples to act as an internal standard for NMR. Samples were then frozen and stored at -80 ºC until time of spectra acquisition. Spectra were acquired at the University of Michigan's Biochemical NMR Core Laboratory on a Varian (now Agilent, Inc., Santa Clara, CA) 500MHz NMR spectrometer with a VNMRS console operated by host software VNMRJ 4.0. Spectra were recorded using 128 scans of a proton-proton-NOESY pulse sequence (commonly called a METNOESY pulse sequence) (23). Spectra were acquired at room temperature (295.45+/-0.3 ºK) using a 5-mm Agilent "One-probe." The pulse sequence is as follows: A 1s recovery delay, which includes a 990ms saturation pulse of 80Hz induced field strength empirically centered on the water resonance, 2 calibrated 90º pulses, a mixing time of 100ms, a final 90º pulse, and an acquisition period of 4s. Optimal excitation pulse widths were obtained by using an array of pulse lengths as previously described (24). NMR spectra were analyzed using Chenomx NMR Suite 8.6 (Chenomx, Inc., Edmonton, AB, Canada). Using the software's Processor module, spectra first had their phase shift adjusted, followed by the excision of the water peak, followed by manual baseline correction. After spectra were processed, the Profiler module of the software was used to identify and quantify compounds relative to the internal standard. Compound identity was determined using Chenomx's internal compound library of 338 compounds, and a 500mHz compound library from HMDB.ca (25) containing 657 compounds. All samples were profiled by a single researcher who was blinded to experimental condition. We detected and profiled 60 metabolites in the kidney samples and 68 metabolites in the liver samples. Metabolite concentrations (μM) were normalized to BCA assay quantified protein concentrations (μg/mL) and stoichiometry was used to obtain final units of nmol/g.

Data Analysis Methods

Demographic data between human cohorts was compared using the Mann-Whitney test in Prism 9 (Version 9.1.0, GraphPad Software, LLC.). We used the metabolomics analysis platform, MetaboAnalyst 5.0 (https://www.metaboanalyst.ca/), to conduct the partial Spearman's rank correlation (for ordinal data: $SOFA_{total}$, $SOFA_{renal}$, $SOFA_{liver}$), partial Pearson's correlation (for continuous data: metabolites, organ biomarkers), 2-way ANOVA analyses, and to impute metabolite missing data using 1/5 the minimum concentration per metabolite. The partial correlation analyses adjusted for age, sex, body mass index (BMI) in the human cohorts, and group, sex, time in the animal analyses, while also correcting for multiple comparisons via False Discovery Rates (FDR). We used RStudio (RStudio Team 2015. RStudio: Integrated Development for R. RStudio, Inc., Boston, MA) to plot the metabolite concentration over time data with subsequent ANOVA Holm's post-hoc testing and the correlation plots.

We subtracted the neurological component of the SOFA score because many of the septic shock patients were sedated which affects the neurological assessment, as has been done previously (13). To be consistent between groups, we removed the neurological score from SOFA in both cohorts and refer to the new score as the $SOFA_{total}$. The pathway analysis used quantitative enrichment analysis which uses a generalized linear model to estimate the association between the metabolite concentrations and the class label (CLP vs sham) (26). The p-values derived from this analysis are plotted against the pathway topology analysis "pathway impact" which represents the importance of a compound within a given metabolic network (26).

3.2.3 Results

Patients with sepsis and septic shock have distinct metabolite signals in the blood that are associated with organ dysfunction.

Using two separate cohorts of patients, one with sepsis (CBR) and one with septic shock (RACE), we found that patients with sepsis had more blood metabolites that correlated with organ dysfunction ($SOFA_{total}$, $SOFA_{renal}$, and $SOFA_{liver}$) than patients with septic shock (**Figure 3-2**). These signals were adjusted for age, sex, and BMI and FDR corrected for multiple comparisons. Notably, in sepsis, there were metabolites that were positively and negatively correlated with $SOFA_{total}$, $SOFA_{renal}$, and $SOFA_{liver}$, whereas in septic shock, there were only positive associations. Apart from the correlation between creatinine and $SOFA_{renal}$, the acylcarnitines were the only measured metabolites that correlated with organ dysfunction in the septic shock cohort.

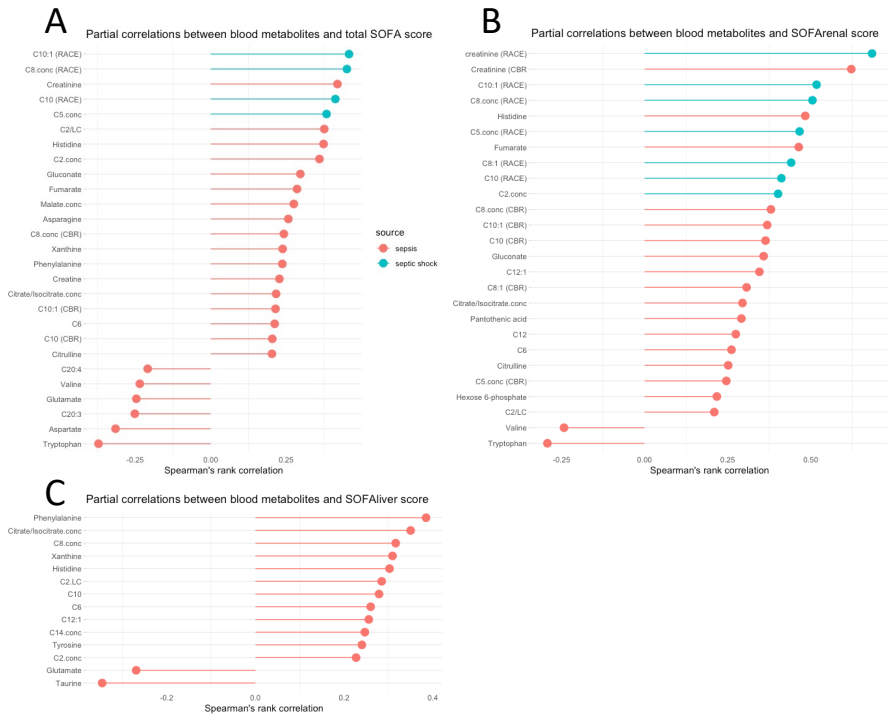

Figure 3-2. Partial correlations between energy metabolites in the blood and organ dysfunction variables
Adjusted for age, sex, and BMI. The partial correlations between (A) SOFA, (B) $SOFA_{renal}$, (C) $SOFA_{liver}$, and energy metabolites measured in the plasma (CBR) and serum (RACE). Correlations with $p<0.05$ were included. Metabolite names with .conc designate quantified concentrations using internal standards.

As such, we assessed the relationship between these blood markers of L-carnitine metabolism (LC, C2, C2/LC) and $SOFA_{total}$, $SOFA_{renal}$, and $SOFA_{liver}$ in the sepsis and septic shock cohorts (**Figures 3-3 and 3-4**.) The found associations persisted when adjusted for age, sex, and BMI in multiple linear regression analyses (**Table 3-5**). The correlation of blood L-carnitine with both $SOFA_{renal}$, and $SOFA_{liver}$ did not become evident until septic shock and the significant correlation with acetylcarnitine (C2) strengthened as sepsis progressed to shock, whereas the correlations with the C2/LC ratio diminished as patients entered shock. In aggregate, these findings corroborate previous findings that sepsis-induced metabolic perturbations in the blood are associated with organ dysfunction (12, 27, 28); we extended them to show that there is a larger and more diverse global metabolic response in early disease (sepsis) that is associated with $SOFA_{renal}$ and $SOFA_{liver}$ than there is in late disease (septic shock). As sepsis progresses, this shift in metabolism leads to an amplification of L-carnitine-related signals.

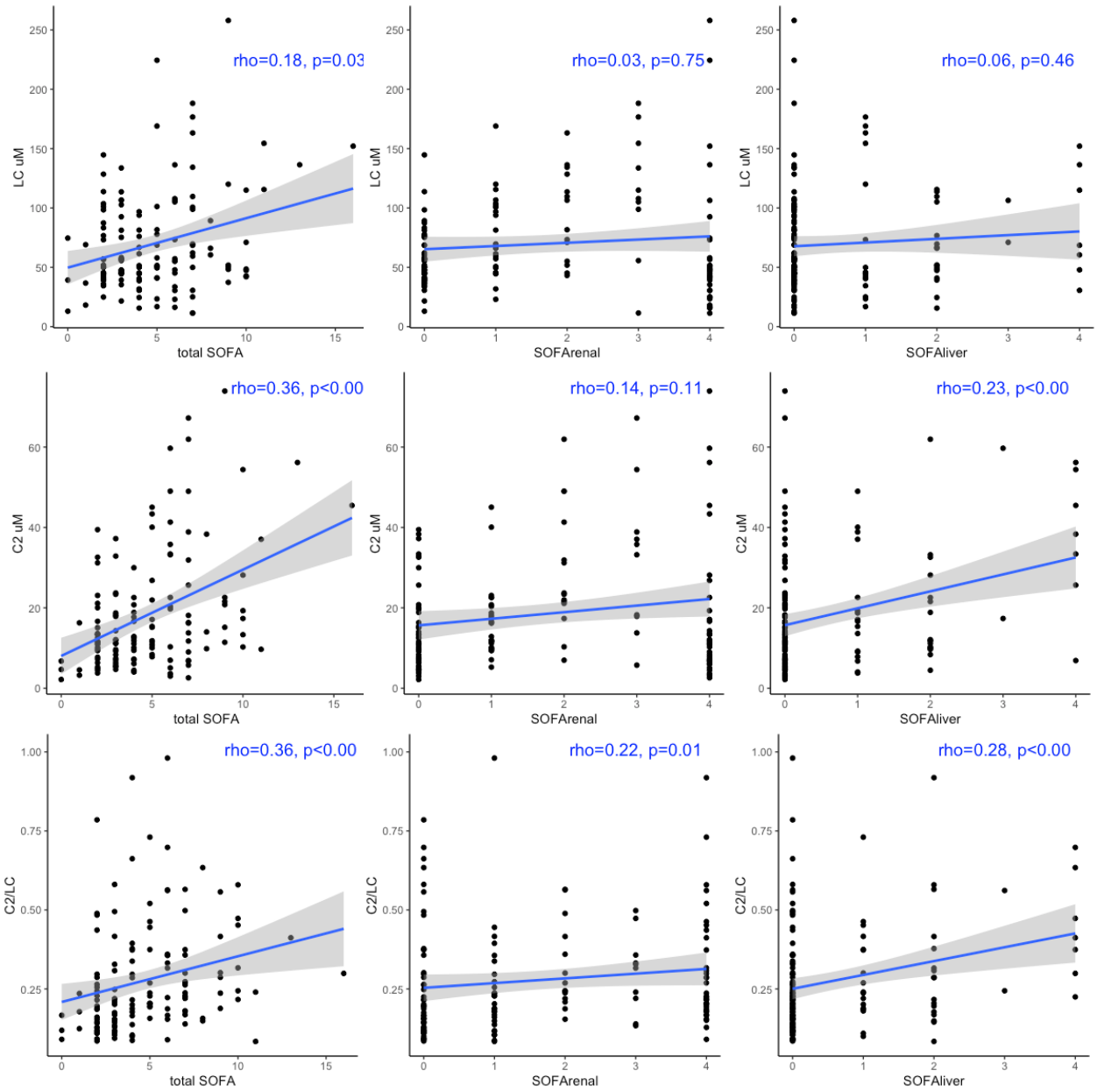

Figure 3-3. Scatter plots of LC, C2, C2/LC plasma concentrations and $SOFA_{total}$, $SOFA_{renal}$, $SOFA_{liver}$ for the sepsis cohort (CBR; n=134).
The Spearman's rank correlation coefficient (rho) and p-value is shown for each association. The shaded area represents the 95% confidence interval around the linear regression best fit line. LC= L-carnitine; C2=acetylcarnitine.

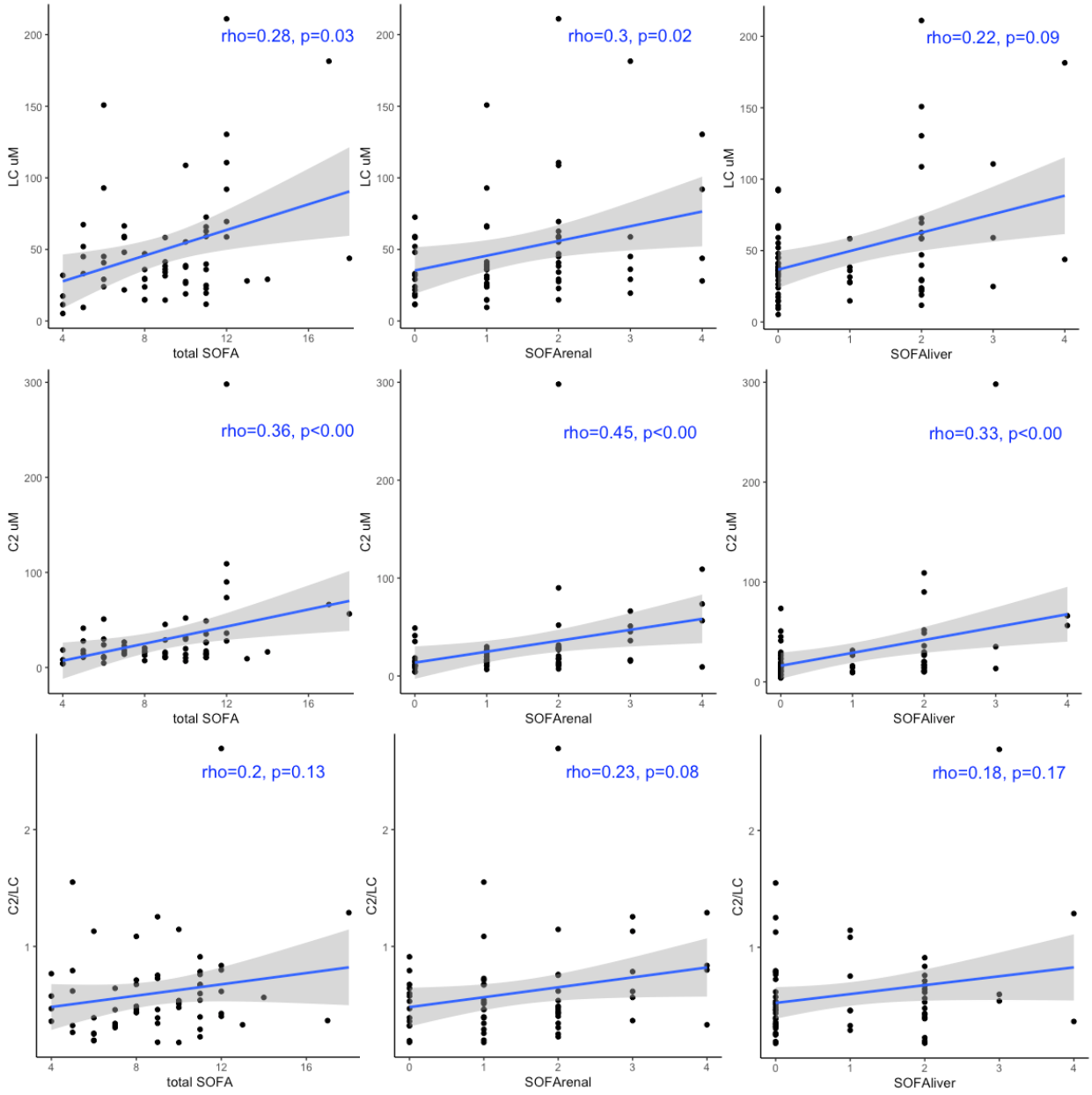

Figure 3-4. Scatter plots between serum LC, C2, C2/LC and SOFA, $SOFA_{renal}$, $SOFA_{liver}$ for the septic shock cohort (RACE; n=61).
Spearman's rank correlation coefficients (rho) with p-values are included. The shaded area represents the 95% confidence interval around the linear regression best fit line. LC= L-carnitine; C2=acetylcarnitine.

Data	Metabolite (y)	Covariate (+Age+Sex+BMI)	slope (p)	adj R^2
RACE	LC	SOFA	0.70 (0.02)	0.09813
RACE	LC	SOFArenal	0.33 (0.07)	0.05438
RACE	LC	SOFAliver	0.42 (0.02)	0.09203
RACE	C2	SOFA	0.84 (<0.00)	0.1746
RACE	C2	SOFArenal	0.62 (<0.00)	0.192
RACE	C2	SOFAliver	0.52 (<0.00)	0.1751
RACE	C2/LC	SOFA	0.15 (0.53)	-0.006383
RACE	C2/LC	SOFArenal	0.29 (0.06)	0.04538
RACE	C2/LC	SOFAliver	0.10 (0.47)	-0.003835
CBR	LC	SOFA	0.19 (0.05)	0.08131
CBR	LC	SOFArenal	0.038 (0.62)	0.05575
CBR	LC	SOFAliver	0.071 (0.47)	0.05779
CBR	C2	SOFA	0.59 (<0.00)	0.1586
CBR	C2	SOFArenal	0.21 (0.04)	0.03045
CBR	C2	SOFAliver	0.38 (<0.00)	0.06847
CBR	C2/LC	SOFA	0.4 (<0.00)	0.1228
CBR	C2/LC	SOFArenal	0.17 (0.02)	0.02993
CBR	C2/LC	SOFAliver	0.31 (<0.00)	0.07596

Table 3-5. Multiple linear regression model results assessing the association between carnitine metabolites and various measures of organ dysfunction.
Adjusted for age, sex, BMI; Metabolites, SOFA variables, and BMI were natural log transformed.

A mouse model of sepsis captures early metabolic changes in blood, kidney, and liver that precede clinically and pathologically detectable organ injury and dysfunction.

Given the associations between metabolites of L-carnitine metabolism and SOFA score in our human cohorts, we first evaluated temporal changes in whole blood levels of LC, C2, and C2/LC. There were no changes in L-carnitine metabolism early in the course of polymicrobial sepsis (6 h). However, alterations in blood L-carnitine were evident by 24 h ($p<0.00$) and progressively declined (30 h, $p<0.00$; 48 h, $p<0.00$) compared with sham animals (**Figure 3-5A**). Similar to observations in the human sepsis data, we found persistent elevations in the blood C2/LC ratio in the CLP mice (24 h, $p<0.00$; 30 h, $p<0.00$; 48 h, $p<0.00$) (**Figure 3-5C**).

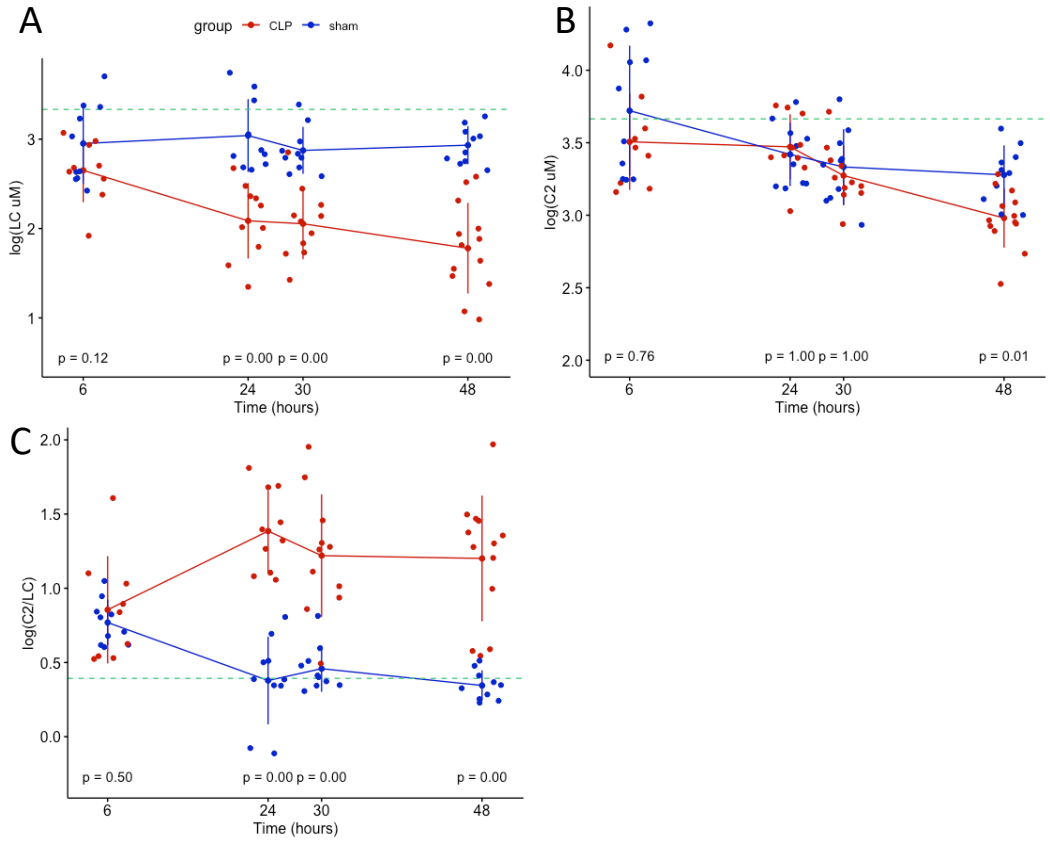

Figure 3-5. Whole blood levels of LC, C2, and C2/LC compared between CLP (red) and sham (blue) animals. Healthy control median value shown by dashed green line with Holm's post-hoc test p-values comparing between CLP and sham per time point. Data were natural log transformed for statistical analysis and are the mean +/- sd.

Despite profound metabolic changes to blood carnitine metabolism, plasma concentrations of creatinine (CRE) and total bilirubin (TBIL), the components of $SOFA_{renal}$ and $SOFA_{liver}$, respectively, were not distinguishable between CLP and sham groups (**Figure 5**). However, other blood measurements of organ function that are not used in the calculation of the SOFA score, such as blood urea nitrogen (BUN), amylase (AMY), total protein (TP), albumin (ALB), and alanine aminotransferase (ALT), became elevated but these changes varied over time and not all were sustained (**Figure 5**). Notably, histological evidence of late-stage apoptotic kidney injury did not occur until 48 hours but was primarily driven by 3 animals (**Figure 6**).

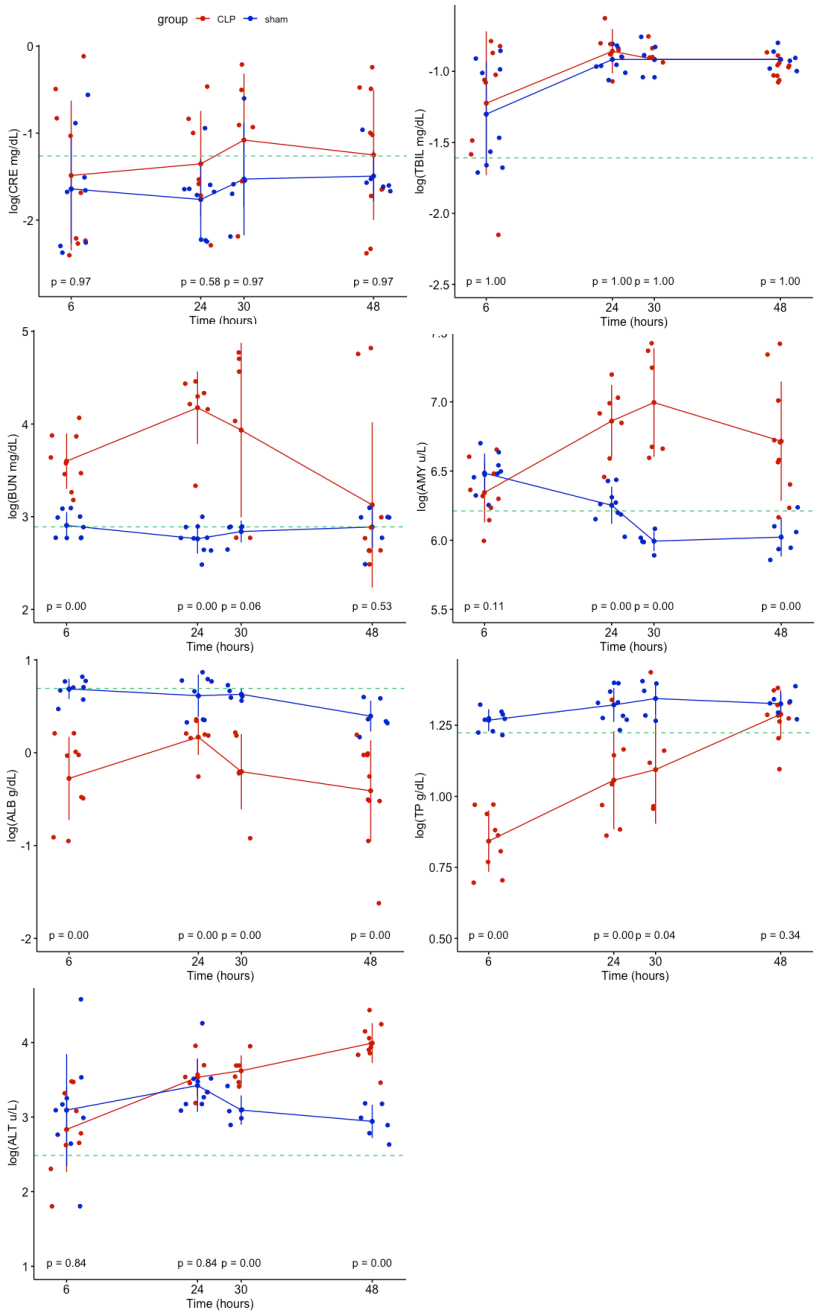

Figure 3-6. Organ function biomarkers compared between CLP (red) and Sham (blue) animals.
Healthy control median value shown by dashed green line with post-hoc p-values included. creatinine (CRE), total bilirubin (TBIL), blood urea nitrogen (BUN), amylase (AMY), albumin (ALB), total protein (TP), and alanine transaminase (ALT)

To understand the findings in blood carnitine metabolites and organ function biomarkers, we measured renal tissue metabolites and found ones that differentiated CLP, sham, and healthy mice using a 2-way ANOVA (**Table 3-6**). Of note, CLP mice had increased concentrations of 3-

hydroxybutyrate, creatine, and histidine over time while adenosine, aspartate, and cystine decreased compared with control animals (**Figure 3-7)**. As a gauge of carnitine metabolic activity, we calculated the organ substrate/product [(acetyl-CoA + L-carnitine)/(acetylcarnitine + CoA)] ratio because it is a surrogate of carnitine acetyltransferase (CAT) activity (**Figure 3-8**). This enzyme catalyzes the production of acetylcarnitine and Coenzyme A (CoA) from acetyl-Coenzyme A and L-carnitine (29). CLP mice had a lower renal CAT activity value compared to sham mice at 24 hours ($p<0.00$), 30 hours ($p=0.01$), and 48 hours ($p<0.00$) (**Figure 3-8A**).

KEGG ID	metabolite	Group (F.val)	Group (adj.p)	Time (F.val)	Time (adj.p)	Interaction (F.val)	Interaction (adj.p)
n/a	CAT	69.99	0.00	3.86	0.02	7.74	0.00
C01089	3-Hydroxybutyrate	52.35	0.00	2.98	0.06	10.43	0.00
C00491	Cystine	50.34	0.00	1.89	0.16	2.25	0.18
C00135	Histidine	41.44	0.00	6.74	0.00	3.15	0.09
C00318	Carnitine (LC)	36.59	0.00	3.04	0.05	1.40	0.39
C00300	Creatine	36.92	0.00	2.41	0.10	11.47	0.00
n/a	Acetyl-CoA/CoA	33.57	0.00	6.30	0.00	8.24	0.00
C00049	Aspartate	33.60	0.00	0.85	0.49	5.47	0.01
C00212	Adenosine	27.37	0.00	3.77	0.03	2.97	0.11
C00025	Glutamate	25.72	0.00	4.03	0.02	0.77	0.60
C00010	Coenzyme A	23.56	0.00	2.02	0.14	8.74	0.00
C00043	UDP-N-Acetylglucosamine	21.53	0.00	3.99	0.02	0.41	0.78
C00543	Dimethylamine	19.90	0.00	3.11	0.05	2.30	0.18
C00189	Ethanolamine	18.40	0.00	13.38	0.00	0.47	0.76
n/a	N-Acetyllactosamine	17.10	0.00	4.84	0.01	2.27	0.18
C00670	sn-Glycero-3-phosphocholine	14.77	0.00	1.13	0.38	9.91	0.00
C01879	Pyroglutamate	14.07	0.00	7.67	0.00	3.24	0.09
C00037	Glycine	13.34	0.00	1.61	0.22	0.31	0.84
C06809	N-Acetylcysteine	12.84	0.00	5.19	0.01	4.17	0.03
C00031	Glucose	12.03	0.00	2.97	0.06	1.22	0.41
C00058	Formate	9.98	0.01	1.00	0.42	2.00	0.23
C00123	Leucine	6.96	0.03	4.42	0.02	1.43	0.39
C01380	Ethylene glycol	6.48	0.03	2.73	0.07	0.59	0.68

*Table 3-6. 2-way ANOVA results of renal metabolites with group, time, and group*time interaction statistics.*
Carnitine acetyltransferase (CAT) = (acetyl-CoA + carnitine)/(acetylcarnitine + CoA)

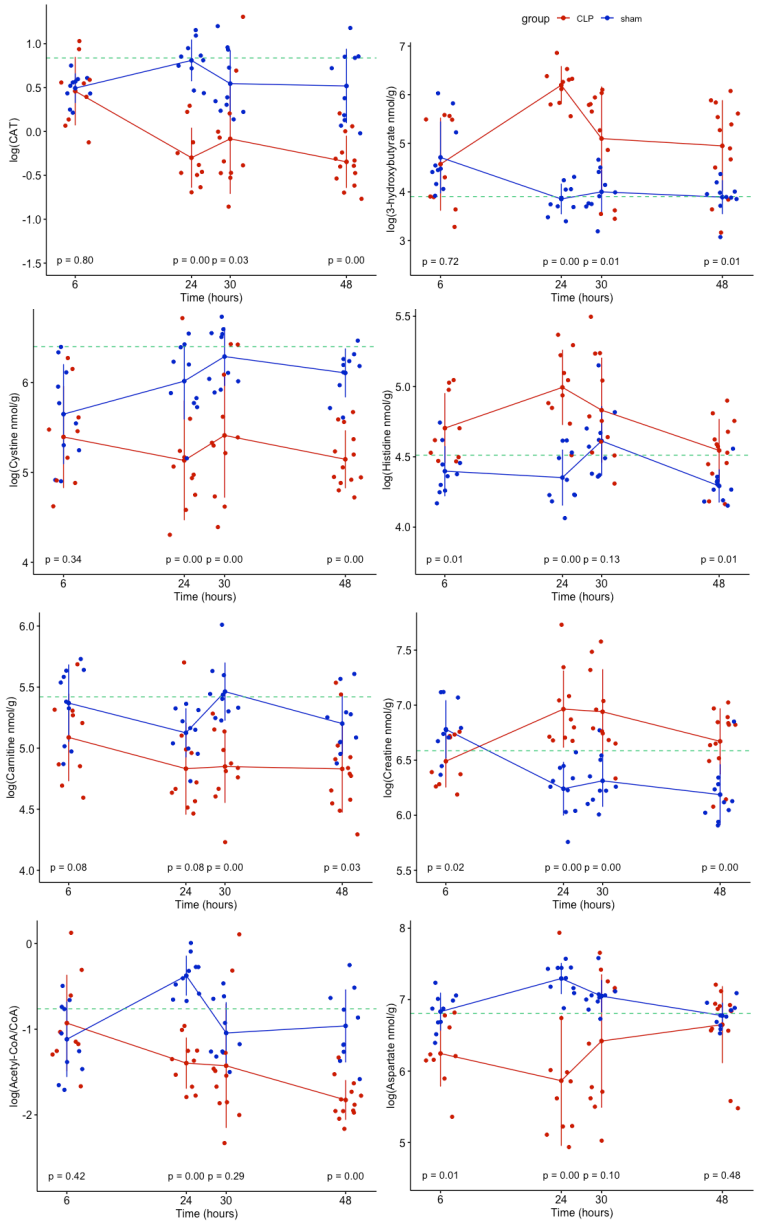

Figure 3-7. Differentiating renal tissue metabolites in the CLP (red) and sham (blue) subjects plotted over time. Adjusted ANOVA Holm's test post-hoc p-values shown per timepoint comparison. The median values for the healthy control animals are represented by the dashed green line. Data are nmol/g of protein that were log transformed for statistical analysis and are the mean +/- sd. Sample sizes were 10 animals for each group at 6 and 24 hours, and 11 at 30 hours and 14 at 48 hours.

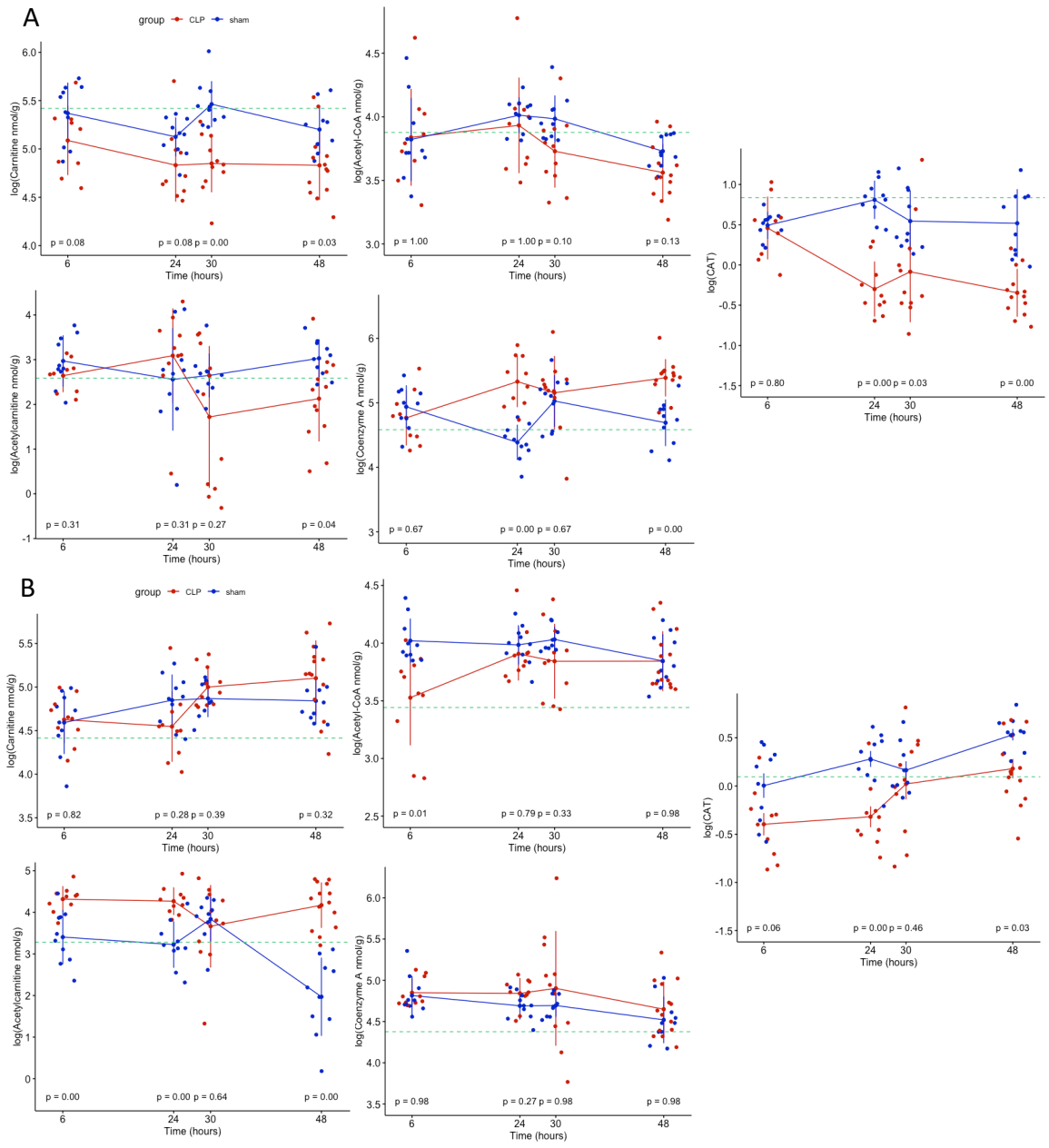

Figure 3-8. Carnitine acetyltransferase substrate and product (A) renal and (B) liver metabolites in the CLP (red) and sham (blue) subjects plotted over time.
Adjusted ANOVA Holm's post-hoc test for multiple comparisons p-values is shown for each timepoint comparison. The median values for the healthy control animals are represented by the dashed green line. Data are nmol/g of protein that were log transformed for statistical analysis and are the mean +/- sd. Sample sizes were 10 animals for each group at 6 and 24 hours, and 11 at 30 hours and 14 at 48 hours. Carnitine acetyltransferase (CAT) = (acetyl-CoA + carnitine)/(acetylcarnitine + CoA)

We applied the same statistical approach to assess changes in liver tissue metabolites (**Table 3-7**). In the liver, CLP mice had elevated levels of 3-hydroxybutyrate, 2-hydroxybutyrate,

N,N-Dimethylglycine, cytidine monophosphate, creatine, uridine monophosphate (UMP), 2-aminobutyrate, and C2 over time (**Figure 3-9)**. CLP mice had a lower liver CAT activity compared to sham (6 hours p=0.06; 24 hours p<0.00, 48 hours p=0.03) (**Figure 3-8B**). The sham metabolite levels closely tracked with the median values from healthy control mice.

KEGG ID	metabolite	Group (F.val)	Group (raw.p)	Group (adj.p)	Time (F.val)	Time (raw.p)	Time (adj.p)
C01089	3-Hydroxybutyrate	99.24	0.00	0.00	4.11	0.01	0.02
C05984	2-Hydroxybutyrate	96.15	0.00	0.00	8.55	0.00	0.00
C01026	N,N-Dimethylglycine	79.39	0.00	0.00	4.61	0.01	0.01
C00055	Cytidine monophosphate	77.50	0.00	0.00	5.27	0.00	0.00
C00300	Creatine	75.63	0.00	0.00	1.96	0.13	0.16
C00105	UMP	65.60	0.00	0.00	8.28	0.00	0.00
C02356	2-Aminobutyrate	58.38	0.00	0.00	23.47	0.00	0.00
C02571	Acetylcarnitine (C2)	57.08	0.00	0.00	5.36	0.00	0.00
C00051	Glutathione	54.15	0.00	0.00	7.45	0.00	0.00
C00041	Alanine	47.68	0.00	0.00	10.61	0.00	0.00
C00135	Histidine	33.57	0.00	0.00	7.79	0.00	0.00
C00064	Glutamine	31.99	0.00	0.00	9.20	0.00	0.00
C00144	Guanosine monophosphate	29.24	0.00	0.00	2.62	0.06	0.08
C00079	Phenylalanine	27.62	0.00	0.00	0.41	0.75	0.77
C00719	Betaine	26.77	0.00	0.00	7.39	0.00	0.00
C00049	Aspartate	26.42	0.00	0.00	32.32	0.00	0.00
C00042	Succinate	25.92	0.00	0.00	1.37	0.26	0.30
C00588	O-Phosphocholine	25.22	0.00	0.00	8.79	0.00	0.00
C00043	UDP-N-Acetylglucosamine	24.67	0.00	0.00	10.47	0.00	0.00
C00082	Tyrosine	24.52	0.00	0.00	12.70	0.00	0.00
C00543	Dimethylamine	24.23	0.00	0.00	7.73	0.00	0.00
n/a	CAT	23.34	0.00	0.00	9.59	0.00	0.00
C00245	Taurine	23.44	0.00	0.00	1.87	0.14	0.17
C00033	Acetate	21.66	0.00	0.00	12.91	0.00	0.00
C06809	N-Acetylcysteine	21.51	0.00	0.00	9.31	0.00	0.00
n/a	Acetyl-CoA/CoA	19.30	0.00	0.00	3.96	0.01	0.02
C00847	4-Pyridoxate	18.50	0.00	0.00	7.19	0.00	0.00
C00299	Uridine	15.14	0.00	0.00	5.51	0.00	0.00
C00020	AMP	10.93	0.00	0.00	2.80	0.05	0.06
C00010	Acetyl-Coenzyme A	10.36	0.00	0.00	1.92	0.13	0.16
C00130	IMP	9.71	0.00	0.00	2.29	0.08	0.11
C00052	UDP-galactose	10.25	0.00	0.00	3.11	0.03	0.05
C00137	myo-Inositol	9.14	0.00	0.01	10.14	0.00	0.00
C00029	UDP-glucose	7.98	0.01	0.01	5.92	0.00	0.00
C00711	Malate	7.10	0.01	0.02	16.98	0.00	0.00
C00208	Maltose	6.25	0.01	0.03	4.08	0.01	0.02
C00047	Lysine	5.97	0.02	0.03	5.84	0.00	0.00
C00159	Mannose	5.76	0.02	0.03	5.22	0.00	0.00
C00073	Methionine	5.75	0.02	0.03	0.69	0.56	0.59
C00611	N-Acetyllactosamine	5.40	0.02	0.04	1.25	0.30	0.34
C00152	Asparagine	5.06	0.03	0.05	0.73	0.54	0.58
C01835	Maltotriose	4.97	0.03	0.05	2.47	0.07	0.09
C00077	Ornithine	4.97	0.03	0.05	3.49	0.02	0.03

*Table 3-7. 2-way ANOVA results of liver metabolites with group, time, and group*time interaction statistics*

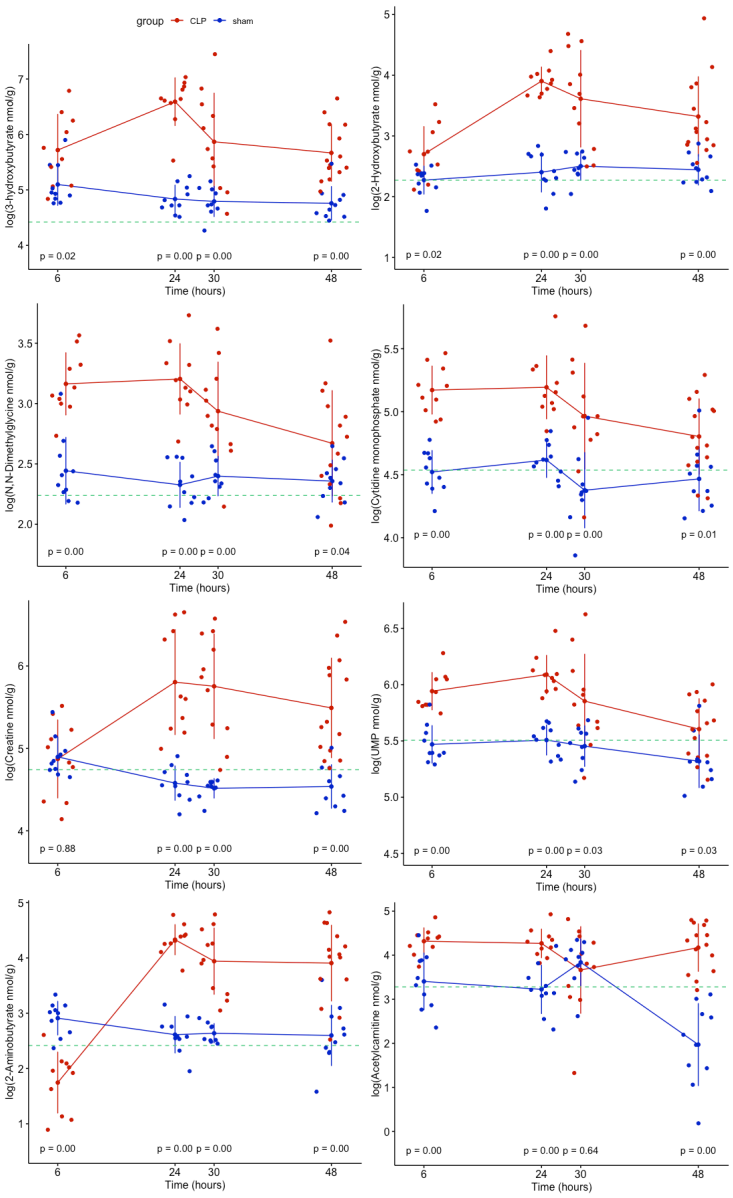

Figure 3-9. Differentiating liver metabolites in the CLP (red) and sham (blue) subjects are plotted over time Adjusted ANOVA Holm's test post-hoc p-values shown per timepoint comparison. The median values for the healthy control animals are represented by the dashed green line. Data are nmol/g of protein that were log transformed for statistical analysis and are the mean +/- sd. Sample sizes were 10 animals for each group at 6 and 24 hours, and 11 at 30 hours and 14 at 48 hours.

To better understand the unique metabolic signals perturbed by sepsis in each organ, the differentiating metabolite concentrations of the kidneys and liver were used in separate pathway analyses. We found that for the 23 differentiating renal tissue metabolites, 27 metabolic pathways were significantly different between the CLP and sham animals (**Figure 3-10A**). The

top five pathways based on the impact score were D-glutamine and D-glutamate metabolism; alanine, aspartate and glutamate metabolism; glycine, serine and threonine metabolism; histidine metabolism; and pantothenate and CoA biosynthesis (**Table 3-8**). For the 30 differentiating liver tissue metabolites, 40 metabolic pathways differentiated CLP and sham animals (**Figure 3-10B**). The top 5 pathways based on pathway impact were phenylalanine, tyrosine and tryptophan biosynthesis; taurine and hypotaurine metabolism; phenylalanine metabolism; alanine, aspartate and glutamate metabolism; and glutathione metabolism (**Table 3-9**).

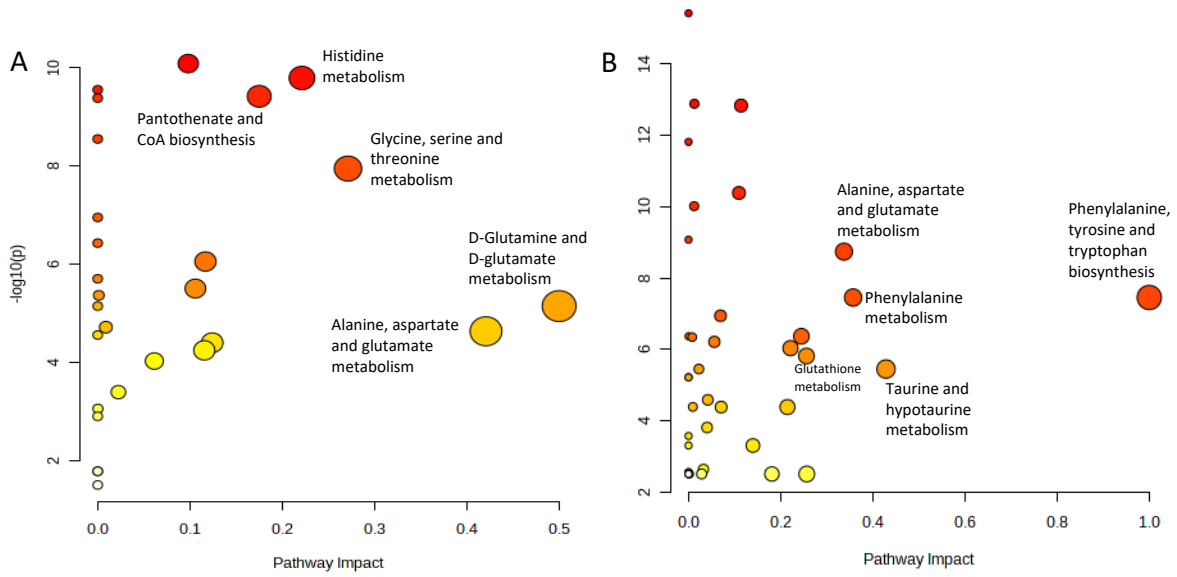

Figure 3-10. Murine metabolic pathway analysis of the differentiating metabolites from the (A) kidney, and (B) liver generated by MetaboAnalyst.
The top 5 pathways based on pathway impact are annotated. Metabolite concentrations from all time points were included from both CLP and sham animals.

Pathway	Total compounds	Hits	Raw p	-LOG10(p)	Holm adjust	FDR	Impact
D-Glutamine and D-glutamate metabolism	6	1	7.03E-06	5.153	9.84E-05	1.27E-05	0.5
Alanine, aspartate and glutamate metabolism	28	3	2.29E-05	4.641	0.0002514	3.63E-05	0.42068
Glycine, serine and threonine metabolism	34	2	1.12E-08	7.9491	2.36E-07	4.34E-08	0.27117
Histidine metabolism	16	3	1.62E-10	9.7913	4.20E-09	2.18E-09	0.22131
Pantothenate and CoA biosynthesis	19	2	3.82E-10	9.4185	9.16E-09	2.24E-09	0.175
Fatty acid degradation	39	1	3.91E-05	4.4074	0.00035225	5.56E-05	0.12404
Arginine biosynthesis	14	2	8.73E-07	6.0591	1.57E-05	2.36E-06	0.11675
Glutathione metabolism	28	3	5.58E-05	4.2533	0.00044646	7.53E-05	0.11548
Glyoxylate and dicarboxylate metabolism	32	3	3.09E-06	5.51	4.94E-05	6.95E-06	0.10582
Arginine and proline metabolism	38	2	8.23E-11	10.085	2.22E-09	2.18E-09	0.09812
Glycerophospholipid metabolism	36	2	9.21E-05	4.0355	0.00064503	0.00011848	0.06138
Primary bile acid biosynthesis	46	1	0.000395	3.4034	0.00237	0.00048478	0.02239
Amino sugar and nucleotide sugar metabolism	37	1	1.89E-05	4.7241	0.0002265	3.19E-05	0.00882
Purine metabolism	66	1	4.24E-06	5.3725	6.36E-05	8.81E-06	0.00117
Glycolysis / Gluconeogenesis	26	1	0.00085597	3.0675	0.0042799	0.0010048	0.00021
Butanoate metabolism	15	2	2.81E-10	9.5517	7.02E-09	2.24E-09	0
beta-Alanine metabolism	21	2	4.14E-10	9.3826	9.53E-09	2.24E-09	0
Cysteine and methionine metabolism	33	1	2.81E-09	8.5507	6.19E-08	1.27E-08	0
Synthesis and degradation of ketone bodies	5	1	1.11E-07	6.9556	2.22E-06	3.74E-07	0
Aminoacyl-tRNA biosynthesis	48	6	3.69E-07	6.4333	7.01E-06	1.11E-06	0
Nicotinate and nicotinamide metabolism	15	1	1.96E-06	5.7087	3.32E-05	4.80E-06	0
Nitrogen metabolism	6	1	7.03E-06	5.153	9.84E-05	1.27E-05	0
Porphyrin and chlorophyll metabolism	30	2	2.72E-05	4.5655	0.00027197	4.08E-05	0
Ether lipid metabolism	20	1	0.0012258	2.9116	0.0049031	0.001379	0
Valine, leucine and isoleucine degradation	40	1	0.016043	1.7947	0.048129	0.01666	0
Valine, leucine and isoleucine biosynthesis	8	1	0.016043	1.7947	0.048129	0.01666	0
Selenocompound metabolism	20	1	0.030504	1.5156	0.048129	0.030504	0

Table 3-8. Metabolic pathway analysis results using differentiating renal metabolites.

Pathway	Total compounds	Hits	Raw p	-LOG10(p)	Holm adjust	FDR	Impact
Phenylalanine, tyrosine and tryptophan biosynthesis	4	2	3.54E-08	7.4507	1.13E-06	1.42E-07	1
Taurine and hypotaurine metabolism	8	1	3.58E-06	5.4461	8.23E-05	7.54E-06	0.42857
Phenylalanine metabolism	12	2	3.54E-08	7.4507	1.13E-06	1.42E-07	0.35714
Alanine, aspartate and glutamate metabolism	28	3	1.83E-09	8.7372	6.04E-08	9.16E-09	0.33734
Fatty acid elongation	39	1	0.0031265	2.5049	0.027896	0.0031265	0.25661
Glutathione metabolism	28	2	1.55E-06	5.8107	3.71E-05	3.64E-06	0.25596
Purine metabolism	66	4	4.31E-07	6.3653	1.25E-05	1.31E-06	0.24495
Histidine metabolism	16	2	9.29E-07	6.0318	2.32E-05	2.32E-06	0.22131
Pyruvate metabolism	22	2	4.17E-05	4.38	0.000741	6.67E-05	0.21462
Fatty acid degradation	39	1	0.0031265	2.5049	0.027896	0.0031265	0.18092
Tyrosine metabolism	42	1	0.00049842	3.3024	0.0064795	0.00068748	0.13972
Glycine, serine and threonine metabolism	34	3	1.48E-13	12.83	5.62E-12	1.97E-12	0.11397
Pyrimidine metabolism	39	4	4.15E-11	10.382	1.50E-09	3.32E-10	0.10946
Glycolysis / Gluconeogenesis	26	2	4.17E-05	4.38	0.000741	6.67E-05	0.07075
Citrate cycle (TCA cycle)	20	2	1.15E-07	6.9395	3.45E-06	4.18E-07	0.06941
beta-Alanine metabolism	21	3	6.18E-07	6.209	1.61E-05	1.65E-06	0.05597
Cysteine and methionine metabolism	33	1	2.62E-05	4.5821	0.00049734	4.76E-05	0.04179
Amino sugar and nucleotide sugar metabolism	37	2	0.00015583	3.8074	0.0023374	0.00023974	0.04019
Galactose metabolism	27	1	0.0023227	2.634	0.02555	0.003097	0.03235
Valine, leucine and isoleucine degradation	40	1	0.0031265	2.5049	0.027896	0.0031265	0.02836
Primary bile acid biosynthesis	46	1	3.58E-06	5.4461	8.23E-05	7.54E-06	0.02239
Propanoate metabolism	23	3	1.32E-13	12.881	5.13E-12	1.97E-12	0.01269
Arginine and proline metabolism	38	1	9.73E-11	10.012	3.41E-09	6.49E-10	0.01212
Glycerophospholipid metabolism	36	1	4.12E-05	4.3855	0.000741	6.67E-05	0.00937
Glyoxylate and dicarboxylate metabolism	32	3	4.57E-07	6.3402	1.25E-05	1.31E-06	0.00794
Fatty acid biosynthesis	47	1	0.0031265	2.5049	0.027896	0.0031265	0.00213
Butanoate metabolism	15	3	3.82E-16	15.418	1.53E-14	1.53E-14	0
Synthesis and degradation of ketone bodies	5	2	1.54E-12	11.813	5.70E-11	1.54E-11	0
Aminoacyl-tRNA biosynthesis	48	5	8.48E-10	9.0714	2.88E-08	4.85E-09	0
Arginine biosynthesis	14	2	4.33E-07	6.3634	1.25E-05	1.31E-06	0
D-Glutamine and D-glutamate metabolism	6	1	6.09E-06	5.2153	0.00012792	1.16E-05	0
Nitrogen metabolism	6	1	6.09E-06	5.2153	0.00012792	1.16E-05	0
Vitamin B6 metabolism	9	1	0.00026959	3.5693	0.0037743	0.00039939	0
Ubiquinone and other terpenoid-quinone biosynthesis	9	1	0.00049842	3.3024	0.0064795	0.00068748	0
Nicotinate and nicotinamide metabolism	15	1	0.0027896	2.5545	0.027896	0.0031265	0
Pantothenate and CoA biosynthesis	19	1	0.0027896	2.5545	0.027896	0.0031265	0
Lysine degradation	25	1	0.0031265	2.5049	0.027896	0.0031265	0
Tryptophan metabolism	41	1	0.0031265	2.5049	0.027896	0.0031265	0
Inositol phosphate metabolism	30	1	0.0031265	2.5049	0.027896	0.0031265	0
Terpenoid backbone biosynthesis	18	1	0.0031265	2.5049	0.027896	0.0031265	0

Table 3-9. Metabolic pathway analysis results using differentiating liver metabolites.

The blood C2/LC ratio is associated with differentiating organ metabolites and organ function biomarkers in the sepsis mouse model.

Since there were correlations between blood C2/LC ratio and all three SOFA measurements ($SOFA_{total}$, $SOFA_{renal}$ and $SOFA_{liver}$) in the human sepsis cohort (**Figure 3-3**) and this signal was also evident in our mouse model, we identified organ metabolites that were

associated with it (**Figure 3-11** and **Table 3-10**). Many of the metabolites correlated to blood C2/LC ratio (11/14 renal; 15/22 liver) were also differentiating between CLP and sham animals, highlighting the sepsis-induced metabolic changes in the organs are reflected in the blood (**Tables 3-6 and 3-7**). The top 10 metabolites that correlated with blood C2/LC ratio were 3-hydroxybutyrate (renal; liver), 2-hydroxybutyrate (liver), creatine (renal; liver), 2-aminobutyrate (liver), glucose (renal, liver), maltotriose (liver), and cystine (renal). Likewise, BUN and AMY were correlated with the C2/LC ratio, respectively ($r= 0.4$, $p=0.003$; $r= 0.5$, $p<0.000$), showing a connection between blood L-carnitine metabolism and organ dysfunction. Various renal and liver metabolites were also found to be correlated with BUN and AMY (**Figure 3-12**), further establishing a connection between organ metabolism and function.

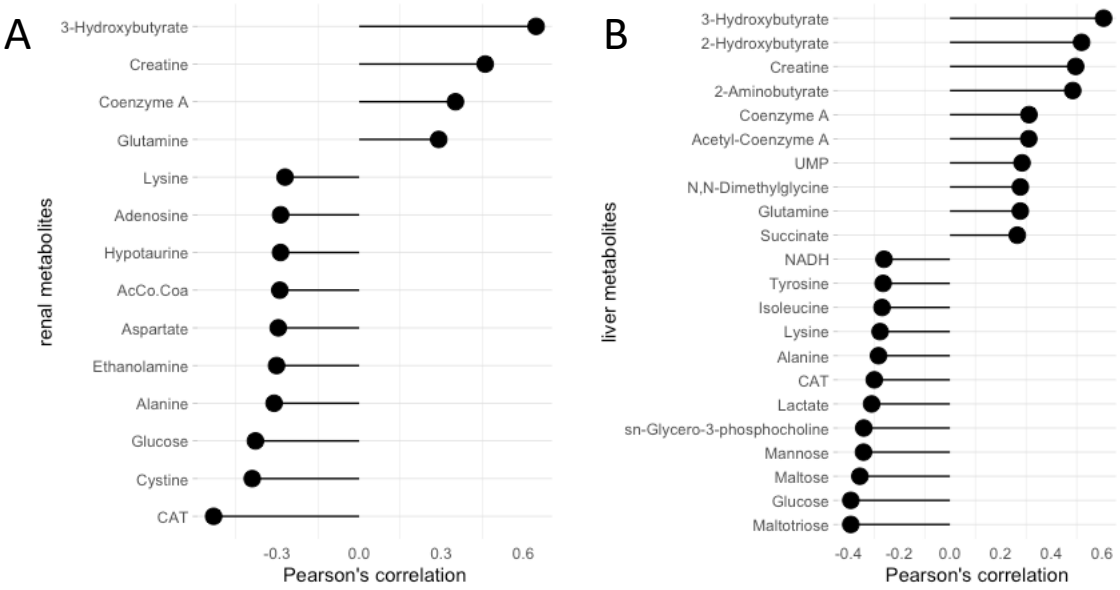

Figure 3-11. Partial correlations between (A) renal and (B) liver metabolites with whole blood C2/LC. Correlations were adjusted for group, sex, and time and corrected for multiple comparisons. Correlations with $p<0.05$ were included. Values reported in Table 3-10.

organ	metabolite	correlation	t-stat	p-value	FDR
kidney	3-Hydroxybutyrate	0.64655	7.9504	5.85E-12	1.90E-10
	CAT	-0.53161	-5.8878	6.99E-08	1.52E-06
	Creatine	0.46061	4.8681	4.92E-06	7.99E-05
	Cystine	-0.3907	-3.9816	0.00014053	0.0018269
	Glucose	-0.37886	-3.8402	0.00023127	0.0025054
	Coenzyme A	0.35191	3.5269	0.00067048	0.0062259
	Alanine	-0.31059	-3.0652	0.0028886	0.02347
	Ethanolamine	-0.3017	-2.9685	0.0038545	0.027838
	Aspartate	-0.29554	-2.9021	0.0046835	0.028437
	Glutamine	0.29076	2.8507	0.0054336	0.028437
	Acetyl-CoA/CoA	-0.28989	-2.8414	0.0055811	0.028437
	Hypotaurine	-0.28718	-2.8124	0.0060623	0.028437
	Adenosine	-0.28684	-2.8088	0.0061249	0.028437
	Lysine	-0.27077	-2.6387	0.0098429	0.042653
liver	3-Hydroxybutyrate	0.60611	7.189	1.94E-10	7.16E-09
	2-Hydroxybutyrate	0.51932	5.733	1.33E-07	3.28E-06
	Creatine	0.49595	5.3881	5.77E-07	1.07E-05
	2-Aminobutyrate	0.48446	5.2243	1.14E-06	1.69E-05
	Maltotriose	-0.39125	-4.0107	0.00012572	0.0013342
	Glucose	-0.39116	-4.0096	0.00012621	0.0013342
	Maltose	-0.35537	-3.5866	0.00054687	0.0050585
	Mannose	-0.34112	-3.4235	0.00093642	0.007207
	sn-Glycero-3-phosphocholine	-0.34006	-3.4114	0.00097391	0.007207
	Coenzyme A	0.31179	3.0958	0.0026247	0.016346
	Acetyl-Coenzyme A	0.31102	3.0873	0.0026933	0.016346
	Lactate	-0.30909	-3.0661	0.0028715	0.016346
	CAT	-0.29854	-2.951	0.0040478	0.021396
	UMP	0.28444	2.799	0.0062848	0.031005
	Alanine	-0.28184	-2.7712	0.0067989	0.031445
	N,N-Dimethylglycine	0.27773	2.7274	0.0076886	0.031836
	Glutamine	0.27749	2.7249	0.007744	0.031836
	Lysine	-0.27566	-2.7054	0.0081748	0.031839
	Isoleucine	-0.26798	-2.6241	0.010223	0.037826
	Succinate	0.26555	2.5985	0.010957	0.038612
	Tyrosine	-0.26372	-2.5793	0.011541	0.03882
	NADH	-0.2603	-2.5434	0.012705	0.040878

Table 3-10. Partial Pearson's correlations between organ metabolites and whole blood C2/LC.
Correlations were adjusted for group, sex, and time.

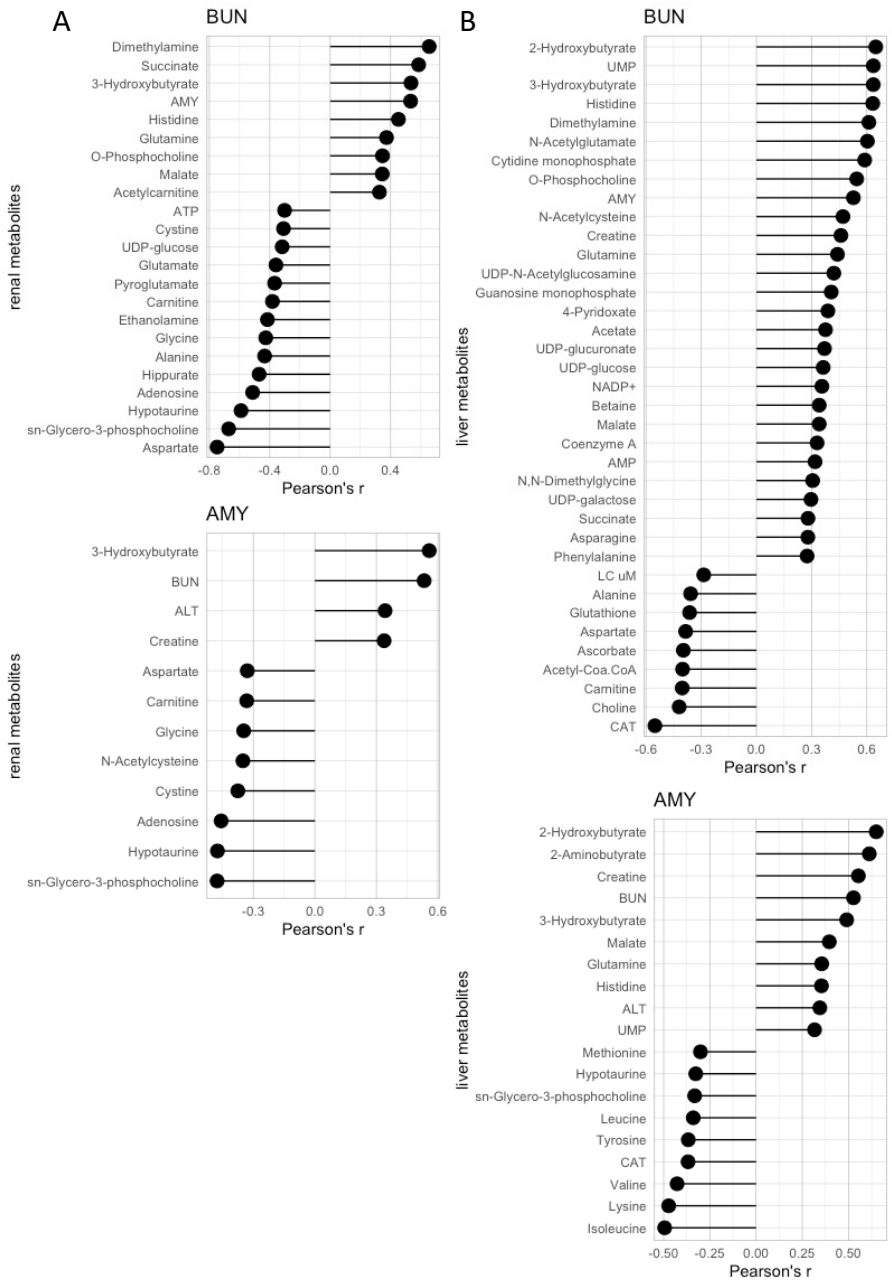

Figure 3-12. Partial Pearson's correlations between (A) renal and (B) liver metabolites with plasma organ function markers, AMY and BUN.
Correlations with $p<0.05$ were included.

Several differentiating metabolites of murine sepsis-induced organ dysfunction are correlated with sepsis-induced organ dysfunction in humans.

We assessed the relationships between the common differentiating metabolites of the kidneys and liver identified in our mouse model with measures of sepsis-induced organ dysfunction in our human cohorts (**Table 3-11**). Consistent with our initial findings (**Figure 3-2**), the metabolic signals of organ dysfunction were more pronounced in patients with sepsis (CBR). Notable, blood levels of histidine, malate, and alanine were positively related to $SOFA_{total}$, $SOFA_{renal}$ and $SOFA_{liver}$ scores; glutamate and aspartate were negatively correlated (**Figure 3-13**). In patients with septic shock (RACE), histidine, lactate, glutamine, and alanine were positively correlated with $SOFA_{total}$, $SOFA_{renal}$ and $SOFA_{liver}$ scores (**Figure 3-14**). To adjust for age, sex, and BMI we conducted multiple linear regressions with the significantly correlated metabolites (**Table 3-12**).

Creatine	Histidine	Aspartate	Lactate
Glutamate	Leucine	Glutamine	Alanine
Succinate	Malate	Taurine	Asparagine
3-hydroxybutyrate*			

Table 3-11. Common metabolites between the sepsis (CBR) and septic shock (RACE) cohorts and the detected compounds in the mouse renal and liver samples.
*indicates a metabolite not detected in CBR, but was found in the other data sets

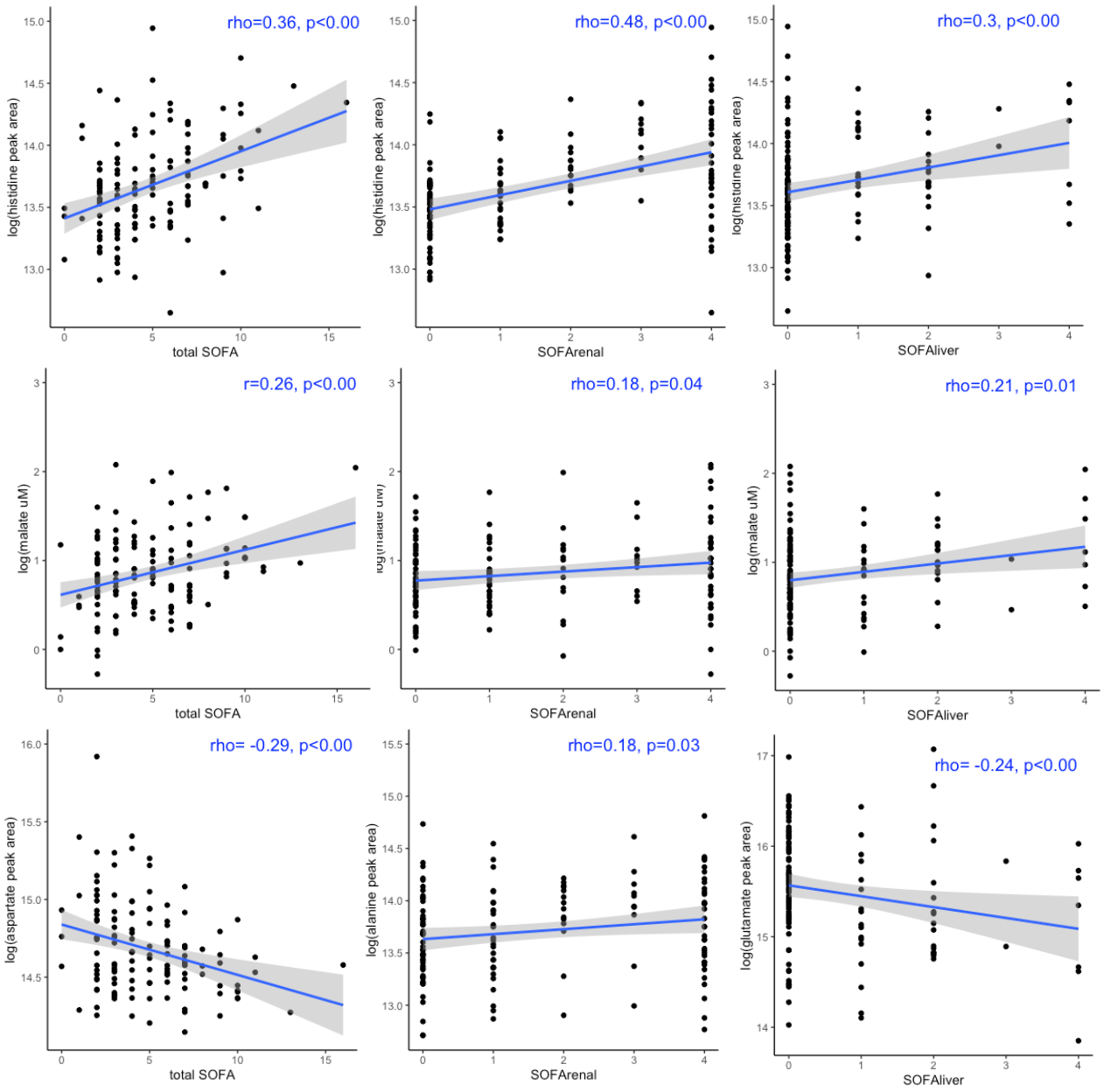

Figure 3-13. Spearman's rank correlations between metabolites and organ dysfunction variables ($SOFA_{total}$, $SOFA_{renal}$, and $SOFA_{liver}$) using the septic cohort (CBR n=134).

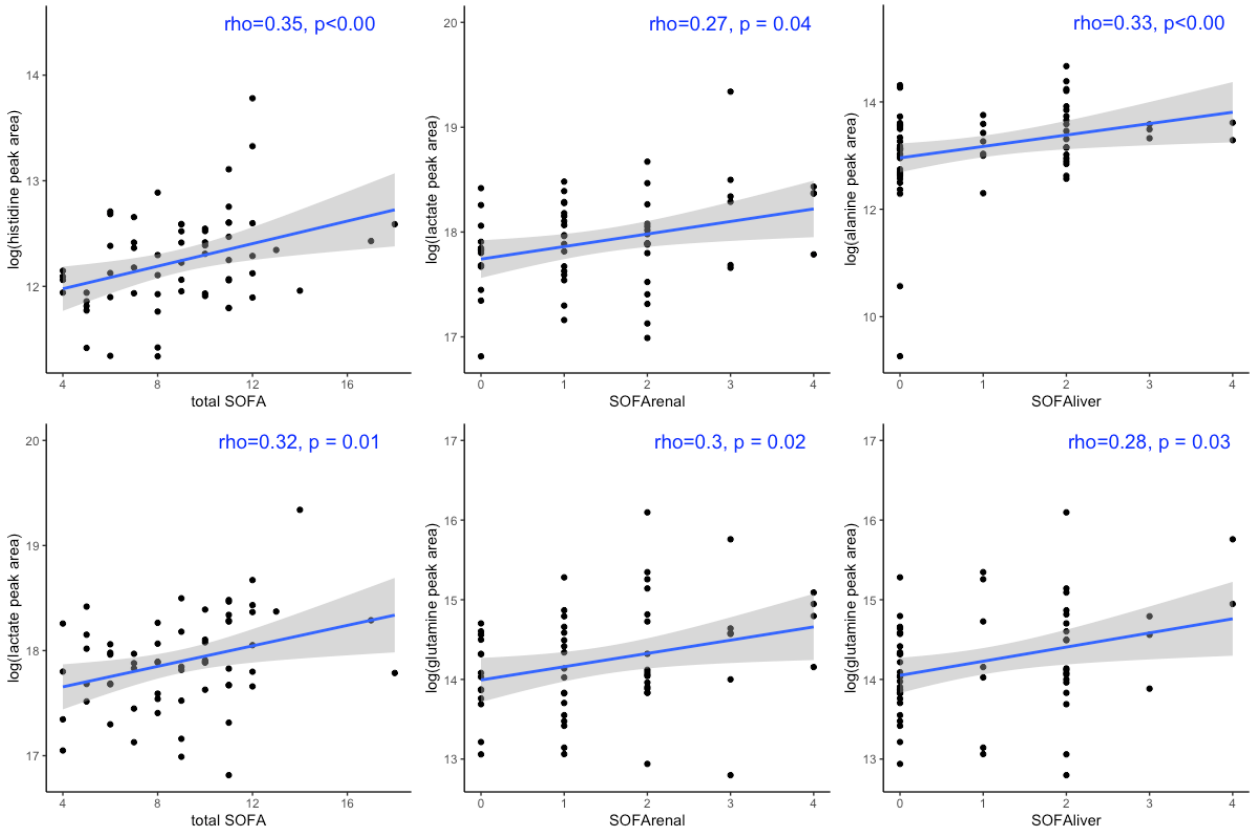

Figure 3-14. Spearman's rank correlations between metabolites and organ dysfunction variables ($SOFA_{total}$, $SOFA_{renal}$, and $SOFA_{liver}$) using the septic shock cohort (RACE, n=61)

Data	Metabolite (y)	Covariate (+Age+Sex+BMI)	slope (p)	adj R^2
RACE	histidine	SOFA	0.34 (0.06)	0.106
RACE	glutamine	SOFA	0.41 (0.14)	0.03004
RACE	lactate	SOFArenal	0.25 (0.05)	0.03089
RACE	glutamine	SOFArenal	0.34 (0.07)	0.0497
RACE	glutamine	SOFAliver	0.27 (0.12)	0.03388
RACE	alanine	SOFAliver	0.35 (0.08)	0.1026
CBR	histidine	SOFA	0.27 (<0.00)	0.1231
CBR	aspartate	SOFA	-0.17 (<0.00)	0.09326
CBR	glutamate	SOFA	-0.27 (0.01)	0.1136
CBR	leucine	SOFA	-0.14 (0.04)	0.03745
CBR	alanine	SOFA	0.16 (0.03)	0.04183
CBR	succinate	SOFA	0.11 (0.12)	0.03369
CBR	malate	SOFA	0.28 (<0.00)	0.09237
CBR	asparagine	SOFA	0.15 (0.01)	0.03092
CBR	histidine	SOFArenal	0.28 (<0.00)	0.2357
CBR	alanine	SOFArenal	0.12 (0.04)	0.04104
CBR	succinate	SOFArenal	0.11 (0.04)	0.04588
CBR	malate	SOFArenal	0.12 (0.04)	0.01695
CBR	histidine	SOFAliver	0.27 (<0.00)	0.1231
CBR	glutamate	SOFAliver	-0.29 (<0.00)	0.1259
CBR	malate	SOFAliver	0.28 (<0.00)	0.09237
CBR	asparagine	SOFAliver	0.12 (0.04)	0.01637

Table 3-12. Multiple linear regression results of differentiating metabolites in the mouse organs were assessed in the human cohorts.
Adjusted for age, sex, and BMI. All continuous variables were natural log-transformed.

Metabolite/Variable	Kidney tissue	Liver tissue	p-value*
L-Carnitine (LC), nmol/g (IQR)	225.9 (197.5, 334.7)	82.7 (64.8, 107)	0.002
Acetylcarnitine (C2), nmol/g (IQR)	13.3 (9.8, 21.4)	26.7 (14, 35.8)	0.03
C2/LC ratio (IQR)	0.06 (0.05, 0.07)	0.27 (0.15, 0.43)	0.002
CAT activity ([(acetyl-CoA + L-carnitine)/(acetylcarnitine + CoA)] (IQR)	2.3 (1.9, 2.7)	1.1 (0.8, 1.3)	0.006

Table 3-13. Kidney and liver tissue carnitine environments in healthy mice (12-13 weeks old).
Data are median values of 10 mice/group; *generated from a Wilcoxon matched pairs signed rank test

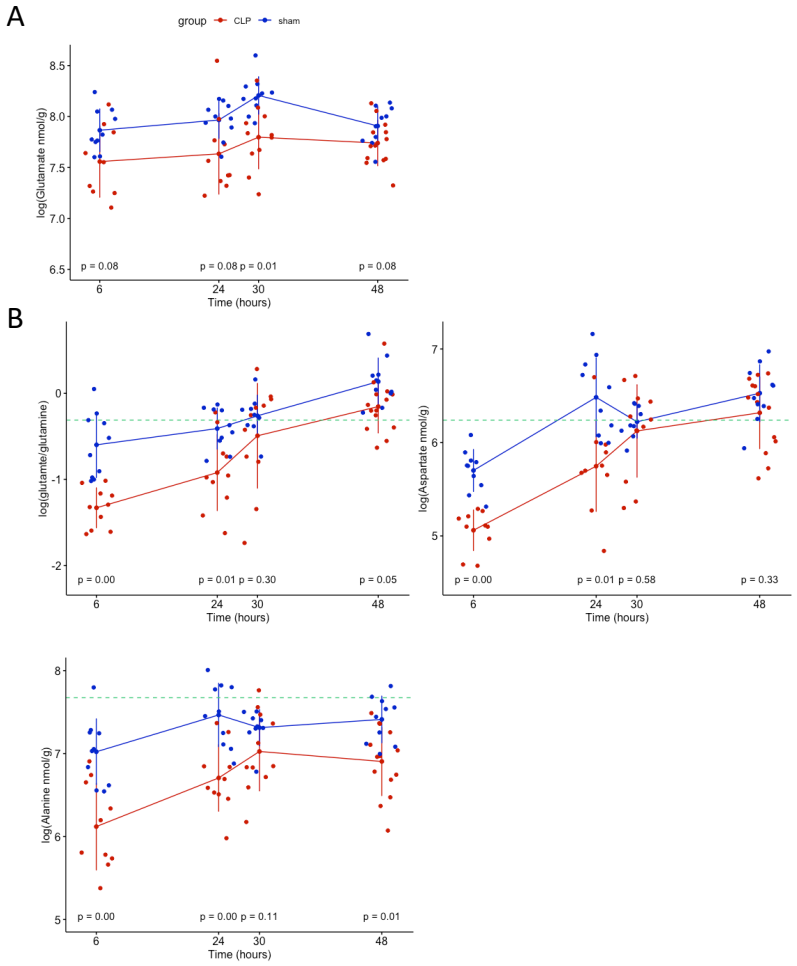

Figure 3-15. Additional differentiating metabolites from the (A) kidneys and (B) livers in the CLP (red) and sham (blue) subjects are plotted over time.
Adjusted ANOVA Holm's test post-hoc p-values shown per timepoint comparison. The median values for the healthy control animals are represented by the dashed green line. Data are nmol/g of protein that were log transformed for statistical analysis and are the mean +/- sd. Sample sizes were 10 animals for each group at 6 and 24 hours, and 11 at 30 hours and 14 at 48 hours.

3.2.4 Discussion

We demonstrate that patients with sepsis and septic shock have distinct blood carnitine metabolite signatures. This was evidenced, in part, by disruption in L-carnitine homeostasis (C2/LC ratio ≥ 0.4 (30)) that was present in approximately 20% and 80% of our sepsis and septic shock patients, respectively. Acetylcarnitine (C2) correlated with $SOFA_{total}$, $SOFA_{renal}$ and $SOFA_{liver}$ in both cohorts. We also found that sepsis patients had evidence of broader derangement in energy metabolism than septic shock patients that correlated with organ dysfunction (as measured by SOFA score) and this signature for either sepsis or septic shock, did not include lactate. Furthermore, the metabolic signatures associated with $SOFA_{renal}$ and $SOFA_{liver}$ were unique. To interrogate these findings, we used a mouse model of polymicrobial sepsis and found that many of these metabolites are distinguishing features at the organ level (kidneys and livers) and do not correlate with the clinically used laboratory values for $SOFA_{renal}$ and $SOFA_{liver}$. These metabolic changes also precede organ-level cellular injury. Collectively, our findings implicate organ level metabolic disruptions that occur early in the course of sepsis are detectable in the blood prior to clinical evidence of organ injury or dysfunction and persist in the later stages of human sepsis and septic shock.

The current clinical paradigm does not accurately capture sepsis-induced metabolic stress of which loss of L-carnitine homeostasis is a key contributor (31). This disruption in mitochondrial metabolic function also extends to the tricarboxylic acid (TCA) cycle. We used an experimental model to show that sepsis-induced metabolic stress is evident in kidney and liver tissue and correlates to the extent of L-carnitine homeostasis loss as measured by the C2/LC ratio in the blood; this was not captured by the correlates of $SOFA_{renal}$ (CRE) and $SOFA_{liver}$ (TBIL).

This is important because metabolic disruptions were evident in renal and liver tissue early (6 hours) after CLP surgery (**Figures 3-7 and 3-9**), suggesting that alterations in metabolic function occur during similar timeframe as the immune response (32). These alterations included organ level changes in carnitine metabolites and substrates of the CAT enzyme that translated to changes in the blood concentrations of L-carnitine (LC), acetylcarnitine (C2) and the C2/LC ratio (**Figure 3-6**). In renal tissue, CAT activity progressively declined in CLP mice (**Figure 3-8A**) which resulted from loss of substrate (L-carnitine and acetyl-CoA. There was an association between kidney calculated CAT activity and blood C2/LC ratio. This association was also evident for kidney CoA (a product of CAT activity) and blood C2/LC. CAT activity in CLP liver tissue was initially lower than sham mice then progressively increased but remained lower than the sham CAT activity; liver tissue acetylcarnitine concentration was persistently elevated over time (**Figure 3-8B**). Liver CAT activity was also inversely associated with blood C2/LC ratio. Notably, in healthy control mice, the kidney and liver tissue have different L-carnitine environments (**Table 3-13**) which may contribute to these findings suggesting that the liver may more readily metabolically adapt to the septic condition to balance the ratio of acetyl-CoA to free CoA (29).

Of the several plasma biomarkers of organ function (BUN, AMY, ALT) that were elevated in CLP mice, AMY and BUN, were correlated with blood C2/LC ratio. We also established a connection between organ function and metabolism by showing correlations between renal and liver metabolites with BUN (renal dysfunction) and AMY (pancreatic and renal dysfunction). Also using the CLP model, others have shown the same directional changes to TBIL, BUN, AMY, ALT, TP, and ALB but confirmed the presence of multiple organ dysfunction which may be due to their reported modest increases to CRE (33-35). In both liver

and renal tissue, polymicrobial sepsis caused alterations in numerous metabolites, many of which correlated to blood C2/LC ratio (**Figure 3-11**). Collectively, at the organ level, they represent disturbances in a number of major metabolic pathways and processes (**Figure 3-10**). For example, glutamate, a non-essential amino acid, participates in several pathways in both the liver and kidney. It is a key regulator of pathways in the liver such as the urea cycle, gluconeogenesis, and amino acid catabolism (36). Decreased plasma levels of glutamate and the glutamate/glutamine ratio have been suggested as more specific markers of liver dysfunction and as early predictors of mortality in septic shock patients (37). Likewise, we showed decreased levels of renal glutamate and the liver glutamate/glutamine ratio in CLP animals (**Figure 3-15**). Aspartate and alanine metabolism was also a reoccurring pathway in both renal and liver metabolomes. Aspartate and alanine are part of the anaplerotic reactions that supply intermediates to the TCA cycle (38). Renal aspartate, liver aspartate, and liver alanine levels were lower in the CLP animals (**Figures E-7 and 3-15**), suggesting that the critical pathways for supplying TCA intermediates were initially adversely impacted by systemic infection. Overall, the rate of the metabolic response in the kidneys and liver indicates an early, measurable signal that precedes or simultaneously presents with clinical measurements (e.g., BUN) of sepsis-induced organ dysfunction and the C2/LC ratio in the blood but not the laboratory values included in $SOFA_{renal}$ (CRE) or $SOFA_{liver}$(TBIL). In both organs, some metabolite concentrations stabilized or move towards healthy control values which may explain, in part, our finding that patients with septic shock had fewer detected metabolic changes in the blood compared with patients with sepsis.

The metabolite profiles detected in the sepsis plasma and septic shock serum reflect many of the same disturbances that we observed in the kidneys and livers of the CLP mice. We found

that many of these metabolites were associated with $SOFA_{total}$, $SOFA_{renal}$, and $SOFA_{liver}$ (**Figures 3-13 and 3-14, Table 3-12**). However, our data reveal distinct metabolic signatures of sepsis and septic shock patients. Sepsis patients had changes in a larger and more diverse group of metabolites that were associated with the organ dysfunction variables when compared to patients with septic shock (**Figure 3-2**). We acknowledge that we did not conduct a comprehensive metabolomics assay but given the importance of the metabolites we measured to the energy economy of the host, we expect greater metabolic derangement in patients with septic shock. Furthermore, the Sepsis-3 guidelines imply that septic shock is associated with greater metabolic abnormalities than sepsis and that these contribute to mortality (6). However, this is primarily based on lactate concentration as a distinguishing feature of sepsis and septic shock. We did not find blood lactate as a metabolic signal associated with $SOFA_{total}$, $SOFA_{renal}$, and $SOFA_{liver}$, in either cohort when corrected for multiple comparisons (**Figure 3-2**). The clinical utility of lactate is well-established (6), but it has recently been recognized as more than a hypoxic waste product (39). It has been found to be in the normal range in many septic patients (40) and its normalization has a modest impact on mortality (41). Here we show that there is a wealth of metabolic information not captured by the lactate signal and the current laboratory measurements used to grossly assess organ function via SOFA score calculations in patients with sepsis. The distinct metabolic response in sepsis patients may reflect an earlier, broader range of disturbed metabolic pathways such as the TCA cycle, glutamate metabolism, aspartate metabolism, and branched-chain amino acid metabolism. Although few metabolic resuscitation therapies have been attempted for sepsis with limited success (5, 42), our findings suggest that the metabolic rescue window may occur early in the course of disease and metabolite stratification could be a useful tool to identify eligible patients (43).

The metabolic signatures associated with organ dysfunction in patients with septic shock are primarily comprised of the short and medium chain acylcarnitines, which reflect incomplete oxidation of fatty acids in the mitochondria or peroxisomes (44). The greater representation of acylcarnitines in septic shock patients may be explained by a shift towards the use of lipids as a fuel source that occurs later in sepsis progression (8). Indeed, septic shock metabolite signatures associated with organ dysfunction were dominated by the acylcarnitines, but they were also highly associated with $SOFA_{total}$, $SOFA_{renal}$, and $SOFA_{liver}$ in the sepsis cohort. Considering that our group and others have shown L-carnitine, acetylcarnitine (C2), and the other acylcarnitines are robust markers of organ dysfunction, mortality, inflammation, and infection in sepsis (10, 12, 13, 19), they may capture important metabolic information that is missed by lactate.

We acknowledge that there are limitations to our study. Our human cohorts were intended to represent the temporal stages of sepsis, but we were not able to combine the data from the two cohorts. This is because the metabolomics data were generated on two separate occasions and in two different types of biofluid, plasma for sepsis and serum for septic shock, that could influence the metabolite profiles (45). As such, it was more appropriate for these data to be analyzed separately. We also were limited to cross-sectional data. Moving forward, and given the value of temporal metabolomics data, it will be important to validate our findings in a larger mixed cohort of sepsis and septic shock patients using time series measurements. We also recognize the limitations of the CLP model and the use of a single sepsis model in our work. A limitation of the CLP model arises from the various model parameters such as needle gauge and cecum ligation length, but we had one person perform the surgeries using previously published methodology (20). Despite these limitations, our findings introduce the concept that metabolic dysfunction occurs early in the course of sepsis, at the organ level and each end organ may have

unique metabolic adaption to the septic insult that ultimately contributes to a blood level signal. Future studies using large animal models could aid in pinpointing specific pathways for metabolic rescue and advance understanding of the metabolic defects that direct organ dysfunction.

In summary, we found that sepsis-induced organ dysfunction and the metabolic response are intertwined early in the course of sepsis and these signals change over sepsis progression. Understanding these early metabolite signals may hold the key to timely identification, leading to the prevention of organ failure, a fundamental goal of the current sepsis and septic shock guidelines (6).

3.3 Acknowledgments

Although the manuscript is in preparation, the following researchers have made vital contributions to the work and will be included as co-authors: Kathleen A. Stringer, Thomas Flott, Laura McLellan, Jean Nemzek, Christopher Fry, Michael A. Puskarich, Alan E. Jones, Michael Maile, Evan Farkash. We would also like to acknowledge the patients for providing vital samples to enable scientific research.

3.4 References

1. Bar-Or D, Carrick M, Tanner A, 2nd, Lieser MJ, Rael LT, Brody E. Overcoming the Warburg Effect: Is it the key to survival in sepsis? J Crit Care. 2018;43:197-201.
2. Englert JA, Rogers AJ. Metabolism, metabolomics, and nutritional support of patients with sepsis. Clin Chest Med. 2016;37(2):321-31.
3. McCall CE, Zhu X, Zabalawi M, Long D, Quinn MA, Yoza BK, et al. Sepsis, pyruvate, and mitochondria energy supply chain shortage. J Leukoc Biol. 2022;112(6):1509-14.
4. Zeng Z, Huang Q, Mao L, Wu J, An S, Chen Z, et al. The Pyruvate Dehydrogenase Complex in Sepsis: Metabolic Regulation and Targeted Therapy. Front Nutr. 2021;8:783164.

5. Jones AE, Puskarich MA, Shapiro NI, Guirgis FW, Runyon M, Adams JY, et al. Effect of Levocarnitine vs Placebo as an Adjunctive Treatment for Septic Shock: The Rapid Administration of Carnitine in Sepsis (RACE) Randomized Clinical Trial. JAMA network open. 2018;1(8):e186076-e.
6. Singer M, Deutschman CS, Seymour CW, Shankar-Hari M, Annane D, Bauer M, et al. The Third International Consensus Definitions for Sepsis and Septic Shock (Sepsis-3). JAMA. 2016;315(8):801-10.
7. Pool R, Gomez H, Kellum JA. Mechanisms of Organ Dysfunction in Sepsis. Crit Care Clin. 2018;34(1):63-80.
8. Arina P, Singer M. Pathophysiology of sepsis. Curr Opin Anaesthesiol. 2021;34(2):77-84.
9. Eckerle M, Ambroggio L, Puskarich MA, Winston B, Jones AE, Standiford TJ, et al. Metabolomics as a Driver in Advancing Precision Medicine in Sepsis. Pharmacotherapy. 2017;37(9):1023-32.
10. Langley RJ, Tsalik EL, van Velkinburgh JC, Glickman SW, Rice BJ, Wang C, et al. An integrated clinico-metabolomic model improves prediction of death in sepsis. Sci Transl Med. 2013;5(195):195ra95.
11. Wardi G, Brice J, Correia M, Liu D, Self M, Tainter C. Demystifying Lactate in the Emergency Department. Ann Emerg Med. 2019.
12. Chung KP, Chen GY, Chuang TY, Huang YT, Chang HT, Chen YF, et al. Increased Plasma Acetylcarnitine in Sepsis Is Associated With Multiple Organ Dysfunction and Mortality: A Multicenter Cohort Study. Crit Care Med. 2019;47(2):210-8.
13. Jennaro TS, Viglianti EM, Ingraham NE, Jones AE, Stringer KA, Puskarich MA. Serum Levels of Acylcarnitines and Amino Acids Are Associated with Liberation from Organ Support in Patients with Septic Shock. J Clin Med. 2022;11(3).
14. Johansson PI, Nakahira K, Rogers AJ, McGeachie MJ, Baron RM, Fredenburgh LE, et al. Plasma mitochondrial DNA and metabolomic alterations in severe critical illness. Crit Care. 2018;22(1):360.
15. Mickiewicz B, Duggan GE, Winston BW, Doig C, Kubes P, Vogel HJ, et al. Metabolic profiling of serum samples by 1H nuclear magnetic resonance spectroscopy as a potential diagnostic approach for septic shock. Crit Care Med. 2014;42(5):1140-9.

16. Rogers AJ, McGeachie M, Baron RM, Gazourian L, Haspel JA, Nakahira K, et al. Metabolomic derangements are associated with mortality in critically ill adult patients. PLoS One. 2014;9(1):e87538.
17. Serkova NJ, Standiford TJ, Stringer KA. The Emerging Field of Quantitative Blood Metabolomics for Biomarker Discovery in Critical Illnesses. Am J Respir Crit Care Med. 2011;184(6):647-55.
18. Peregrín-Alvarez JM, Sanford C, Parkinson J. The conservation and evolutionary modularity of metabolism. Genome Biol. 2009;10(6):R63.
19. Puskarich MA, Evans CR, Karnovsky A, Das AK, Jones AE, Stringer KA. Septic Shock Nonsurvivors Have Persistently Elevated Acylcarnitines Following Carnitine Supplementation. Shock. 2018;49(4):412-9.
20. Carpenter KC, Zhou Y, Hakenjos JM, Fry CD, Nemzek JA. Thermoneutral Housing Temperature Improves Survival in a Murine Model of Polymicrobial Peritonitis. Shock. 2020;54(5):688-96.
21. Maksimovic I, Zhang S, Vuckovic I, Irazabal MV. Kidney harvesting and metabolite extraction for metabolomics studies in rodents. Methods Cell Biol. 2019;154:15-29.
22. Nagana Gowda GA, Abell L, Tian R. Extending the Scope of (1)H NMR Spectroscopy for the Analysis of Cellular Coenzyme A and Acetyl Coenzyme A. Analytical chemistry. 2019;91(3):2464-71.
23. Lacy P, McKay RT, Finkel M, Karnovsky A, Woehler S, Lewis MJ, et al. Signal intensities derived from different NMR probes and parameters contribute to variations in quantification of metabolites. PLoS One. 2014;9(1):e85732.
24. Trexel J, Yoon GS, Keswani RK, McHugh C, Yeomans L, Banerjee R, et al. Macrophage-Mediated Clofazimine Sequestration is Accompanied by a Shift in Host Energy Metabolism. Journal of Pharmaceutical Sciences. 2017;106(4):1162-74.
25. Wishart DS, Guo A, Oler E, Wang F, Anjum A, Peters H, et al. HMDB 5.0: the Human Metabolome Database for 2022. Nucleic Acids Res. 2022;50(D1):D622-d31.
26. Xia J, Wishart DS. Web-based inference of biological patterns, functions and pathways from metabolomic data using MetaboAnalyst. Nat Protoc. 2011;6(6):743-60.

27. Rogers AJ, Leligdowicz A, Contrepois K, Jauregui A, Vessel K, Deiss TJ, et al. Plasma Metabolites in Early Sepsis Identify Distinct Clusters Defined by Plasma Lipids. Crit Care Explor. 2021;3(8):e0478.
28. Puskarich MA, McHugh C, Flott TL, Karnovsky A, Jones AE, Stringer KA. Serum Levels of Branched Chain Amino Acids Predict Duration of Cardiovascular Organ Failure in Septic Shock. Shock. 2021;56(1):65-72.
29. Schroeder MA, Atherton HJ, Dodd MS, Lee P, Cochlin LE, Radda GK, et al. The cycling of acetyl-coenzyme A through acetylcarnitine buffers cardiac substrate supply: a hyperpolarized 13C magnetic resonance study. Circ Cardiovasc Imaging. 2012;5(2):201-9.
30. Reuter SE, Evans AM. Carnitine and acylcarnitines: pharmacokinetic, pharmacological and clinical aspects. Clinical pharmacokinetics. 2012;51(9):553-72.
31. Noland RC, Koves TR, Seiler SE, Lum H, Lust RM, Ilkayeva O, et al. Carnitine insufficiency caused by aging and overnutrition compromises mitochondrial performance and metabolic control. J Biol Chem. 2009;284(34):22840-52.
32. Boomer JS, Green JM, Hotchkiss RS. The changing immune system in sepsis: is individualized immuno-modulatory therapy the answer? Virulence. 2014;5(1):45-56.
33. Stortz JA, Hollen MK, Nacionales DC, Horiguchi H, Ungaro R, Dirain ML, et al. Old Mice Demonstrate Organ Dysfunction as well as Prolonged Inflammation, Immunosuppression, and Weight Loss in a Modified Surgical Sepsis Model. Crit Care Med. 2019;47(11):e919-e29.
34. Li JL, Li G, Jing XZ, Li YF, Ye QY, Jia HH, et al. Assessment of clinical sepsis-associated biomarkers in a septic mouse model. J Int Med Res. 2018;46(6):2410-22.
35. Mei SH, Haitsma JJ, Dos Santos CC, Deng Y, Lai PF, Slutsky AS, et al. Mesenchymal stem cells reduce inflammation while enhancing bacterial clearance and improving survival in sepsis. Am J Respir Crit Care Med. 2010;182(8):1047-57.
36. Brosnan JT. Glutamate, at the interface between amino acid and carbohydrate metabolism. J Nutr. 2000;130(4S Suppl):988s-90s.
37. Poeze M, Luiking YC, Breedveld P, Manders S, Deutz NE. Decreased plasma glutamate in early phases of septic shock with acute liver dysfunction is an independent predictor of survival. Clin Nutr. 2008;27(4):523-30.
38. Owen OE, Kalhan SC, Hanson RW. The key role of anaplerosis and cataplerosis for citric acid cycle function. J Biol Chem. 2002;277(34):30409-12.

39. Chen YJ, Mahieu NG, Huang X, Singh M, Crawford PA, Johnson SL, et al. Lactate metabolism is associated with mammalian mitochondria. Nat Chem Biol. 2016;12(11):937-43.
40. Sauer CM, Gómez J, Botella MR, Ziehr DR, Oldham WM, Gavidia G, et al. Understanding critically ill sepsis patients with normal serum lactate levels: results from U.S. and European ICU cohorts. Sci Rep. 2021;11(1):20076.
41. Jones AE, Shapiro NI, Trzeciak S, Arnold RC, Claremont HA, Kline JA, et al. Lactate clearance vs central venous oxygen saturation as goals of early sepsis therapy: a randomized clinical trial. JAMA. 2010;303(8):739-46.
42. Iglesias J, Vassallo AV, Patel VV, Sullivan JB, Cavanaugh J, Elbaga Y. Outcomes of Metabolic Resuscitation Using Ascorbic Acid, Thiamine, and Glucocorticoids in the Early Treatment of Sepsis: The ORANGES Trial. Chest. 2020;158(1):164-73.
43. Puskarich MA, Jennaro TS, Gillies CE, Evans CR, Karnovsky A, McHugh CE, et al. Pharmacometabolomics identifies candidate predictor metabolites of an L-carnitine treatment mortality benefit in septic shock. Clin Transl Sci. 2021;14(6):2288-99.
44. McCann MR, George De la Rosa MV, Rosania GR, Stringer KA. L-Carnitine and Acylcarnitines: Mitochondrial Biomarkers for Precision Medicine. Metabolites. 2021;11(1).
45. Vignoli A, Tenori L, Morsiani C, Turano P, Capri M, Luchinat C. Serum or Plasma (and Which Plasma), That Is the Question. J Proteome Res. 2022;21(4):1061-72.

Chapter 4 Conclusions and Future Directions

The work presented in this dissertation sought to elucidate the metabolic relationships between measures of C2 in the blood with various assessments of mitochondrial function to mechanistically validate C2 as a candidate biomarker in sepsis. While acknowledging the broad range of biological responsibilities performed by the mitochondria, we focused on the energetic metabolism component of mitochondrial function. The justification for this was due to the well-established reputation that C2 and the carnitine pool are representative biomarkers of disrupted mitochondrial fatty acid oxidation (1). I also highlighted the extent to which these metabolites can inform of the metabolic status in various clinical conditions, with an emphasis on sepsis and septic shock. Since mitochondrial dysfunction is one of the proposed mechanisms contributing to sepsis-induced organ dysfunction or failure (2, 3), it was imperative to establish a connection between measured C2 in the blood and mitochondrial dysfunction in the context of sepsis.

Measuring mitochondrial oxygen consumption rates (mOCR) is considered the gold standard for assessing mitochondrial function due to the direct connection to energy production in the form of ATP (4). The method itself is technically challenging and cost prohibitive in many settings. Both limitations are barriers preventing the direct measurement of mOCR in patients. Furthermore, it would be difficult to routinely acquire tissue biopsies from a critically ill patient population such as those with sepsis or septic shock. The use of platelets as a “circulating organ” circumvents the challenges with obtaining tissue biopsies but does not overcome the technical and financial barriers (5, 6). A more clinically translatable solution to assess mitochondrial

function is possible by establishing a relationship between metabolite signals in the blood and mOCR in platelets, which has been suggested as a more complete method for assessing mitochondrial function (7). We illustrated the feasibility of this approach using a stepwise forward-backward variable selection method to generate multiple linear regression models using the mOCR data and NMR metabolomics data from either platelets or whole blood. The whole blood metabolite model with a positive predicted-R^2 and a significant ANOVA p-value included acetylcarnitine and leucine as covariates associated with basal mOCR. Indeed, acetylcarnitine was shown to be associated with the unstimulated measurement of mOCR. The β-coefficient of the acetylcarnitine term was negative which implies that the metabolite concentration was inversely related to mitochondrial function at baseline. Lower baseline mOCR represents the downregulation of the anti-inflammatory/oxidative phosphorylation response that was discussed in Chapter 1. The inability to restore this homeostatic metabolic process is associated with negative outcomes in sepsis (8, 9). We showed higher levels of acetylcarnitine in the blood are related to this negative metabolic state. Thus, measurements of acetylcarnitine in the blood could serve as a biomarker of downregulated mitochondrial oxidative phosphorylation and the subsequent poor clinical consequences. Thus, it is possible to assess mitochondrial function by measuring acetylcarnitine rather than measuring mOCR directly. Measurement of metabolites in the routinely drawn blood samples affords a more clinically translatable method to assess mitochondrial health in patients with sepsis. Although quantifying metabolites is not without technical drawbacks, the widespread implementation of the metabolite biomarker serum lactate illustrates it is not a major limitation.

To further credential C2 as a biomarker reflecting comprehensive metabolism, I sought to identify relationships between C2 with intermediates of the TCA cycle and to explore the

potential origins of the blood C2 signal by investigating its relationship to changes in organ metabolites, specifically, acetyl-CoA. I found that the relationship between C2 and the TCA cycle intermediate, malate, was stronger in the septic shock non-survivors when compared to the survivors, suggesting that disruptions in this critical metabolic pathway is closely linked to mortality and is reflected in changes in blood C2. Indeed, our data show support that C2 reflects a broader mitochondrial dysfunction interpretation, encompassing not just disruptions in fatty acid oxidation, but also the TCA cycle. The subsequent analysis using a less sick sepsis cohort did not show a similar mortality driven relationship between those metabolites, suggesting that the different metabolic response between sepsis and septic shock is driven by severity of illness and not mortality. The differing relationships observed between the blood measurements of L-carnitine (LC), C2, and the C2/LC ratio with measures of organ dysfunction further corroborate that severity of illness is reflected by distinct metabolite profiles. This finding led to the utilization of a sepsis mouse model to further elucidate the associations between blood carnitine metabolism with changes in organ function and metabolism.

Briefly, conditions of high stress and high energetic demands provoke an adaptive metabolic response to conserve highly valued acetyl- groups by combining acetyl-CoA with LC to produce C2 and free CoA, which is facilitated by carnitine acetyltransferase (CAT) (10). By measuring the ratio of the substrates to the products [(acetyl-CoA + L-carnitine)/(acetylcarnitine + CoA)] of this adaptive pathway, I was able to evaluate how sepsis-induced changes in the organ CAT enzyme activity of the septic mice are reflected in disrupted carnitine metabolism in the blood. Compared to the sham controls, the septic mice had decreased blood concentrations of LC and increased levels of the C2/LC ratio. The independent components of the CAT activity ratio varied between the kidney and liver tissues, but notably, the liver C2 concentrations were

elevated in the septic animals compared to the sham controls. Furthermore, the CAT activity measurement was lower in both the kidney and liver tissues, meaning a shift in production of C2 and free CoA. The data suggest that the kidney and liver cells upregulated this adaptive metabolic pathway as a response to sepsis. The sepsis mouse model was intended to capture the beginning of sepsis which allowed us to observe the production of C2 in the organs but was too early to see the transition into the blood. The model also enabled the chronological characterization of sepsis-induced changes in organ metabolism and organ dysfunction through the plasma measurements of clinical biomarkers and histopathological staining. Importantly, I observed robust sepsis-induced disruptions in kidney and liver metabolism that preceded widespread and clinically detectable organ injury and dysfunction. The profound disruptions in organ metabolism were also reflected by changes in the blood measurements of the C2/LC ratio. Not only does this finding strengthen the biomarker potential of blood carnitine metabolism, but it also shows the close connection between organ metabolism and sepsis-induced organ dysfunction at the start of sepsis. These findings provide the foundational pathophysiological knowledge that could lead to new therapeutic targets intended to prevent or mitigate sepsis-induced organ dysfunction, the primary driver of mortality in patients with sepsis.

The identified association between whole blood C2 and platelet mOCR established that measurements of C2 in the blood have the potential to serve as a surrogate measure of mitochondrial energetic dysfunction. Research highlighting the importance of mitochondrial dysfunction in the progression of sepsis-induced organ dysfunction is growing but has not translated into clinical practice applications yet (2, 11). The current clinical paradigm relies on the measurement of one metabolite biomarker, lactate, to represent the whole metabolic derangement inflicted by sepsis (12), but this likely does not capture the full picture. There is an

abundance of literature highlighting the breadth of sepsis-induced disruptions to the metabolism (13-15), many of which have consistently identified C2 as a predictor of organ dysfunction and mortality (16, 17). Future studies are necessary to validate these findings in larger and more diverse cohorts but also to understand what changes could be made in the care of sepsis patients based on the knowledge gained from using C2 as a surrogate measure of mitochondrial dysfunction. One possible action is through the use of metabolic resuscitation strategies. Although few have been successful in the improvement of outcomes, using metabolic stratification has been shown as a viable method to identify patients that would derive a benefit from such a therapeutic intervention (18-20). Utilizing metabolic stratification in pre-clinical models could improve the success of translating therapies between animal and human sepsis, which has been attempted in other disease states (21). Additionally, employing a pre-clinical mouse model of early sepsis revealed key insights in the tandem development and progression of sepsis-mediated changes in organ metabolism and function. While other researchers have reported disruptions in organ metabolism (22, 23) and function (24), we made longitudinal observations tracking the chronological progression of both. Like all animal models, the findings require rigorous validation before the successful translation into human studies. It would also be insightful to explore the metabolic changes of other major organs such as the heart and lungs, extend the model timepoints to align with human sepsis and septic shock more closely, and study targeted metabolic therapies using the model. In aggregate, the data presented provide evidence to support the use of C2 as a candidate biomarker for the comprehensive assessment of metabolism in patients with sepsis.

4.1 References

1. Dambrova M, Makrecka-Kuka M, Kuka J, Vilskersts R, Nordberg D, Attwood MM, et al. Acylcarnitines: Nomenclature, Biomarkers, Therapeutic Potential, Drug Targets, and Clinical Trials. Pharmacol Rev. 2022;74(3):506-51.
2. Arina P, Singer M. Pathophysiology of sepsis. Curr Opin Anaesthesiol. 2021;34(2):77-84.
3. Brealey D, Singer M. Mitochondrial Dysfunction in Sepsis. Curr Infect Dis Rep. 2003;5(5):365-71.
4. Brand M, Nicholls D. Assessing mitochondrial dysfunction in cells. Biochem J. 2011;435(Pt 2):297-312.
5. Sjovall F, Morota S, Hansson MJ, Friberg H, Gnaiger E, Elmer E. Temporal increase of platelet mitochondrial respiration is negatively associated with clinical outcome in patients with sepsis. Crit Care. 2010;14(6):R214.
6. Puskarich MA, Kline JA, Watts JA, Shirey K, Hosler J, Jones AE. Early alterations in platelet mitochondrial function are associated with survival and organ failure in patients with septic shock. J Crit Care. 2016;31(1):63-7.
7. Jones AE, Sheng L, Acevedo A, Veliova M, Shirihai OS, Stiles L, et al. Forces, fluxes, and fuels: tracking mitochondrial metabolism by integrating measurements of membrane potential, respiration, and metabolites. Am J Physiol Cell Physiol. 2021;320(1):C80-c91.
8. Han SH, Malaga-Dieguez L, Chinga F, Kang HM, Tao J, Reidy K, et al. Deletion of Lkb1 in Renal Tubular Epithelial Cells Leads to CKD by Altering Metabolism. J Am Soc Nephrol. 2016;27(2):439-53.
9. Singer M. Critical illness and flat batteries. Crit Care. 2017;21(Suppl 3):309.
10. Schroeder MA, Atherton HJ, Dodd MS, Lee P, Cochlin LE, Radda GK, et al. The cycling of acetyl-coenzyme A through acetylcarnitine buffers cardiac substrate supply: a hyperpolarized 13C magnetic resonance study. Circ Cardiovasc Imaging. 2012;5(2):201-9.
11. Singer M. The role of mitochondrial dysfunction in sepsis-induced multi-organ failure. Virulence. 2014;5(1):66-72.
12. Singer M, Deutschman CS, Seymour CW, Shankar-Hari M, Annane D, Bauer M, et al. The Third International Consensus Definitions for Sepsis and Septic Shock (Sepsis-3). JAMA. 2016;315(8):801-10.

13. Eckerle M, Ambroggio L, Puskarich MA, Winston B, Jones AE, Standiford TJ, et al. Metabolomics as a Driver in Advancing Precision Medicine in Sepsis. Pharmacotherapy. 2017;37(9):1023-32.
14. Puskarich MA, Finkel MA, Karnovsky A, Jones AE, Trexel J, Harris BN, et al. Pharmacometabolomics of l-carnitine treatment response phenotypes in patients with septic shock. Annals of the American Thoracic Society. 2015;12(1):46-56.
15. Langley RJ, Tsalik EL, van Velkinburgh JC, Glickman SW, Rice BJ, Wang C, et al. An integrated clinico-metabolomic model improves prediction of death in sepsis. Sci Transl Med. 2013;5(195):195ra95.
16. Chung KP, Chen GY, Chuang TY, Huang YT, Chang HT, Chen YF, et al. Increased Plasma Acetylcarnitine in Sepsis Is Associated With Multiple Organ Dysfunction and Mortality: A Multicenter Cohort Study. Crit Care Med. 2019;47(2):210-8.
17. Puskarich MA, Evans CR, Karnovsky A, Das AK, Jones AE, Stringer KA. Septic Shock Nonsurvivors Have Persistently Elevated Acylcarnitines Following Carnitine Supplementation. Shock. 2018;49(4):412-9.
18. Iglesias J, Vassallo AV, Patel VV, Sullivan JB, Cavanaugh J, Elbaga Y. Outcomes of Metabolic Resuscitation Using Ascorbic Acid, Thiamine, and Glucocorticoids in the Early Treatment of Sepsis: The ORANGES Trial. Chest. 2020;158(1):164-73.
19. Jones AE, Puskarich MA, Shapiro NI, Guirgis FW, Runyon M, Adams JY, et al. Effect of Levocarnitine vs Placebo as an Adjunctive Treatment for Septic Shock: The Rapid Administration of Carnitine in Sepsis (RACE) Randomized Clinical Trial. JAMA network open. 2018;1(8):e186076-e.
20. Puskarich MA, Jennaro TS, Gillies CE, Evans CR, Karnovsky A, McHugh CE, et al. Pharmacometabolomics identifies candidate predictor metabolites of an L-carnitine treatment mortality benefit in septic shock. Clin Transl Sci. 2021;14(6):2288-99.
21. Thorens B, Rodriguez A, Cruciani-Guglielmacci C, Wigger L, Ibberson M, Magnan C. Use of preclinical models to identify markers of type 2 diabetes susceptibility and novel regulators of insulin secretion - A step towards precision medicine. Mol Metab. 2019;27s(Suppl):S147-s54.

22. Hao Y, Zheng H, Wang RH, Li H, Yang LL, Bhandari S, et al. Maresin1 Alleviates Metabolic Dysfunction in Septic Mice: A (1)H NMR-Based Metabolomics Analysis. Mediators Inflamm. 2019;2019:2309175.
23. Izquierdo-García JL, Nin N, Ruíz-Cabello J, Rojas Y, de Paula M, López-Cuenca S, et al. A metabolomic approach for diagnosis of experimental sepsis. Intensive Care Med. 2011;37(12):2023-32.
24. Li JL, Li G, Jing XZ, Li YF, Ye QY, Jia HH, et al. Assessment of clinical sepsis-associated biomarkers in a septic mouse model. J Int Med Res. 2018;46(6):2410-22.